Department of Clinical Pharmacology
University of Helsinki
Finland

Role of CYP2C8 in the metabolism of montelukast and imatinib

Studies *in vitro*, *in silico* and in humans

Anne Filppula

ACADEMIC DISSERTATION

To be presented,
with permission of the Faculty of Medicine of the University of Helsinki,
for public examination in Lecture Hall 3 of Biomedicum Helsinki, Haartmaninkatu 8,
on November 14th, 2014, at 12 noon.

Helsinki 2014

Supervisors: Professor Janne T Backman, MD, PhD
Department of Clinical Pharmacology
University of Helsinki and HUSLAB, Helsinki University Central Hospital
Helsinki, Finland

Professor *Emeritus* Pertti J Neuvonen, MD, PhD
Department of Clinical Pharmacology
University of Helsinki and HUSLAB, Helsinki University Central Hospital
Helsinki, Finland

Reviewers: Associate Professor Nina Isoherranen, PhD
University of Washington
Seattle, USA

Adjunct Professor Mikko Koskinen, PhD
Head of DMPK
Orion Corporation
Espoo, Finland

Opponent: Professor Kim Brøsen, MD, PhD
Clinical Pharmacology
University of Southern Denmark
Odense, Denmark

ISBN 978-951-51-0240-9 (paperback)
ISBN 978-951-51-0241-6 (PDF, http://ethesis.helsinki.fi)

Unigrafia Oy, Helsinki 2014

To my family

TABLE OF CONTENTS

LIST OF FIGURES

LIST OF TABLES

ABBREVIATIONS AND DEFINITIONS

[I]	Inhibitor concentration
[S]	Substrate concentration
ABC	Adenosine triphosphate-binding cassette
AIC	Akaike information criterion
ALL	Acute lymphoblastic leukaemia
ATP	Adenosine triphosphate
AUC	Area under concentration-time curve
B/P	Blood-to-plasma ratio
BCR	Breakpoint cluster region
BCRP	Breast cancer resistance protein
c.	Nucleotide position in the coding deoxyribonucleic acid
CAR	Constitutive androstane receptor
CL	Clearance
C_{max}	Peak concentration
CML	Chronic myelogenous leukaemia
C_{trough}	Trough concentration
CV	Coefficient of variation
CYP	Cytochrome pigment 450
CysLT	Cysteinyl leukotriene
EM	Extensive metaboliser
EMA	European Medicines Agency
F	Bioavailability
FDA	Food and Drug Administration
F_G	Extent of bioavailability across the intestinal wall
f_m	Fraction metabolised
FMO	Flavin-containing monooxygenase
f_u	Fraction unbound
GIST	Gastrointestinal stromal tumour
HLM	Human liver microsomes
HMG-CoA	3-hydroxy-3-methyl-glutaryl-coenzyme A
IC_{50}	Inhibitor concentration producing 50% inhibition
IM	Intermediate metaboliser
ISEF	Intersystem extrapolation factor
k_a	Absorption rate constant
k_{deg}	First-order degradation rate constant of an enzyme
k_{dep}	First-order depletion rate constant
k_e	Elimination rate constant
K_i	Reversible inhibition constant
K_I	Inhibitor concentration supporting half of the maximal rate of inactivation

k_{inact}	Maximal rate of inactivation
K_m	Michaelis-Menten constant
k_{obs}	Inactivation rate constant for a particular inhibitor concentration
LC-MS/MS	Liquid chromatography-tandem mass spectrometry
MBI	Mechanism-based inhibitor
MIC	Metabolic inhibitory complex / metabolic intermediate complex
MPPGL	Microsomal protein per gram liver
mRNA	Messenger ribonucleic acid
n/a	Not available
n/d	Not determined
NADPH	Nicotinamide adenine dinucleotide phosphate (reduced form)
NSAID	Non-steroidal anti-inflammatory drug
OAT	Organic anion transporter
OATP	Organic anion-transporting polypeptide
OCT	Organic cation transporter
OCTN	Novel organic cation/carnitine transporter
PBPK	Physiologically based pharmacokinetic
PDGFR	Platelet-derived growth factor receptor
P-gp	P-glycoprotein
PM	Poor metaboliser
POR	Cytochrome P450 oxidoreductase
PPAR	Peroxisome proliferator activated receptor
PXR	Pregnane X receptor
r	Partition ratio
r^2	Coefficient of determination
RA	Relative abundance
RAF	Relative activity factor
SLC	Solute carrier
SNP	Single nucleotide polymorphism
$t_{½}$	Elimination half-life
t_{max}	Time to peak concentration
UGT	Uridine-5'-diphosphate glucuronosyltransferase
v	Reaction velocity
V_d	Volume of distribution
V_{max}	Maximum reaction velocity

LIST OF ORIGINAL PUBLICATIONS

This thesis is based on the following original publications, which are referred to in the text as studies **I-V**:

I **Filppula AM**, Laitila J, Neuvonen PJ, and Backman JT (2011) Reevaluation of the microsomal metabolism of montelukast: major contribution by CYP2C8 at clinically relevant concentrations. Drug Metab Dispos 39:904-911.

II Karonen T, **Filppula A**, Laitila J, Niemi M, Neuvonen PJ, and Backman JT (2010) Gemfibrozil markedly increases the plasma concentrations of montelukast: a previously unrecognized role for CYP2C8 in the metabolism of montelukast. Clin Pharmacol Ther 88:223-230.

III **Filppula AM**, Laitila J, Neuvonen PJ, and Backman JT (2012) Potent mechanism-based inhibition of CYP3A4 by imatinib explains its liability to interact with CYP3A4 substrates. Br J Pharmacol 165:2787-2798.

IV **Filppula AM**, Neuvonen M, Laitila J, Neuvonen PJ, and Backman JT (2013) Autoinhibition of CYP3A4 leads to important role of CYP2C8 in imatinib metabolism: variability in CYP2C8 activity may alter plasma concentrations and response. Drug Metab Dispos 41:50-59.

V **Filppula AM**, Tornio A, Niemi M, Neuvonen PJ, and Backman JT (2013) Gemfibrozil impairs imatinib absorption and inhibits the CYP2C8-mediated formation of its main metabolite. Clin Pharmacol Ther 94:383-393.

 Study **II** is also included in the academic dissertation of Tiina Karonen.

ABSTRACT

The drug-metabolising enzyme cytochrome P450 (CYP) 2C8 is involved in the elimination of several important drugs. Inhibition of CYP2C8 may therefore cause clinically relevant drug-drug interactions. Gemfibrozil, a lipid-lowering agent, is a strong CYP2C8 inhibitor, which has increased the plasma exposure to many CYP2C8 substrates several-fold in clinical studies. The asthma drug montelukast is also a potent CYP2C8 inhibitor *in vitro*; however, it does not affect the pharmacokinetics of CYP2C8 substrates *in vivo*. In turn, the cancer drug imatinib is a CYP2C8 and CYP3A4 substrate *in vitro*, but CYP3A4 inhibitors have little effect on its concentrations *in vivo*. This thesis aimed to study the discrepancies between these *in vitro* and *in vivo* findings, and to determine the role of CYP2C8 in the metabolism of montelukast and imatinib.

The work comprised *in vitro* experiments, physiologically based pharmacokinetic (PBPK) simulations, and two clinical studies with a two-phase, randomised, placebo-controlled crossover design. In microsomal incubations, among ten CYP enzymes tested, CYP2C8 metabolised montelukast most extensively. Its contribution to the *in vivo* metabolism of montelukast was estimated to exceed 70%. In accordance with the prediction, gemfibrozil increased the area under the plasma concentration time-curve (AUC) of montelukast by 4.5-fold in healthy subjects.

Based on microsomal data, the roles of CYP2C8 and CYP3A4 were estimated at 40 and 57%, respectively, of the hepatic clearance of imatinib. However, imatinib also inhibited CYP3A4 irreversibly, suggesting that it can inhibit its own CYP3A4-mediated metabolism. In healthy subjects, gemfibrozil had no effect on imatinib AUC, while it unexpectedly reduced imatinib absorption. Gemfibrozil also reduced the AUC of the main metabolite of imatinib, N-desmethylimatinib, by 48%. PBPK simulations suggested that the findings could be explained by a complex interaction involving simultaneous inhibition of an uptake transporter involved in imatinib absorption and of CYP2C8 by gemfibrozil. Furthermore, multiple-dose simulations suggested that because imatinib inhibits CYP3A4, the role of CYP2C8 in imatinib pharmacokinetics increases with time.

The findings of this work propose that CYP2C8 is the main enzyme involved in the pharmacokinetics of montelukast, contributing to about 80% of its elimination. Because montelukast is generally well-tolerated and safe, it could serve as a CYP2C8 marker substrate drug in interaction studies. The results for imatinib indicate that it is an irreversible CYP3A4 inhibitor, which suggests that concomitant use of imatinib with CYP3A4 substrates may increase the risk of concentration-dependent adverse drug reactions. In addition, the findings propose that during long-term treatment, the elimination of imatinib relies more on CYP2C8 than on CYP3A4. Collectively, these studies strengthen the position of CYP2C8 as a pivotal drug-metabolising enzyme. In addition, they highlight the importance of carefully validated *in vitro* experimental conditions and demonstrate the usefulness of PBPK simulations to explain complex drug-drug interactions.

YHTEENVETO

Sytokromi P450 (CYP) 2C8 -entsyymi osallistuu monen lääkeaineen metaboliaan, joten sen esto voi johtaa kliinisesti merkittäviin yhteisvaikutuksiin. Lipidilääke gemfibrotsiili on voimakas CYP2C8-estäjä. Se moninkertaistaa eräiden CYP2C8-substraattien pitoisuudet plasmassa. Astmalääke montelukasti on myös vahva CYP2C8-estäjä *in vitro*, mutta ei vaikuta CYP2C8-substraattien plasmapitoisuuksiin *in vivo*. Syöpälääke imatinibi puolestaan on CYP2C8- ja CYP3A4-substraatti *in vitro*, mutta CYP3A4-estäjillä on ollut vain vähäinen vaikutus imatinibin pitoisuuksiin *in vivo*. Tämän väitöskirjatyön tavoitteena oli selvittää näitä *in vitro*- ja *in vivo* -havaintojen välillä olevia epäjohdonmukaisuuksia, sekä tutkia CYP2C8-entsyymin merkitystä montelukastin ja imatinibin metaboliassa.

Väitöskirja koostuu *in vitro* -töistä, fysiologiaan perustuvista farmakokineettisistä (PBPK) simulaatioista, sekä kahdesta lumekontrolloidusta yhteisvaikutustutkimuksesta. CYP2C8 oli tärkein kymmenestä CYP-entsyymistä, joiden osuutta montelukastin metaboliaan testattiin mikrosomi-inkubaatioissa, ja sen osuudeksi montelukastin *in vivo* -metaboliassa arvioitiin yli 70 %. Gemfibrotsiili nosti koehenkilöillä montelukastin plasmapitoisuus-aika-kuvaajan alaisen pinta-alan (AUC:n) 4,5-kertaiseksi.

In vitro -tulosten perusteella lasketut CYP2C8:n ja CYP3A4:n osuudet imatinibin maksapuhdistumassa olivat 40 % ja 57 %. Toisaalta imatinibi oli myös CYP3A4:n irreversiibeli estäjä *in vitro*, mikä viittaa siihen, että imatinibi voi estää omaa CYP3A4-välitteistä metaboliaansa. Yllättäen gemfibrotsiili pienensi imatinibin imeytymistä koehenkilöillä, mutta ei aiheuttanut muutosta imatinibin AUC:ssa. Lisäksi imatinibin päämetaboliitin, N-desmetyyli-imatinibin, AUC laski 48 %. PBPK-simulaatioiden mukaan nämä havainnot ovat selitettävissä monimutkaisella yhteisvaikutuksella, jossa gemfibrotsiili estää sekä imatinibin imeytymiseen osallistuvaa sisäänottotransportteria että sen metaboliassa tärkeää CYP2C8:aa. Toistuvan annostelun simulaatioiden mukaan imatinibin aiheuttama CYP3A4-esto voi johtaa siihen, että CYP2C8:n rooli imatinibin farmakokinetiikassa kasvaa ajan myötä.

Väitöskirjatutkimuksessa tehtyjen havaintojen perusteella CYP2C8 vastaa noin 80 % montelukastin eliminaatiosta ja on siten tärkein entsyymi sen metaboliassa. Koska montelukasti on yleisesti ottaen hyvin siedetty ja turvallinen lääke, se voisi toimia CYP2C8:n mallisubstraattina yhteisvaikutustutkimuksissa. Imatinibi osoittautui olevan irreversiibeli CYP3A4-estäjä, joten sen yhtäaikainen käyttö CYP3A4-substraattien kanssa voi lisätä niiden pitoisuusriippuvaisia haittavaikutuksia. Jatkuvassa käytössä imatinibin eliminaatio vaikuttaa olevan enemmän riippuvainen CYP2C8:sta kuin CYP3A4:sta. Yhteenvetona voidaan todeta, että nämä tutkimukset vahvistavat CYP2C8-entsyymin tärkeyttä lääkeaineita metaboloivana entsyyminä. Ne myös korostavat tarkasti validoitujen *in vitro* -olosuhteiden merkitystä ja osoittavat PBPK-simulaatioiden käyttökelpoisuuden monimutkaisten lääkeyhteisvaikutusten selittämisessä.

SAMMANFATTNING

Enzymet cytokrom P450 (CYP) 2C8 deltar i nedbrytningen av flertalet läkemedel. Blockering av detta enzym kan därmed leda till kliniskt relevanta läkemedelsinteraktioner. Det lipidsänkande läkemedlet gemfibrozil är en stark CYP2C8-hämmare som har orsakat kraftigt förhöjda plasmakoncentrationer av flera CYP2C8-substrat. Astmaläkemedlet montelukast är också en potent CYP2C8-hämmare *in vitro*, men dess effekt på farmakokinetiken hos CYP2C8-substrat *in vivo* är obetydlig. Cancerläkemedlet imatinib metaboliseras sin tur av både CYP2C8 och CYP3A4 *in vitro*, men CYP3A4-hämmare har påverkat dess koncentrationer endast i låg grad *in vivo*. Målet med denna avhandling var att utreda motsättningarna mellan dessa *in vitro*- och *in vivo*-observationer samt att undersöka betydelsen av CYP2C8 i metabolismen av montelukast och imatinib.

Arbetet genomfördes i form av *in vitro*-experiment, fysiologiskt baserade farmakokinetiska (PBPK) simulationer och två placebokontrollerade interaktionsstudier. Av de tio CYP-enzym som testades i mikrosomala inkubationer, metaboliserades montelukast i störst utsträckning av CYP2C8 och enzymets andel i montelukasts *in vivo*-metabolism uppskattades till >70 %. I enlighet med denna prediktion förhöjde gemfibrozil montelukasts yta under plasmakoncentration-tid-kurvan (AUC) 4,5-faldigt hos friska försökspersoner.

På basen av *in vitro*-data uppskattades betydelsen av CYP2C8 och CYP3A4 i imatinibs hepatiska clearance till 40 respektive 57 %. Imatinib visade sig även vara en irreversibel CYP3A4-hämmare, vilket tyder på att imatinib kan hämma sin egen CYP3A4-katalyserade metabolism. I den kliniska studien minskade gemfibrozil oväntat på imatinibs absorption medan imatinibs AUC förblev opåverkad. Därtill sjönk AUC av imatinibs primära metabolit N-desmetylimatinib med 48 % vid samtidigt intag av gemfibrozil. Enligt PBPK-simulationer kan dessa observationer förklaras av en komplex interaktion där gemfibrozil hämmar en upptagstransportör som deltar i imatinibs absorption samtidigt som den hämmar imatinibs metabolism via CYP2C8. Enligt resultat från flerdos-simulationer leder imatinibs hämning av CYP3A4 till att betydelsen av CYP2C8 i imatinibs farmakokinetik ökar med tiden.

Enligt observationerna i denna avhandling svarar CYP2C8 för ungefär 80 % av montelukasts elimination och är därmed det huvudsakliga enzymet i dess metabolism. Eftersom montelukast generellt anses vara ett vältolererat och tryggt läkemedel, tyder resultaten på att montelukast kunde användas som ett markörsubstrat för CYP2C8 i interaktionsstudier. Iakttagelserna för imatinibs del tyder på att det hämmar CYP3A4 irreversibelt, vilket indikerar att samtidigt intag av imatinib och CYP3A4-substrat kan öka risken för koncentrationsberoende biverkningar. Under långtidsbehandling med imatinib verkar imatinibs elimination vara mera beroende av CYP2C8 än CYP3A4. Observationerna från studierna i denna avhandling stärker CYP2C8:s roll som ett viktigt läkemedelsmetaboliserande enzym. Därtill belyser de vikten av noggrant validerade experimentella *in vitro*-betingelser samt demonstrerar hur PBPK-simulationer kan användas till att förklara komplexa läkemedelsinteraktioner.

INTRODUCTION

Drug-drug interactions occur when one drug causes clinically relevant changes in the plasma concentrations and/or pharmacological effect of another drug. In most cases, two or more drugs can be safely and successfully administered together. Occasionally, however, drug-drug interactions arise that can have serious clinical consequences, including lack of therapeutic effect, adverse drug reactions, and even fatalities (EMA, 2013). Inhibition of the drug-metabolising cytochrome P450 (CYP) enzymes is the most important cause of harmful drug-drug interactions (Pelkonen *et al.*, 2008). Highly expressed in the liver, about ten individual CYPs play a significant role in the metabolism of drugs. Therefore, when characterising the interaction potential of a drug that undergoes metabolism, it is important to determine the CYP enzymes possibly involved. Correspondingly, drugs should also be tested for their potential to inhibit and induce different CYPs. These risk assessment studies typically include a combination of *in vitro* (laboratory), *in silico* (computational), and *in vivo* (animal and human) methods.

The role of CYP2C8 in drug metabolism was long considered to be of little importance. However, during the last 15 years, it has received increasing attention as more CYP2C8 substrates and inhibitors have been identified, its structure has been elucidated, and genetic CYP2C8 polymorphisms have been characterised (Schoch *et al.*, 2004, Lai *et al.*, 2009, Aquilante *et al.*, 2013b). The significance of CYP2C8 was recognised following a severe interaction between the strong CYP2C8 inhibitor gemfibrozil and cerivastatin that resulted in cases of fatal rhabdomyolysis (Backman *et al.*, 2002, Huang *et al.*, 2008). Gemfibrozil has also increased the concentrations of many other CYP2C8 substrate drugs several-fold (Niemi *et al.*, 2003a, Niemi *et al.*, 2003b, Jaakkola *et al.*, 2005, Niemi *et al.*, 2006, Tornio *et al.*, 2007, Tornio *et al.*, 2008, Backman *et al.*, 2009, Honkalammi *et al.*, 2012, Aquilante *et al.*, 2013a), and is therefore recommended as a CYP2C8 inhibitor drug in clinical interaction studies (FDA, 2011, EMA, 2013). In addition, gemfibrozil is an inhibitor of the hepatic uptake transporter organic anion-transporting polypeptide (OATP) 1B1, which likely explains its interactions with pravastatin and rosuvastatin (Kyrklund *et al.*, 2003, Schneck *et al.*, 2004), which are not metabolised by CYP2C8.

The leukotriene receptor antagonist montelukast also interacts with CYP2C8. It is a selective, competitive inhibitor of CYP2C8 *in vitro* (Walsky *et al.*, 2005b). In a screening study, montelukast was the most potent CYP2C8 inhibitor among 209 drugs tested (Walsky *et al.*, 2005a), and crystallographic studies have shown that montelukast fits the active site cavity of CYP2C8 well (Schoch *et al.*, 2008). However, despite its ability to inhibit CYP2C8 *in vitro*, montelukast has not affected the plasma concentrations of the CYP2C8 substrates pioglitazone, repaglinide, and rosiglitazone in healthy volunteers (Jaakkola *et al.*, 2006b, Kajosaari *et al.*, 2006, Kim *et al.*, 2007). The lack of *in vivo* inhibitory effect suggests that the

concentrations of montelukast at the CYP2C8 enzyme site in hepatocytes are too low for it to cause inhibition, in line with its very small unbound fraction in plasma (Singulair Clinical Pharmacology and Biopharmaceutic Review(s), 1998).

In contrast, the tyrosine kinase inhibitor imatinib is a relatively strong CYP3A4 inhibitor *in vivo*, but appears to affect CYP3A4 weakly *in vitro*. Imatinib has increased the plasma exposure to the CYP3A4 substrate simvastatin almost four-fold in healthy volunteers (O'Brien *et al.*, 2003), but this interaction cannot be explained based on its reported inhibition potency of CYP3A4 *in vitro* (Gleevec Clinical Pharmacology and Biopharmaceutic Review(s), 2001). In addition, imatinib is mainly metabolised by CYP3A4 (Marull and Rochat, 2006, Rochat *et al.*, 2008, Gleevec label, 2014). Despite the proposed role of CYP3A4 in its metabolism, the CYP3A4 inhibitor ketoconazole increased the area under plasma concentration-time curve (AUC) of imatinib after a single imatinib dose only moderately (by 1.4-fold) (Dutreix *et al.*, 2004), while the strong CYP3A4 inhibitor ritonavir had no effect on its plasma exposure after multiple imatinib doses (van Erp *et al.*, 2007). Furthermore, the elimination of the CYP3A4 substrates erythromycin and midazolam correlated with imatinib elimination in the beginning of imatinib treatment, but no longer at steady state (Gurney *et al.*, 2007). Thus, imatinib steady state pharmacokinetics has been suggested to rely on enzymes other than CYP3A4 (van Erp *et al.*, 2007). In 2010, an *in vitro* study indicated involvement of CYP2C8 in the main metabolic pathway of imatinib, the formation of the pharmacologically active metabolite N-desmethylimatinib (Nebot *et al.*, 2010). However, the study did not contain quantitative extrapolations of the obtained *in vitro* findings to clinical relevance. In addition, the finding did not mechanistically explain why imatinib is sensitive to CYP3A4 inhibition in the beginning of therapy, but no longer at steady state.

The purpose of this work was to investigate the role of CYP2C8 in the metabolism of montelukast and imatinib to provide explanations to the inconsistencies documented in the literature. For montelukast, we first conducted an *in vitro* metabolism study, followed by an interaction study in humans with gemfibrozil as the CYP2C8 inhibitor drug. In turn, for imatinib, in order to understand the role of CYP2C8 in its metabolism, we first examined its inhibitory effects on CYP3A4 *in vitro*. Then, using an integrated *in vitro*, *in silico*, and *in vivo* approach, we carried out *in vitro* metabolism experiments, physiologically based pharmacokinetic (PBPK) simulations, and an interaction study with gemfibrozil in healthy subjects, to examine the importance of CYP2C8 in its elimination.

REVIEW OF THE LITERATURE

1. Drug-metabolising enzymes and drug transporters

Pharmacokinetics describes the passage of a drug through the body. Following oral administration, a drug usually undergoes several pharmacokinetic processes, including absorption, distribution, and metabolism, before it is excreted from the body. These processes define the relationship between the drug dose and its concentration in the body in relation to time. Because the effect of a drug is usually related to its concentration at the site of action, the pharmacokinetics of a drug will influence its pharmacological response and toxicity (Tozer and Rowland, 2006).

The liver and the intestine are the major sites for drug metabolism. About 70% of clinically used drugs undergo metabolism as their main elimination route (Pelkonen *et al.*, 2008). Typically, these drugs are relatively lipophilic and need to be metabolised to become more hydrophilic so that they are easily excreted from the body (Murray, 1997). In contrast, hydrophilic drugs tend to be excreted unchanged. Drug metabolism is commonly divided into phase I and phase II reactions (Testa and Kramer, 2006), although these reaction types can be overlapping or only one can occur. Phase I enzymes, such as aldehyde dehydrogenases, carboxyl ester hydrolases, CYPs, flavin-containing monooxygenases (FMOs) and numerous others, perform functionalisation reactions that introduce or expose a functional group in the drug molecule. In phase II, enzymes including *N*-acetyltransferases (NATs), glutathione S-transferases (GSTs), uridine-5'-diphosphate glucuronosyltransferases (UGTs) and many others, catalyse conjugation reactions that attach highly hydrophilic moieties to the drug or its phase I metabolite. In addition to its protective detoxification function, metabolism may occasionally lead to the formation of reactive and toxic metabolites (Murray, 1997).

Currently under intensive study, membrane transporters also play an important role in drug exposure. These proteins mediate the transport of endogenous compounds, drugs and other xenobiotics into and out from cells, thus contributing to their distribution and elimination. Although transporters are present with varying abundance in all body tissues, those that are important in pharmacokinetics are mainly expressed in the intestine, kidney, and liver (Figure 1) (Giacomini and Sugiyama, 2011). Together, drug-metabolising enzymes and transporters determine the intracellular and plasma concentrations of numerous drugs, and influence their systemic and site-specific effects and toxicities.

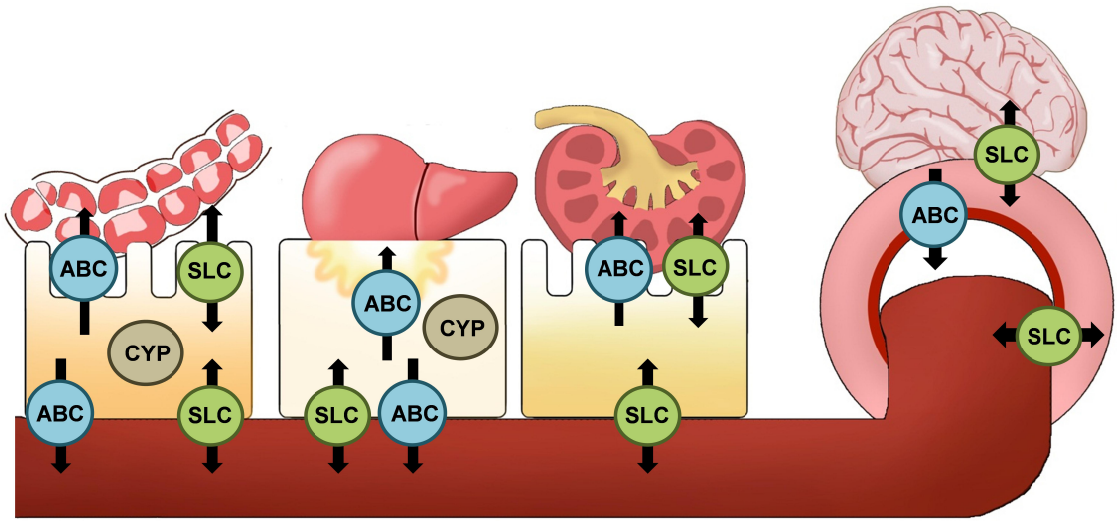

Figure 1. Localisation of CYP enzymes and drug transporters (adapted from Giacomini and Sugiyama (2011)). Drug-metabolising enzymes, including the CYPs, are mainly located in the liver and intestine. Drug transporters important in pharmacokinetics are primarily found in the intestine, liver, and kidney. They can also be found in other organs and tissues, e.g. in the blood-brain barrier. ABC, adenosine triphosphate-binding cassette transporter; CYP, cytochrome P450; SLC, solute carrier transporter.

1.1. Human CYP enzymes

CYP enzymes are a superfamily of important haem-containing proteins that mediate the metabolism of a wide range of endogenous and foreign compounds. CYPs are found throughout nature; in animals, plants, insects, lower eukaryotes, and bacteria (Nelson, 2009). In humans, about a dozen individual CYPs are important in the metabolism of drugs (Pelkonen *et al.*, 2008, Zanger and Schwab, 2013).

Discovery. The CYP enzymes were discovered in the 1950s when it was noted that carbon monoxide inhibited reactions in adrenal and liver microsomes (Conney *et al.*, 1957, Ryan and Engel, 1957). Findings demonstrated that the addition of carbon monoxide to microsomal suspensions containing reduced nicotinamide adenine dinucleotide (NADH) or dithionite resulted in the appearance of a broad absorption peak at 450 nm in the ultraviolet visible spectra (Garfinkel, 1958, Klingenberg, 1958). This carbon monoxide-binding pigment was identified as a haemoprotein, and it was tentatively named "P-450" for "pigment 450"(Omura and Sato, 1962). It soon became evident that this pigment was able to metabolise drugs (Estabrook *et al.*, 1963, Cooper *et al.*, 1965). Initially, this system was thought to be one enzyme, but in the 1970s it was clear that several different CYP enzymes exist. Intensive studies were subsequently undertaken to characterise and isolate the different forms.

Classification. CYP enzymes are divided into families and subfamilies based upon their amino acid sequence similarities. Members of a family share >40% amino acid identity, while subfamily members are >55% identical (Madan *et al.*, 2002). Altogether 18 families and 44

subfamilies of *CYP* genes have been identified in humans (Nelson, 2009). The CYP1, CYP2, and CYP3 families metabolise approximately 75% of clinical drugs that undergo metabolism, while other CYP families are primarily important in the biosynthesis and metabolism of endogenous compounds, such as bile acids, eicosanoids, fatty acids, steroids, and vitamins (Nebert and Russell, 2002, Guengerich, 2008). CYP3A4 is the major drug-metabolising CYP enzyme in the liver and intestine, and is involved in the metabolism of about 50% of clinically used drugs (Pelkonen *et al.*, 2008). Other important drug-metabolising CYP enzymes in the liver include CYP1A2, CYP2A6, CYP2B6, CYP2C8, CYP2C9, CYP2C19, CYP2D6, CYP2E1, and CYP3A5 (Figure 2). In turn, CYP1A1, CYP1B1, and CYP2J2 are mainly expressed extra-hepatically (Zanger and Schwab, 2013).

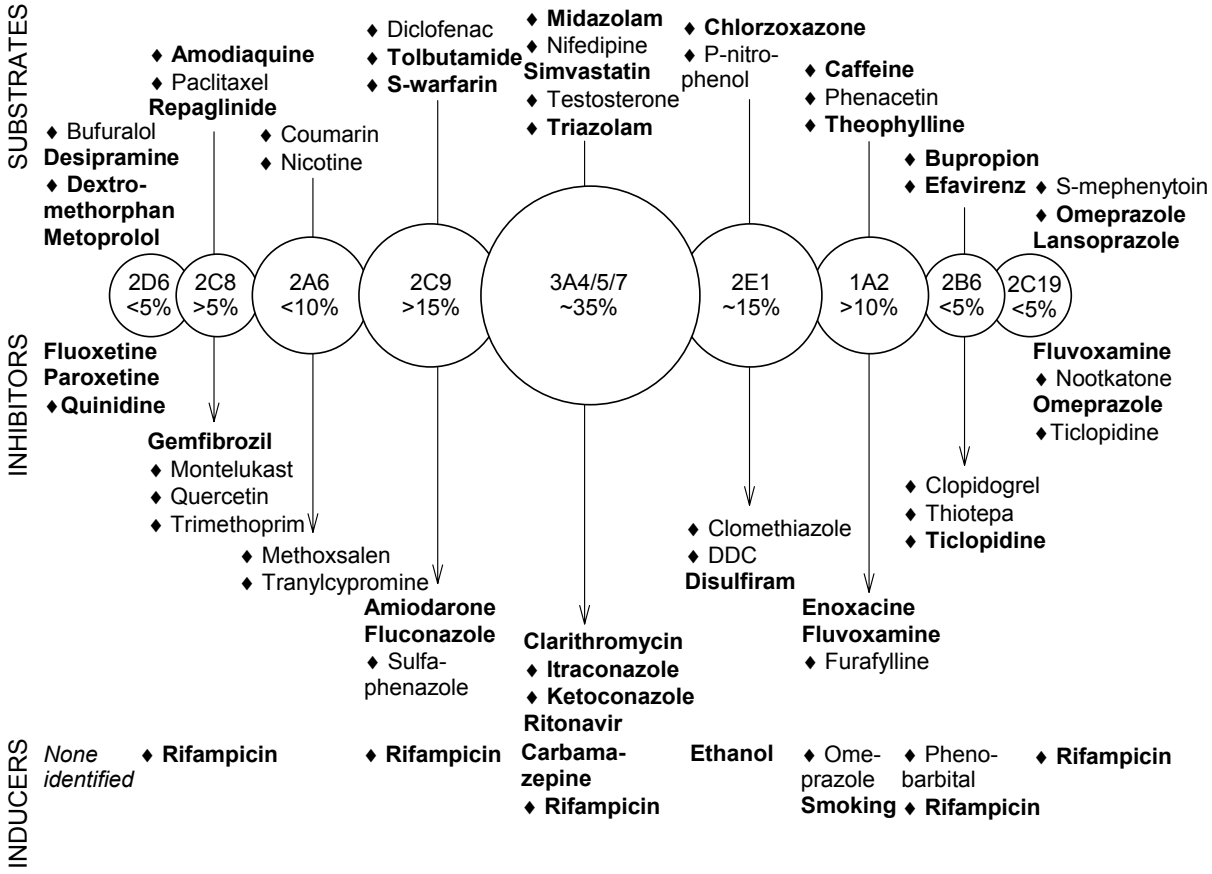

Figure 2. Abundance of drug-metabolising CYP isoforms in the liver (Rostami-Hodjegan and Tucker, 2007, Pelkonen *et al.*, 2008, Achour *et al.*, 2014), and examples of their marker substrates, inhibitors, and inducers (FDA, 2011, EMA, 2013), adapted from Pelkonen *et al.* (2008). Substrates, inhibitors, and inducers recommended for *in vitro* studies are marked with a diamond (♦), and for *in vivo* studies in bold font. The importance of a particular CYP isoform in drug metabolism does not necessarily correspond to its abundance in the liver. DDC, diethyl dithiocarbamate.

Genes. In the human genome, 57 genes encoding CYP enzymes and 58 pseudogenes (defective genes) have been identified (Nelson *et al.*, 2004, Ingelman-Sundberg and Sim, 2010). The *CYP* genes are highly polymorphic (http://www.cypalleles.ki.se). Mutations in *CYP* genes may lead to enzyme variants with higher, lower, or no activity, or to the absence of enzyme. In particular, CYP2A6, CYP2B6, CYP2C8, CYP2C9, CYP2C19, CYP2D6, and CYP3A5 have several polymorphisms, which affect their function. Carriers of variant *CYP* alleles can generally be divided into three major phenotypes: extensive metabolisers (EMs), intermediate metabolisers (IMs), and poor metabolisers (PMs). EMs carry at least one functional allele and exhibit a normal enzyme function. IMs carry one defective allele or two partially defective alleles, while PMs are homozygous for the defective allele, leading to a reduced or no enzyme activity, respectively (Ingelman-Sundberg and Sim, 2010). Moreover, CYP2D6 ultra-rapid metabolisers (UMs) carry multiple functional alleles. In addition to affecting the metabolism of drugs, genetic variants of CYP enzymes may also be a determinant for the extent of drug-drug interactions. For instance, individuals with high activity variants are expected to be more sensitive to CYP inhibition as compared to individuals with low activity variants (Konig *et al.*, 2013).

Expression. The liver and intestine are the most important sites for CYP-mediated metabolism (Pelkonen *et al.*, 2008), but CYPs can be found throughout the body, in particular at interfaces, such as the nasal and lung epithelia, and skin. In the cells, drug-metabolising CYP enzymes are mainly located in the endoplasmic reticulum with their active sites exposed at the cytosolic side of the membrane (Edwards *et al.*, 1991, Lin and Lu, 2001, Cribb *et al.*, 2005). The expression levels of CYP enzymes vary considerably between individuals and populations (Shimada *et al.*, 1994). Important sources for inter-individual variability in CYP concentrations and activities include genetic polymorphisms, epigenetics, and other internal and external factors such as age, disease, environmental chemicals, medication, nutrition, and sex (Meyer, 1996, Zanger and Schwab, 2013).

Reaction. The CYP enzymes are haem-thiolate proteins, containing well-conserved helices (A-L) and folds. The I and L helices are associated with the haem (iron protoporphyrin IX) (Guengerich, 2001). In the resting state of the enzyme, the haem iron is in ferric state (Fe^{3+}) and bound to water. When reduced to ferrous state (Fe^{2+}), it can bind ligands such as oxygen and carbon monoxide.

CYPs mainly catalyse oxidative reactions, such as carbon hydroxylation, heteroatom oxygenation, dealkylation, and epoxidation (Lin and Lu, 1998, Guengerich, 2001). For example, CYP-mediated hydroxylation plays an important role in the synthesis of cholesterol and in its further metabolism to steroid hormones and bile salts. CYPs are called mixed function oxidases or monooxygenases because they incorporate one atom of molecular oxygen into substrate and the other one is reduced to water (Scheme 1).

$$RH + O_2 + NADPH + H^+ \rightarrow ROH + H_2O + NADP^+$$ (Scheme 1.)

For their activity, CYPs need to be integrated into a membrane that contains CYP oxidoreductase (POR) and, for some reactions, cytochrome b5. The CYP catalytic cycle consists of at least seven steps: 1) binding of substrate to the ferric form of the CYP, 2) reduction of the haem iron from ferric to ferrous state by an electron donated by nicotinamide adenine dinucleotide phosphate (NADPH) via POR, 3) binding of oxygen, 4) transfer of a second electron from POR and/or cytochrome b5, 5) cleavage of the O-O bond, 6) substrate oxygenation, and 7) product release and return of the enzyme to its resisting state (Lin and Lu, 1998, Guengerich, 2001). If carbon monoxide binds to the ferrous iron, the catalytic cycle is interrupted. This reaction yields the classic CO difference spectrum with a maximum at 450 nm.

Most CYP oxidation reactions follow traditional Michaelis-Menten kinetics according to Scheme 2 and Equation 1:

$$E + S \rightleftharpoons E \times S \longrightarrow E + P \qquad \text{(Scheme 2.)}$$

where E represents the enzyme, S the substrate, E×S the enzyme-substrate complex, and P is the product. Under steady state conditions, Equation 1 can describe the reaction (Korzekwa, 2002):

$$v = \frac{V_{max} \times [S]}{K_m + [S]} \qquad \text{(Equation 1.)}$$

where v represents the reaction velocity, V_{max} is the reaction velocity at saturating substrate concentrations, [S] is the substrate concentration, and K_m is the Michaelis-Menten constant. This constant describes the concentration of substrate giving half maximal velocity, and is a useful descriptor of the binding affinity of the substrate for the enzyme.

Some CYP reactions, however, show unusual enzyme kinetics, including activation, autoactivation, partial inhibition, biphasic saturation, and substrate inhibition (Korzekwa, 2002). Although these reactions have been described for most CYPs, they have primarily been associated with CYP3A4 (Tracy, 2006).

CYP2C subfamily. Members of the human CYP2C subfamily include CYP2C8, CYP2C9, CYP2C18, and CYP2C19. Together, these enzymes metabolise about 20-30% of clinical drugs, and account for almost 30% of the total hepatic CYP amount (Totah and Rettie, 2005, Rostami-Hodjegan and Tucker, 2007, Lai *et al.*, 2009, Zanger and Schwab, 2013, Achour *et al.*, 2014). The *CYP2C* genes are located on chromosome 10q24 arranged as centromere-*CYP2C18*-*CYP2C19*-*CYP2C9*-*CYP2C8*-telomere (Gray *et al.*, 1995). *CYP2C8* (31 kilobases, nine exons) is the smallest of the human *CYP2C* genes (Klose *et al.*, 1999). Although the CYP2C isoforms show high amino acid identity (>77%), they exhibit variation in their protein

expression and substrate specificities (Klose *et al.*, 1999, Totah and Rettie, 2005, Niwa and Yamazaki, 2012). CYP2C8, CYP2C9, and CYP2C19 are primarily located in the liver. Even though it has high messenger ribonucleic acid (mRNA) levels in hepatocytes, CYP2C18 is poorly translated into protein (Zanger and Schwab, 2013), and is, in contrast to the other CYP2C isoforms, not inducible (Gerbal-Chaloin *et al.*, 2001, Rae *et al.*, 2001). CYP2C9 is considered to be the most important isoform of the subfamily due to its high liver expression and participation in the metabolism of several important drugs such as S-warfarin, phenytoin, and non-steroidal anti-inflammatory drugs (NSAIDs). Similarly, CYP2C19 metabolises several drug classes, including antidepressants, benzodiazepine, and proton pump inhibitors. The substrates of CYP2C9 and CYP2C19 tend to be mildly acidic and mildly basic, respectively (Totah and Rettie, 2005). CYP2C8 differs from the CYP2C9 and CYP2C19 due to its substrate specificity and large active site cavity.

1.1.1. CYP2C8

Although CYP2C8 was early known to metabolise arachidonic acid, carbamazepine, retinol, and retinoic acid (Leo *et al.*, 1989, Kerr *et al.*, 1994, Rifkind *et al.*, 1995), its importance as a drug-metabolising enzyme was undervalued for some time. Over the last 15 years, CYP2C8 has gradually gained increased attention as clinically relevant CYP2C8 substrates and inhibitors have been identified, functional *CYP2C8* single nucleotide polymorphisms (SNPs) have been characterised, and its crystal structure has been resolved. Following a pharmacokinetic interaction between gemfibrozil and cerivastatin that resulted in rhabdomyolysis cases, the role of CYP2C8 was recognised by drug regulatory authorities (Backman *et al.*, 2002, Chang *et al.*, 2004, Huang *et al.*, 2008).

Expression and regulation. CYP2C8 is primarily expressed in the liver, where it is expressed at 22-30 pmol/mg microsomal protein, thus accounting for about 6-7% of the total hepatic CYP content (Rowland Yeo *et al.*, 2004, Rostami-Hodjegan and Tucker, 2007, Kawakami *et al.*, 2011, Ohtsuki *et al.*, 2012, Achour *et al.*, 2014). CYP2C8 mRNA has been detected in several extrahepatic tissues (Zeldin *et al.*, 1995, McFayden *et al.*, 1998, Klose *et al.*, 1999, Thum and Borlak, 2000, Nishimura *et al.*, 2003), but immunochemistry has detected extrahepatic CYP2C8 protein only in kidney and adrenal cortical cells, heart, salivary ducts, intestine, and tonsils (Enayetallah *et al.*, 2004, Delozier *et al.*, 2007). In the liver, the protein expression of CYP2C8 is correlated with CYP3A4 > CYP2D6 > CYP2C9 > CYP2C19 (Naraharisetti *et al.*, 2010, Achour *et al.*, 2014). Induction studies suggest that CYP2C8 is regulated by several nuclear receptors, including the pregnane X receptor (PXR), the constitutive androstane receptor (CAR), the glucocorticoid receptor (GR), and the vitamin D receptor (VDR) (Gerbal-Chaloin *et al.*, 2001, Ferguson *et al.*, 2005, Chen and Goldstein, 2009). The *in vivo* turn-over half-life of hepatic CYP2C8 protein has been estimated to 22 h (Backman *et al.*, 2009). Following induction or mechanism-based inhibition, the half-life of

the CYP determines the time required for complete recovery of the enzymatic activity (Yang *et al.*, 2008). In comparison, CYP1A2, CYP2D6, CYP2E1, and CYP3A4 have estimated *in vivo* half-lives of 36-100 h (Obach *et al.*, 2007, Yang *et al.*, 2008, Grimm *et al.*, 2009).

Structure. In 2004, the first paper reporting determination of the structure of CYP2C8 by X-ray crystallography was published (Schoch *et al.*, 2004). The molecular weight of CYP2C8 approximated to 54 kDa, and one single crystal diffracted to 2.7 Å. CYP2C8 crystallised as a symmetric dimer, formed by extensive interaction between the F, F', G, and G' helices. Later, it has been shown that CYP2C8 exists as a dimer also in natural membranes (Hu *et al.*, 2010). As compared to other CYP isoforms, CYP2C8 has a large active site cavity (1438 $Å^3$) (Schoch *et al.*, 2004), which is consistent with its ability to metabolise large substrates, such as cerivastatin and paclitaxel (Lai *et al.*, 2009). The topology of the active site is trifurcated, resembling a T or Y shape (Schoch *et al.*, 2008). In comparison, the active site cavity of CYP3A4 is more uniformly distributed, but its volume (1386 $Å^3$) is similar to that of CYP2C8 (Yano *et al.*, 2004). These findings likely explain why CYP2C8 and CYP3A4 often have common substrates but yield different metabolite profiles. In fact, CYP2C8 has more substrates in common with CYP3A4 than with CYP2C9 (Totah and Rettie, 2005).

Substrates, inhibitors, and inducers. CYP2C8 metabolises about 5-8% of drugs that undergo metabolism (Zanger *et al.*, 2008, Lai *et al.*, 2009, Zanger and Schwab, 2013). Due to its large, sinuous active site, CYP2C8 can accommodate substrates of different sizes and structures. Its substrates do not share any common structures or chemical patterns, but many of them are large organic anions at physiological pH with oxidation sites located ~13 Å from the anionic group (Melet *et al.*, 2004). CYP2C8 metabolises drugs from several different therapeutic classes; typical CYP2C8 substrates include antimalarial agents, glitazone antidiabetic drugs, NSAIDs, opioids, and statins (Table 1). In addition, CYP2C8 is involved in the metabolism of several members of the new protein kinase inhibitor drug class, such as dabrafenib, erlotinib, pazopanib, and ponatinib. Amodiaquine N-deethylation, paclitaxel 6α-hydroxylation, and rosiglitazone para-hydroxylation are recommended *in vitro* marker reactions of CYP2C8 activity, and amodiaquine, repaglinide, and rosiglitazone are suitable *in vivo* CYP2C8 probe drugs, according to regulatory authorities (FDA, 2011, EMA, 2013). Except for metabolism of drugs, CYP2C8 is also involved in the metabolism of endogenous compounds such as arachidonic acid and retinoids (Zeldin *et al.*, 1995, Nadin and Murray, 1999).

Several reversible and irreversible CYP2C8 inhibitors have been identified in the literature (Table 2). Montelukast, quercetin, and trimethoprim are recommended as selective CYP2C8 inhibitors for *in vitro* studies (FDA, 2011, EMA, 2013). Unusually, two phase II glucuronide metabolites, gemfibrozil 1-*O*-β glucuronide and clopidogrel acyl 1-β-D-glucuronide, affect CYP2C8 by strong mechanism-based inhibition (Backman *et al.*, 2002, Ogilvie *et al.*, 2006, Tornio *et al.*, 2014). Gemfibrozil has increased the plasma exposure to many CYP2C8

substrates several-fold *in vivo* (Backman *et al.*, 2002, Niemi *et al.*, 2003a, Niemi *et al.*, 2003b, Jaakkola *et al.*, 2005, Tornio *et al.*, 2008, Backman *et al.*, 2009, Honkalammi *et al.*, 2012, Aquilante *et al.*, 2013a), and is recommended as a CYP2C8 inhibitor drug in clinical drug-drug interaction studies (FDA, 2011, EMA, 2013).

CYP2C8 is the most inducible member of the CYP2C subfamily (Gerbal-Chaloin *et al.*, 2001, Feidt *et al.*, 2010). Typical inducers such as dexamethasone, phenobarbital, and rifampicin have increased its mRNA and protein expression several-fold in hepatocytes (Gerbal-Chaloin *et al.*, 2001, Rae *et al.*, 2001, Raucy *et al.*, 2002, Madan *et al.*, 2003). *In vivo*, rifampicin has reduced the plasma exposure to several CYP2C8 substrates (Niemi *et al.*, 2000, Niemi *et al.*, 2004, Park *et al.*, 2004, Jaakkola *et al.*, 2006a), and it is the preferred CYP2C8 inducer for use both in *in vitro* and clinical studies (FDA, 2011, EMA, 2013).

Table 1. Examples of CYP2C8 substrate drugs (adapted from (Lai *et al.*, 2009)).

Drug	Therapeutic use	References
Amiodarone	Antiarrhythmic	(Ohyama *et al.*, 2000)
Amodiaquine	Antimalarial (histamine N-methyltransferase inhibitor)	(Li *et al.*, 2002)
Buprenorphine	Analgesic (opioid)	(Picard *et al.*, 2005)
Cerivastatin	Hypolipidemic (HMG-CoA reductase inhibitor)	(Wang *et al.*, 2002)
Chloroquine	Antimalarial (histamine N-methyltransferase inhibitor)	(Kim *et al.*, 2003)
Dabrafenib	Anticancer (BRAF inhibitor)	(Lawrence *et al.*, 2014)
Enzalutamide	Anticancer (androgen receptor antagonist)	(Xtandi Clinical Pharmacology and Biopharmaceutic Review(s), 2012)
R-ibuprofen	Analgesic, anti-inflammatory (NSAID)	(Hamman *et al.*, 1997)
Loperamide	Antidiarrheal (opioid)	(Kim *et al.*, 2004)
Paclitaxel	Anticancer (mitotic inhibitor)	(Rahman *et al.*, 1994)
Pioglitazone	Antidiabetic (PPARγ agonist)	(Jaakkola *et al.*, 2006c)
Repaglinide	Antidiabetic drug (insulin secretagogue)	(Bidstrup *et al.*, 2003, Kajosaari *et al.*, 2005a)
Rosiglitazone	Antidiabetic drug (PPARγ agonist)	(Baldwin *et al.*, 1999)
Simvastatin acid	Active metabolite of simvastatin; hypolipidemic (HMG-CoA reductase inhibitor)	(Prueksaritanont *et al.*, 2003)
Tazarotenic acid	Active metabolite of tazaratone; antipsoriatic, antiacne	(Attar *et al.*, 2003)
Troglitazone	Antidiabetic drug (PPARγ agonist)	(Yamazaki *et al.*, 1999)
Zopiclone	Sedative	(Becquemont *et al.*, 1999)

HMG-CoA, 3-hydroxy-3-methyl-glutaryl-coenzyme A; NSAID, non-steroidal anti-inflammatory drug; PPARγ, peroxisome proliferator activated receptor gamma.

Table 2. Examples of CYP2C8 inhibitor drugs and their effects on CYP2C8 activity in HLM.

Inhibitor	Mode of inhibition	Effect on CYP2C8*	References
Amiodarone	Irreversible or quasi-irreversible (MBI)	K_I = 51 μM k_{inact} = 0.029 1/min	(Polasek *et al.*, 2004)
Clopidogrel acyl 1-β-D-glucuronide	Irreversible or quasi-irreversible (MBI)	IC_{50} = 56.4 μM IC_{50} = 12.0 μM** K_I = 9.9 μM k_{inact} = 0.047 1/min	(Tornio *et al.*, 2014)
Clotrimazole	Reversible	IC_{50} = 0.78 μM	(Walsky *et al.*, 2005a)
Felodipine	Reversible	IC_{50} = 1.2 μM	(Walsky *et al.*, 2005a)
Gemfibrozil	Reversible (competitive)	IC_{50} = 91-120 μM K_i = 75-76 μM	(Wang *et al.*, 2002, Ogilvie *et al.*, 2006)
Gemfibrozil 1-*O*-β glucuronide	Irreversible (MBI)	IC_{50} = 24 μM IC_{50} = 1.8 μM** K_I =20-52 μM k_{inact} = 0.21 1/min	(Ogilvie *et al.*, 2006)
Ketoconazole	Reversible (non-competitive)	K_i = 11.8 μM	(Bun *et al.*, 2003)
Lovastatin	Reversible	IC_{50} = 15 μM K_i = 8.4 μM	(Tornio *et al.*, 2005)
Montelukast	Reversible (competitive)	IC_{50} = 0.020-2.0 μM K_i = 0.014-0.15 μM	(Walsky *et al.*, 2005a, Walsky *et al.*, 2005b)
Nilotinib	Reversible (competitive)	IC_{50} = 0.4-0.7 μM K_i = 0.10-0.90 μM	(Kim *et al.*, 2013b, Wang *et al.*, 2014)
Phenelzine	Irreversible or quasi-irreversible (MBI)	K_I = 54 μM k_{inact} = 0.17 1/min	(Polasek *et al.*, 2004)
Pioglitazone	Reversible (competitive)	IC_{50} = 9.4 μM K_i = 1.7 μM	(Sahi *et al.*, 2003)
Quercetin	Reversible (competitive)	IC_{50} = 3.1-8.4 μM K_i = 3.1-10.1 μM	(Bun *et al.*, 2003, Walsky and Obach, 2004)
Rosiglitazone	Reversible (competitive)	IC_{50} = 9.6 μM K_i = 5.6 μM	(Sahi *et al.*, 2003)
Trimethoprim	Reversible (competitive)	IC_{50} = 54 μM K_i = 32 μM	(Wen *et al.*, 2002)
Troglitazone	Reversible (competitive)	IC_{50} = 2.3-20 μM K_i = 2.6 μM	(Yamazaki *et al.*, 2000, Sahi *et al.*, 2003)
Vilazodone	Reversible (competitive)	IC_{50} = 1.8 μM K_i = 0.46 μM	(Viibryd Clinical Pharmacology and Biopharmaceutics Review(s), 2010)
Zafirlukast	Reversible	IC_{50} = 0.39 μM	(Walsky *et al.*, 2005a)

* Inhibitory effect on amodiaquine N-deethylation or paclitaxel 6α-hydroxylation in HLM. ** IC_{50} after a 30-min pre-incubation of inhibitor with NADPH in HLM. CYP, cytochrome P450; HLM, human liver microsomes; IC_{50}, inhibitor concentration producing 50% inhibition; K_i, reversible inhibition constant; K_I, inhibitor concentration supporting half of the maximal rate of inactivation; k_{inact}, maximal rate of inactivation; MBI, mechanism-based inhibitor.

Polymorphisms. More than 450 *CYP2C8* SNPs have been identified (Lai *et al.*, 2009). Some of these SNPs have been associated with variability in CYP2C8-mediated metabolism and changed drug response. To date, 16 *CYP2C8* alleles have been identified and named *CYP2C8*1A* (wild type) to *CYP2C8*14* (http://www.cypalleles.ki.se). Due to discrepancies between *in vitro* and *in vivo* data, and substrate-dependent functional effects, however, the polymorphic *CYP2C8* alleles have not been assigned an activity level or phenotype.

Except for rare variants with no (*CYP2C8*5*, *CYP2C8*7*, *CYP2C8*11*), reduced (*CYP2C8*8*, *CYP2C8*14*), unchanged (*CYP2C8*6*, *CYP2C8*9*, *CYP2C8*10*, *CYP2C8*13*) or unknown activity (*CYP2C8*12*), *CYP2C8*2*, *CYP2C8*3*, and *CYP2C8*4* are common and have possibly clinical relevance (http://www.cypalleles.ki.se) (Dai *et al.*, 2001, Bahadur *et al.*, 2002, Aquilante *et al.*, 2013b, Zanger and Schwab, 2013). As compared to *CYP2C8*1*, *CYP2C8*2* (c.805A>T, rs11572103) has been associated with reduced enzyme activity *in vitro* and *in vivo* (Dai *et al.*, 2001, Parikh *et al.*, 2007, Gao *et al.*, 2010, Aquilante *et al.*, 2013c, Yu *et al.*, 2013). The *CYP2C8*2* allele is rare in Caucasians and Asians (<3%), but common in Africans with a frequency of ~20% (Dai *et al.*, 2001, Parikh *et al.*, 2007, Kudzi *et al.*, 2009, Pechandova *et al.*, 2012, Wu *et al.*, 2013).

The available evidence for the activity of *CYP2C8*3* (c.416G>A, rs11572080 and c.1196A>G, rs10509681) is conflicting (Aquilante *et al.*, 2013b). For instance, as compared to CYP2C8.1, CYP2C8.3 has exhibited reduced activity for the metabolism of amodiaquine, arachidonic acid, and paclitaxel, while amiodarone concentrations were not affected by this polymorphism *in vitro* (Dai *et al.*, 2001, Soyama *et al.*, 2001, Bahadur *et al.*, 2002, Soyama *et al.*, 2002, Parikh *et al.*, 2007). For cerivastatin, pioglitazone, and repaglinide, however, *CYP2C8*3* has been associated with an increased *in vitro* metabolism (Muschler *et al.*, 2009, Kaspera *et al.*, 2010, Yu *et al.*, 2013). In clinical studies, this allele has been associated with unchanged and decreased plasma concentrations of paclitaxel, repaglinide, and rosiglitazone (Niemi *et al.*, 2003c, Henningsson *et al.*, 2005, Niemi *et al.*, 2005b, Bidstrup *et al.*, 2006, Kirchheiner *et al.*, 2006, Stage *et al.*, 2013). The *CYP2C8*3* allele is relatively common in Caucasians (frequency of 7-23%), but rare in Africans and Asians (Dai *et al.*, 2001, Bahadur *et al.*, 2002, Nakajima *et al.*, 2003, Halling *et al.*, 2005, Parikh *et al.*, 2007, Kudzi *et al.*, 2009, Pedersen *et al.*, 2010, Pechandova *et al.*, 2012, Wu *et al.*, 2013). There is a strong partial linkage disequilibrium between *CYP2C8*3* and *CYP2C9*2*, a reduced function allele of CYP2C9 (Bahadur *et al.*, 2002, Alessandrini *et al.*, 2013, Aquilante *et al.*, 2013b); more than 95% of *CYP2C8*3* allele carriers have also been reported to be carriers of *CYP2C9*2* (Yasar et al., 2002).

*CYP2C8*4* (c.792C>G, rs1058930) has a frequency of ~7% in Caucasians (Bahadur *et al.*, 2002, Totah and Rettie, 2005, Daily and Aquilante, 2009, Pechandova *et al.*, 2012) but is uncommon or absent in Africans and Asians (Kudzi *et al.*, 2009, Wu *et al.*, 2013). It has been associated with reduced or unchanged *in vitro* enzyme activity (Bahadur *et al.*, 2002,

Rodriguez-Antona *et al.*, 2008, Singh *et al.*, 2008, Smith *et al.*, 2008, Gao *et al.*, 2010, Jiang *et al.*, 2011, Yu *et al.*, 2013). The *in vivo* effect of CYP2C8.4 is unclear because the number of subjects carrying this variant in pharmacogenetic studies has been low.

1.1.2. CYP3A4

CYP3A4 is the most important CYP enzyme. Its expression level in the liver is approximately 58-146 pmol/mg microsomal protein (Shimada *et al.*, 1994, Lin *et al.*, 2002, Westlind-Johnsson *et al.*, 2003, Wolbold *et al.*, 2003, Kawakami *et al.*, 2011, Ohtsuki *et al.*, 2012), and its population variability is very high (Zanger and Schwab, 2013). A recent estimate of its liver expression is 93 pmol/mg (Achour *et al.*, 2014), thus suggesting that CYP3A4 constitutes for about 30% of the total hepatic CYP amount. CYP3A4 is also the main CYP enzyme expressed in the intestine, where it significantly contributes to the first-pass elimination of orally administered drugs (Pelkonen *et al.*, 2008).

CYP3A4 is involved in the metabolism of about 50% of clinically used drugs (Pelkonen *et al.*, 2008). Its activate site is large and flexible, allowing it to accommodate many structurally different substrates. It is also able to bind and metabolise multiple substrates simultaneously (Williams *et al.*, 2004). Typical CYP3A4 marker substrate drugs include midazolam, simvastatin, and testosterone, while ketoconazole, itraconazole, and ritonavir are examples of strong CYP3A4 inhibitors (Figure 2) (FDA, 2011, EMA, 2013). Rifampicin and St John's Wort are CYP3A4 inducers recommended for use in interaction studies.

More than 40 *CYP3A4* variant alleles have been identified (http://www.cypalleles.ki.se), but few of them appear to have clinical significance. *CYP3A4*22* (15389C>T, rs35599367) has been associated with reduced CYP3A4 activity. In a clinical study, patients who were carriers of the T allele required 1.7-five-fold reduced statin doses, as compared to non-T carriers (Wang *et al.*, 2011). Furthermore, *CYP3A4*22* has been associated with decreased 2-OH-atorvastatin/atorvastatin AUC ratio and with simvastatin lipid-lowering response in other studies (Elens *et al.*, 2011, Klein *et al.*, 2012). In turn, *CYP3A4*18A* (20070T>C, rs28371759) has been suggested to result from a gain-of-function mutation (Kang *et al.*, 2009), and has been associated with low bone mass.

1.2. Drug transporters

Drugs cross cell membranes via passive diffusion, facilitated diffusion, and active transport (Giacomini and Sugiyama, 2011). Evidence suggests that involvement of transport proteins in the transport of drugs across biological barriers may be more the rule than the exception (Dobson and Kell, 2008). Drug transporters are involved in both pharmacodynamic and pharmacokinetic processes of drugs. Those important in pharmacokinetics are primarily

located in the intestinal, renal, and hepatic epithelia, where they selectively mediate drug absorption and disposition (Figure 1) (Giacomini and Sugiyama, 2011). They work together with drug-metabolising enzymes to eliminate drugs and their metabolites. Based on their function, drug transporters can be divided into uptake and efflux transporters (Konig *et al.*, 2013). All uptake transporters belong to the solute carrier (SLC) superfamily, while most efflux transporters are members of the adenosine triphosphate (ATP)-binding cassette (ABC) superfamily (Konig *et al.*, 2013). Except for mediating tissue-specific drug distribution, transporters may also serve as protective barriers to organs and cells. For example, in the blood-brain barrier, the efflux transporter P-glycoprotein (P-gp) protects the central nervous system from a variety of compounds. On the other hand, drug transporters may also play critical roles in drug resistance, e.g. overexpression of P-gp in tumour cells may result in resistance due to increased efflux of anticancer drugs (Giacomini and Sugiyama, 2011).

SLC superfamily. SLC transporters mediate either drug entry into or drug efflux out from cells (Giacomini and Sugiyama, 2011). They transport their substrates across membranes through numerous mechanisms, including facilitated diffusion, ion coupling, or ion exchange (Hediger *et al.*, 2004, Giacomini and Sugiyama, 2011). Altogether 55 SLC families with more than 350 transporter coding genes have been identified in the human genome (Hediger *et al.*, 2004, He *et al.*, 2009). Examples of SLC transporters include the OATPs, organic anion transporters (OATs), organic cation transporters (OCTs), multidrug and toxic compound extrusion transporters (MATE), novel organic cation/carnitine transporters (OCTNs), and peptide transporters (PEPTs). OATPs primarily mediate the uptake of amphipathic compounds. Their substrates include endogenous substances such as bile salts, steroid conjugates, thyroid hormones, and drugs such as statins. OATP1B1, highly expressed on the sinusoidal membrane of hepatocytes, is known to mediate uptake of statins into the liver (Niemi *et al.*, 2011), where they exert their pharmacological effect.

ABC superfamily. ABC transporters mediate unidirectional efflux of solutes across membranes. They limit the entry of drugs into tissues or enhance their removal from tissues. ABC transporters are primary active transporters that couple with ATP hydrolysis, and often work against high concentration gradients. The 49 genes that have been identified as ABC transporters are grouped into seven families (ABCA to ABCG) (Giacomini and Sugiyama, 2011). Important ABC transporters include P-glycoprotein (P-gp, ABCB1, multidrug resistance protein 1, MDR1), the bile salt export pump (BSEP, ABCB11), the multi-drug resistance-associated protein family (MRP; ABCC1-ABCC6), and the breast cancer resistance protein (BCRP, ABCG2). P-gp is the most studied efflux transporter and it has a wide range of substrates, many of which also are substrates of CYP3A4 (Konig *et al.*, 2013). In the intestine, P-gp and CYP3A4 reduce the absorption of many drugs and other xenobiotics, thereby functioning as an initial protective barrier, preventing foreign compounds from reaching the systemic circulation (Zhang and Benet, 2001).

Transporter polymorphisms. Similarly, as for CYP enzymes, genetic polymorphisms in transporter genes may cause marked variability in drug concentrations and response. Numerous polymorphisms have been identified, but the best characterised functionally relevant polymorphisms to date are *OATP1B1* c.521T>C (rs4149056) and *ABCG2* c.421C>A (rs2231142) (Giacomini *et al.*, 2013). *SLCO1B1* c.521T>C causes an amino acid change in the transport protein (Tirona *et al.*, 2001), resulting in a significantly impaired transport activity both *in vitro* and *in vivo*. Clinically, c.521T>C is associated with increased plasma exposure to several statins (Pasanen *et al.*, 2006, Niemi *et al.*, 2011). Because myopathy is a concentration-dependent adverse reaction to statins, this SNP may increase the risk of simvastatin-induced myopathy (Link *et al.*, 2008). Also *ABCG2* c.421C>A is associated with impaired transport activity *in vitro* (Furukawa et al., 2009), and it has been linked to increased plasma concentrations of its substrate drugs, such as gefitinib, rosuvastatin, and sunitinib (Cusatis *et al.*, 2006, Zhang *et al.*, 2006b, Keskitalo *et al.*, 2009, Mizuno *et al.*, 2010, Tomlinson *et al.*, 2010).

2. Pharmacokinetic drug interactions

Drug-drug interactions occur when one drug alters the pharmacokinetics and/or pharmacological effect of another drug. Usually, co-administration of two drugs does not result in undesired pharmacokinetic or pharmacodynamic alterations. However, if a kinetic interaction is evident, its clinical relevance depends on whether the variation in the plasma and/or tissue exposure to the affected drug is large enough to produce a clinically important change in its effect and/or toxicity (Tozer and Rowland, 2006). Drug-drug interactions can have serious clinical consequences in terms of lack of therapeutic effect, severe adverse reactions, and even fatalities (EMA, 2013). Interactions have resulted in early termination of drug development, refusal of approval, prescribing restrictions, and withdrawals of drugs from the market (Zhang *et al.*, 2006a).

Pharmacokinetic interactions can originate from any of the pharmacokinetic processes of a drug; from its absorption, distribution, metabolism, or elimination (Tozer and Rowland, 2006). Metabolism-based interactions are generally due to inhibition or induction of CYP enzymes. Similarly, inhibition and induction of drug transporters may also result in interactions. The interaction outcome largely depends on three key factors; the perpetrator drug (e.g. interaction mechanism, potency, dose), the affected drug (e.g. importance of the affected enzyme/transporter in its pharmacokinetics, presence of alternative elimination routes, therapeutic window), and the patient (e.g. age, disease, concomitant medications, genetics), in addition to the site of interaction.

The therapeutic window of a drug defines the concentration range where the benefit/risk ratio of a drug is optimal; the effect will be small below this range, while the risk for toxicity

increases at concentrations above the window. A drug with a narrow therapeutic window is thus sensitive to changes in its concentrations. The therapeutic window of a drug can be quantified by the therapeutic index, which is classically defined according to Equation 2:

$$Therapeutic\ index = \frac{TD_{50}}{ED_{50}} \qquad \text{(Equation 2.)}$$

where TD_{50} is the dose that causes a toxic response in 50% of subjects, while ED_{50} is the dose that causes a pharmacological response in 50% of subjects (Baca and Golan, 2012). However, as there may be marked inter-individual variability in drug concentration levels at the same dose, the therapeutic index (or safety margin) is nowadays primarily based on drug exposure rather than dose (Muller and Milton, 2012). It is thus regarded as the ratio of the highest exposure to the drug that causes no toxicity to the exposure that produces the desired response. Accordingly, a high therapeutic index will represent a large therapeutic window.

2.1. Inhibition of drug-metabolising enzymes

Inhibition of CYP enzymes is the most important cause of harmful drug-drug interactions (Pelkonen *et al.*, 2008). Pharmacokinetically, CYP inhibition may lead to increased bioavailability and decreased clearance of drugs that depend on these enzymes for their elimination. For pro-drugs, CYP inhibition may reduce the formation of their pharmacologically active species. CYP inhibition may thus result in both an increased and reduced therapeutic effect as well as increased toxicity. Based on the effect on the inhibited enzyme, CYP inhibition mechanisms are generally divided into reversible, quasi-irreversible, and irreversible inhibition.

2.1.1 Reversible inhibition

Direct, reversible inhibition occurs when a parent drug inhibits CYPs without requiring metabolism (Madan *et al.*, 2002). The binding of direct inhibitors to the enzymes is usually weak; bonds are formed and broken down easily (Pelkonen *et al.*, 2008). Thus, the onset and offset of inhibition are rapid, and inhibition does not result in a long-term inactivation of the enzyme. Direct, reversible inhibition can further be divided into three subtypes: competitive, non-competitive, and uncompetitive inhibition. Competitive inhibition is the most common inhibition mechanism and occurs when the substrate and inhibitor compete for binding to the active site of the enzyme (Korzekwa, 2002, Madan *et al.*, 2002). Thus, a competitive inhibitor will increase the K_m of the substrate (Table 3). In non-competitive inhibition, the inhibitor binds to another site than the substrate, which causes conformational changes of the enzyme. The alterations do not affect the binding of the substrate but the enzymatic reaction is inhibited; hence the K_m of the substrate is unaffected, while its V_{max} is decreased.

Uncompetitive inhibitors bind directly to the enzyme-substrate complex, and inhibit it, leading to a reduction of both V_{max} and K_m. Thus, competitive and non-competitive CYP inhibition will result in a decrease in the intrinsic clearance (V_{max}/K_m) of the substrate, while uncompetitive inhibitors have minimal effect on the intrinsic clearance at low substrate concentrations (Lin and Lu, 1998, Obach, 2008). In addition to the above mechanisms, mixed inhibition is often observed; herein both competitive and non-competitive inhibition occur (Table 3) (Madan *et al.*, 2002, Pelkonen *et al.*, 2008).

The kinetics and affinity with which a reversible inhibitor binds to the CYP enzyme can be defined by its inhibition constant K_i. This constant describes the dissociation of the enzyme-inhibitor complex. Modifications of the Michaelis-Menten equation can be used to calculate the K_i value and for graphical determination of the inhibition mechanism, according to Equations 3, 4, 5, and 6 for competitive, non-competitive, uncompetitive, and mixed inhibition (Table 3), respectively.

Table 3. Direct, reversible inhibition mechanisms (Fowler and Zhang, 2008).

Inhibition mechanism	Equation		Change in substrate		
			V_{max}	K_m	V_{max}/K_m
Competitive	$v = \frac{V_{max} \times [S]}{K_m \times (1 + [I]/K_i) + [S]}$	(Equation 3.)	-	↑	↓
Non-competitive	$v = \frac{V_{max} \times [S]}{K_m \times (1 + [I]/K_i) + [S] \times (1 + [I]/K_i)}$	(Equation 4.)	↓	-	↓
Uncompetitive	$v = \frac{V_{max} \times [S]}{K_m + (1 + [I]/K_i) \times [S]}$	(Equation 5.)	↓	↓	-
Mixed	$v = \frac{V_{max} \times [S]}{K_m \times (1 + [I]/K_i) + [S] \times (1 + [I]/K_i')}$	(Equation 6.)	↓	↑↓	-↓

[I], inhibitor concentration; K_i, reversible inhibition constant; K_I, inhibitor concentration supporting half of the maximal rate of inactivation; K_m, Michaelis-Menten constant; [S], substrate concentration; v, reaction rate; V_{max}, maximum velocity.

Other reversible inhibitors include slow- and tight-binding inhibitors. These inhibitors typically bind to and/or dissociate from the target enzyme slowly (Copeland, 2005), which leads to a time-dependence for the onset of inhibition. Inhibition by slow- and tight-binding inhibitors may seem irreversible because the dissociation rate of the enzyme-inhibitor complex may be too slow to be experimentally measured, but the inhibition is most often reversible (Silverman, 1995, Copeland, 2005). Slow- and tight-binding CYP inhibitors are rare but some clinical examples exist, such as clotrimazole, itraconazole, and ketoconazole (Gibbs *et al.*, 1999, Pearson *et al.*, 2006, Ogilvie *et al.*, 2008, Peng *et al.*, 2012).

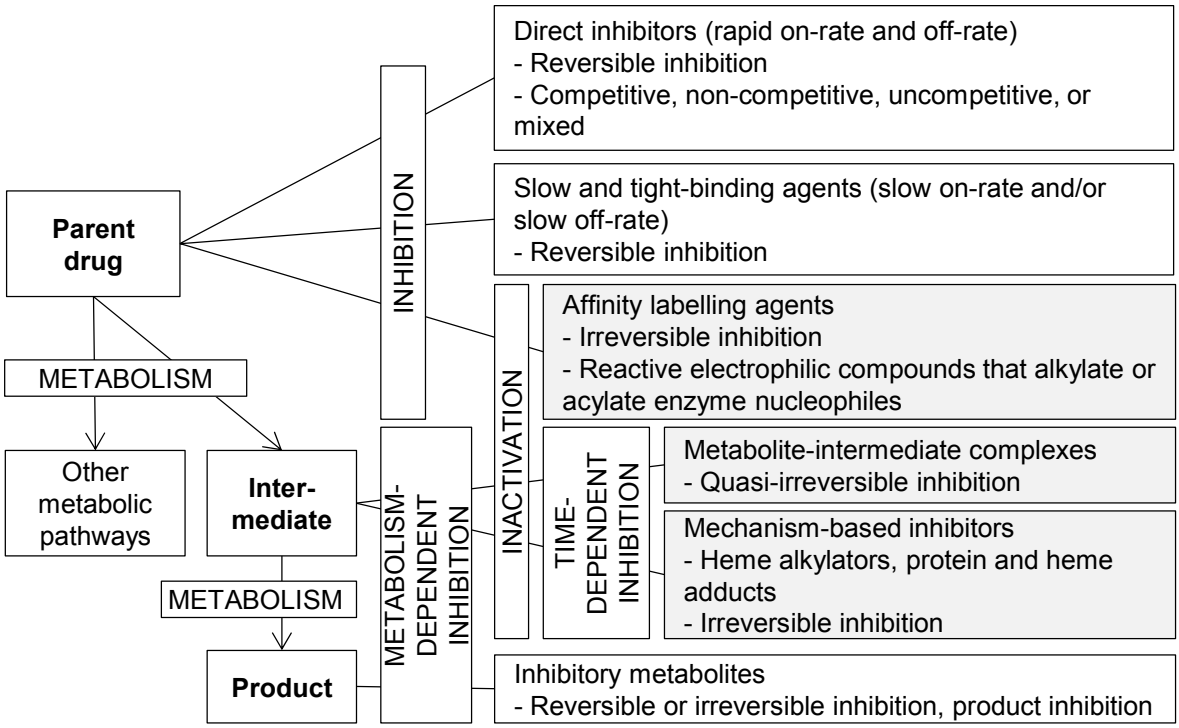

Figure 3. Examples of different inhibition mechanisms. Inhibition of CYPs can be due to inhibition by the parent inhibitor drug, a metabolic intermediate, or a product (metabolite). Inhibitors causing irreversible inhibition are marked grey.

2.1.2 Quasi-irreversible and irreversible inhibition

Inhibitors causing quasi-irreversible or irreversible inhibition are commonly referred to as inactivators. Affinity labelling agents typically contain reactive electrophilic elements that alkylate or acylate enzyme nucleophiles, forming irreversible, covalent bonds (Silverman, 1995, Copeland, 2005). Due to their reactivity, which may cause toxicity and adverse reactions, affinity labelling agents are usually not suitable as drugs (Silverman, 1995).

Reactive metabolic intermediates of a drug may also inactivate CYP enzymes (Figure 3). In quasi-irreversible inhibition, these agents complex with the ferrous haem iron of the CYP, forming inactivating metabolic intermediate complexes (MICs). MICs exhibit an absorbance maximum in the Soret region between 448 and 456 nm (Franklin, 1991), and spectral measurements can thus be used to assess whether the inactivation occurs via formation of MICs. *In vitro*, the enzyme activity can be restored by irradiation, addition of potassium ferricyanide, or incubation with highly lipophilic compounds, which dissociates or displaces the MIC from the enzyme (Ullrich and Schnabel, 1973, Elcombe *et al.*, 1975, Dickins *et al.*, 1979, Lin and Lu, 1998). However, inhibition by MICs is generally regarded as quasi-irreversible, as the *in vivo* activity of the CYP is expected to be restored only by synthesis of new enzyme (Lin and Lu, 1998).

In turn, irreversible inhibitors inactivate the CYP enzyme through haem alkylation and/or covalent binding to the protein (Silverman, 1995, Lin and Lu, 1998). In general, modification of the haem always inactivates the CYP, while changes in the protein cause loss of enzyme activity only if amino acids essential for substrate binding, electron transfer, and oxygen activation, are modified. Reactive metabolic intermediates causing irreversible CYP inhibition are denoted mechanism-based inhibitors (Silverman, 1995, Lin and Lu, 1998).

2.1.2.1 Mechanism-based inhibition

A mechanism-based enzyme inhibitor is an unreactive compound that is metabolised by an enzyme to an intermediate that, before leaving the active site, inactivates it (Silverman, 1995). Due to the irreversible nature of the inhibition, synthesis of new enzyme is required to restore enzyme activity. Therefore, the effects of mechanism-based inhibition can be more serious and persist longer than those of reversible inhibition (Ghanbari *et al.*, 2006).

Scheme 3 describes the process of mechanism-based inhibition (Silverman, 1995). First, the unreactive inhibitor drug (I) binds to the active site of the enzyme (E), in a similar manner as a typical substrate or competitive inhibitor of the enzyme. Next, however, a new complex (E×I') is formed in a step (k_2) that is usually unidirectional, and responsible for the observed time-dependence of the inactivation. The formed complex can have several fates: 1) if it is unreactive but forms a tight complex, the inhibition may be result from a non-covalent tight-binding complex, 2) the intermediate is reactive and undergoes nucleophilic, electrophilic, or radical reactions (k_4) to form a covalent complex (E×I''), 3) the species generated could be released (k_3) from the enzyme as a stable end product (P), or, in some instances, as a reactive intermediate (I') that can react with cellular constituents (Silverman, 1995, Kalgutkar *et al.*, 2007). Reactive intermediates that are released into the cytosol are often inactivated by glutathione, and the resulting conjugates can usually be detected in plasma or urine.

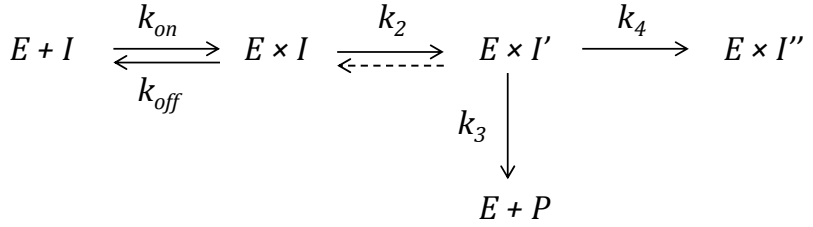

(Scheme 3.)

The efficiency of a mechanism-based inhibitor can be described by its partition ratio (r) k_3/k_4, which depicts the ratio of the end product release to enzyme inactivation. Thus, when r is 0, every turnover of inactivator produces inactivated enzyme (Silverman and Invergo, 1986). Mechanism-based inactivation can further be described by Equation 7:

$$k_{obs} = \frac{k_{inact} \times [I]}{K_I + [I]}$$ (Equation 7.)

where k_{obs} is the observed initial rate of inactivation, k_{inact} is the maximal inactivation rate, K_I is the inactivation constant defined as the inhibitor concentration supporting half of the maximal rate of inactivation, and [I] is the inhibitor concentration. *In vitro*, for a drug to be classified as a mechanism-based inhibitor, it needs to fulfil several criteria, for instance, time- and NADPH-dependency, saturation, involvement of catalytic step, and irreversibility (Silverman, 1995, Fontana *et al.*, 2005). Structural elements of a drug may indicate a potential for mechanism-based inhibition. Numerous structures, such as side chains with unsaturated carbon-carbon bonds and furan ring systems, alkylamino and methylenedioxy groups have been associated with this inhibition type (Murray, 1997). However, *in vitro* experiments are the best way to determine the mechanism-based inhibition potential of a drug (section 4.2.).

Clinical relevance. Mechanism-based inhibition can be of greater concern than reversible inhibition as the clinical outcome may be a more profound and long-lasting inhibition than what could be expected based on the dose or drug exposure (Ghanbari *et al.*, 2006). In fact, among drugs that cause interactions, mechanism-based inhibitors of CYPs represent several of those agents causing interactions of the greatest extent (Table 4) (Venkatakrishnan *et al.*, 2007). For instance, mibefradil, a mechanism-based inhibitor of CYP3A4, was withdrawn partially because of unmanageable drug-drug interactions. In a clinical study, a low mibefradil dose of 50 mg once daily for three days increased the plasma exposure to triazolam by nine-fold (Table 4) (Backman *et al.*, 1999). However, many important drugs that have been identified as mechanism-based inhibitors of CYPs are used clinically, but often with contraindications and restrictions to use with such drugs that might be subject to inhibition. Of the 129 identified CYP inhibitors on the United States market in 2009, 24 (19%) were mechanism-based inhibitors (Isoherranen *et al.*, 2009). Eight of these drugs have caused strong interactions *in vivo* (defined as a ≥five-fold increase in AUC of the victim drug), including clarithromycin (CYP3A4), nefazodone (CYP3A4), nelfinavir (CYP3A4), paroxetine (CYP2D6), ritonavir (CYP3A4), saquinavir (CYP3A4), ticlopidine (CYP2C19), and troleandomycin (CYP3A4). Since 2009, several other drugs have been identified as mechanism-based inhibitors. For instance, many protein kinase inhibitors are mechanism-based inhibitors of CYP3A4 *in vitro* (Kenny *et al.*, 2012, Filppula *et al.*, 2014). Compounds other than drugs may also affect CYPs by mechanism-based inhibition, such as components in grapefruit juice and liquorice root.

Apart from the risk of long-lasting drug-drug interactions, mechanism-based inhibitors that bind covalently to CYP enzymes and other cellular proteins are of additional concern due to the risk of idiosyncratic drug reactions (Ghanbari *et al.*, 2006). Tienilic acid, a mechanism-based inhibitor of CYP2C9 (Lecoeur *et al.*, 1994), was withdrawn because of hepatotoxicity mediated by an auto-immune response.

Table 4. Examples of drug-drug interactions due to mechanism-based inhibition of CYP enzymes.

MBI	Victim drug	Inhibited enzyme	Change in C_{max}	AUC	$t_{½}$	References
Clopidogrel*	repaglinide	CYP2C8	↑ 2.5-fold	↑ 5.1-fold	↑ 1.4-fold	(Tornio *et al.*, 2014)
Paroxetine	S-metoprolol	CYP2D6	↑ 2.0-fold	↑ 5.1-fold	↑ 2.1-fold	(Hemeryck *et al.*, 2000)
Mibefradil	triazolam	CYP3A4	↑ 1.8-fold	↑ 9.0-fold	↑ 4.9-fold	(Backman *et al.*, 1999)
Ticlopidine	omeprazole	CYP2C19	↑ 3.0-fold	↑ 6.2-fold	↑ 2.6-fold	(Ieiri *et al.*, 2005)

* The glucuronide metabolite of clopidogrel is a mechanism-based inhibitor of CYP2C8. AUC, area under concentration-time curve; C_{max}, peak concentration; CYP, cytochrome P450; MBI, mechanism-based inhibitor; $t_{½}$, elimination half-life.

2.1.3 Inhibition by metabolites

Except for reactive metabolic intermediates, other drug metabolites may also inhibit CYP enzymes and contribute to drug-drug interactions. Not taking circulating inhibitory metabolites into account when predicting the inhibitory potential of a drug may cause significant underpredictions of its possible interactions (Yeung *et al.*, 2011). For instance, inhibitory metabolites of the CYP3A4 inhibitor itraconazole have been estimated to account for about 50% of its total inhibitory effect on CYP3A4 *in vivo* (Templeton *et al.*, 2008, Templeton *et al.*, 2010). Other examples of drugs with metabolites causing reversible or irreversible CYP inhibition include bupropion, clopidogrel (Table 4), fluoxetine, and gemfibrozil (Stevens and Wrighton, 1993, Ogilvie *et al.*, 2006, Reese *et al.*, 2008, Sager *et al.*, 2014, Tornio *et al.*, 2014). Product inhibition ("feedback inhibition") occurs when a metabolite (product) inhibits an enzyme involved in the metabolism of the parent drug (Figure 3).

2.2. Induction of drug-metabolising enzymes

In comparison to direct inhibition of CYPs, enzyme induction is a slow process. Induction of drug-metabolising enzymes usually increases the elimination of the victim drug, which may result in reduced plasma concentrations and therapeutic failure. In turn, if the drug is a pro-drug, induction may lead to an increased formation of the active agent.

Enzyme induction leads in general to increased protein synthesis or reduced enzyme turnover due to increased gene transcription, or mRNA or enzyme stabilisation, respectively (Brown *et al.*, 1954, Conney, 1967, Gonzalez, 2007). CYPs are typically induced by transcriptional gene activation (Sinz *et al.*, 2008). In general, the CYP1A subfamily is induced by aryl

hydrocarbon receptor ligands, while PXR and CAR mediate induction of the CYP2 and CYP3 families. Many other drug-metabolising enzymes and drug transporters are also induced by these nuclear receptors. The receptors are activated by ligand (inducer) binding, which causes conformational changes, leading to release of co-repessors and recruitment of co-activators and dimerisation partners. In turn, these processes result in chromatin remodelling and transcriptional activation. Transcription regulation is achieved through binding of the receptor to deoxyribonucleic acid (DNA) response elements present in the promoter region of target genes (Wang and LeCluyse, 2003).

Clinical relevance. The induced increase in enzyme protein levels causes an increased enzyme activity. *In vitro*, an increase in the V_{max} of the victim drug is observed, while its K_m is unaffected, thus leading to an increased intrinsic metabolic clearance (V_{max}/K_m). Clinically, the resulting increase in hepatic clearance may cause reduced plasma exposure to the victim drug (Table 5) (Sinz *et al.*, 2008), and loss of drug response. For instance, reduced efficacy has been observed in cases where CYP3A4 induction has led to reduced ethinyloestradiol levels from oral contraceptives or lowered cyclosporine concentrations in transplant patients, resulting in unwanted pregnancies or organ rejection, respectively (Sinz *et al.*, 2008). Other possible outcomes of CYP induction include an increased formation of active or toxic metabolites, enhanced activation of pro-drugs, and hypertrophy of hepatocytes. Autoinduction occurs when the inducer compound induces its own metabolism, for instance, artemisinin and carbamazepine are both substrates and inducers of CYP2B6 and CYP3A4, respectively (Bertilsson *et al.*, 1980, Simonsson *et al.*, 2003). Well-known CYP inducers include carbamazepine, phenobarbital, phenytoin, rifampicin (Table 5), and St John's Wort (Pelkonen *et al.*, 2008). Similarly as for CYP inhibition, compounds other than drugs may also cause CYP induction. For instance, ethanol induces CYP2E1, while tobacco smoking causes an up-regulation of CYP1A2 (Figure 2).

Table 5. Examples of drug-drug interactions mainly due to CYP induction by rifampicin.

Victim drug	Induced enzyme(s)	Change in C_{max}	AUC	$t_{½}$	References
Midazolam	CYP3A4	↓ 95%	↓ 98%	↓ 63%	(Backman *et al.*, 1998)
Pioglitazone	CYP2C8	↔	↓ 54%	↓ 53%	(Jaakkola *et al.*, 2006a)
Repaglinide	CYP2C8, CYP3A4	↓ 79%	↓ 80%	↔	(Bidstrup *et al.*, 2004)
Rosiglitazone	CYP2C8, CYP2C9	↓ 31%	↓ 66%	↓ 62%	(Park *et al.*, 2004)
Simvastatin acid	CYP3A4, CYP2C8	↓ 90%	↓ 93%	↔	(Kyrklund *et al.*, 2000)

AUC, area under concentration-time curve; C_{max}, peak concentration; CYP, cytochrome P450; $t_{½}$, elimination half-life.

2.3. Transporter interactions

Inhibition or induction of drug transporters may also result in altered tissue distribution and plasma concentrations of their substrate drugs. The outcome depends on the importance of the transporter in the pharmacokinetics of the drug, but also on the type (uptake/efflux) and localisation of the transporter affected (Endres *et al.*, 2006, Giacomini and Sugiyama, 2011). For instance, inhibition of an uptake transporter located in the intestine may result in reduced absorption of its substrates, while inhibition of an intestinal efflux transporter may lead to an increased drug exposure (EMA, 2013). Inhibition of transporters is complex and may involve several mechanisms, including traditional competitive, non-competitive and uncompetitive inhibition of the transporter, or interaction with the ATP hydrolysis of ABC transporters (Lin, 2003, Giacomini and Sugiyama, 2011). However, evaluation of the role of a single transporter in a drug-drug interaction may be challenging. Many transporters and CYPs show overlapping substrate specificities, and several membrane transporters are regulated by the same nuclear receptors as CYPs, such as CAR and PXR (Tirona, 2011, Yoshida *et al.*, 2012).

Clinical relevance. Today it is evident that transporter inhibition or induction may cause clinical significant drug-drug interactions (Table 6). As compared to interactions due to transporter inhibition, however, the number of documented interactions resulting from transporter induction is small (Konig *et al.*, 2013). Some interactions affecting transporters change the concentrations of a drug within a particular tissue, without altering its concentrations in plasma (Endres et al., 2006). This is possible because the amount of drug distributing into a specific tissue is only a small fraction of the total drug amount in the body, or its clearance may be mainly due to processes other than transport, such as metabolism. For instance, the P-gp inhibitor verapamil increases the concentration of cyclosporine in the brain, but not in plasma (Sasongko et al., 2005).

Table 6. Examples of drug-drug interactions due to transporter inhibition or induction.

Perpetrator drug	Victim drug	Affected transporter	Change in C_{max}	AUC	$t_{½}$	References
Cyclosporine	repaglinide	OATP1B1* (liver)	↑ 1.8-fold	↑ 2.4-fold	↔	(Kajosaari *et al.*, 2005b)
Cyclosporine	rosuvastatin	OATP1B3** (liver)	↑ 10.6-fold	↑ 5.0-fold	↓ 53%	(Simonson *et al.*, 2004)
Grapefruit juice	aliskiren	OATP2B1** (intestine)	↓ 81%	↓ 61%	↓ 10%	(Tapaninen *et al.*, 2010)
Itraconazole	digoxin	P-gp (kidney)	↔	↑ 1.7-fold	↔	(Jalava *et al.*, 1997)
Rifampicin***	digoxin	P-gp (intestine)	↓ 58%	↓ 30%	↔	(Greiner *et al.*, 1999)

* CYP3A4 inhibition also involved. ** Other transporters may also be involved. ***Inducer. AUC, area under concentration-time curve; C_{max}, peak concentration; OATP, organic anion transporting polypeptide; P-gp, P-glycoprotein; $t_{½}$, elimination half-life.

3. Guidelines on the investigation of drug-drug interactions in drug development

Drug-drug interaction studies aim to determine whether there is a potential for clinically relevant interactions between the study drug and other drugs. In drug development, these studies should be conducted early as part of the assessment of the safety and effectiveness of the drug, but also during its clinical use after approval (FDA, 2012, EMA, 2013). The most recent guidelines on the investigation of pharmacokinetic drug-drug interactions in drug development from European and United States drug regulatory authorities include the Guideline on the Investigation of Drug Interactions of the European Medicines Agency (EMA) published in 2013, and the corresponding draft guidance from the United States Food and Drug Administration (FDA), issued in February 2012 (FDA, 2012, EMA, 2013).

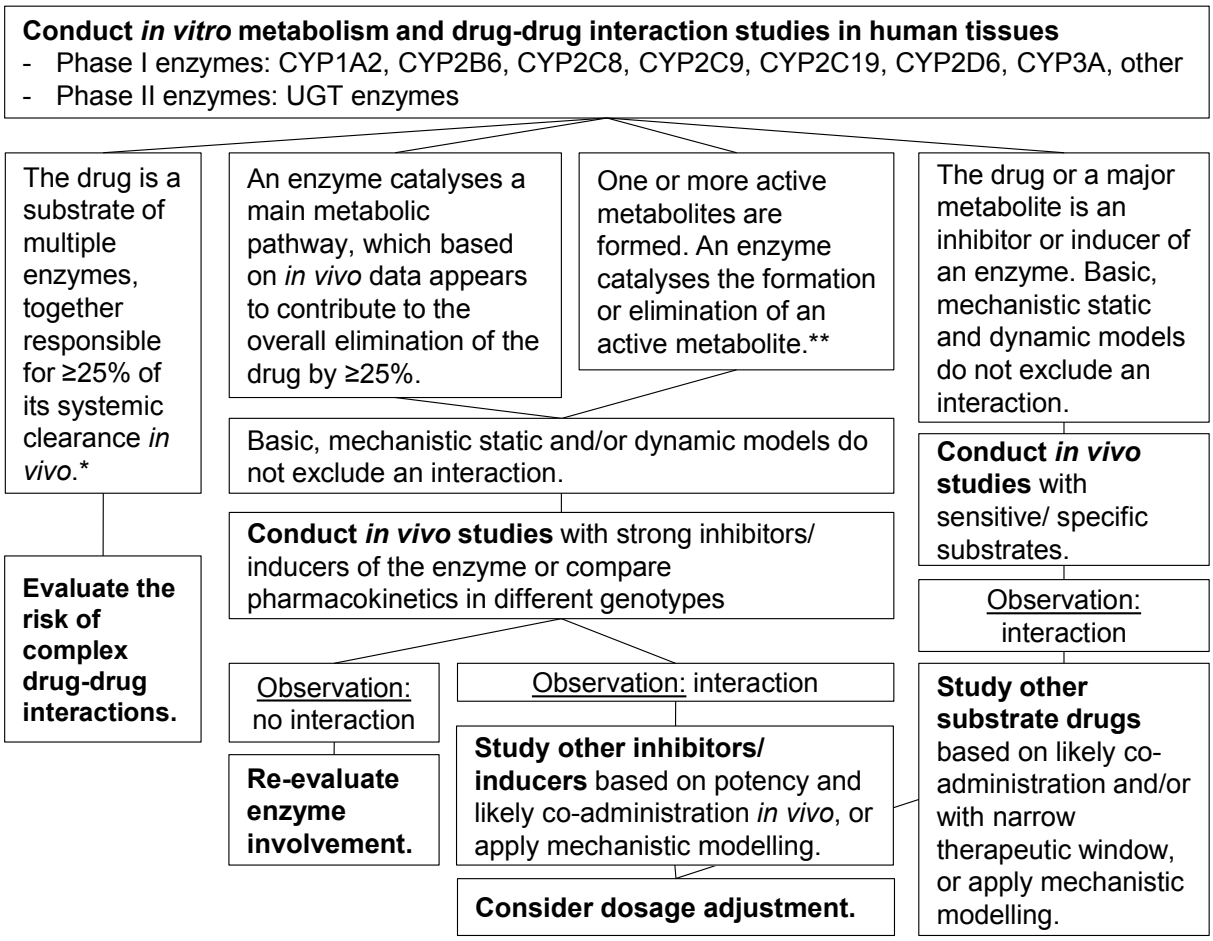

Figure 4. Decision tree for investigation of metabolism-based drug-drug interactions (modified from FDA (2012) and EMA (2013)). * Specific for FDA. ** Specific for EMA. CYP, cytochrome P450; UGT, uridine-5'-diphosphate glucuronosyltransferase.

The interaction potential of a drug can be assessed using *in vitro* (laboratory), *in silico* (computational), and *in vivo* (animal and human) methods. If the investigations indicate that the drug is likely to cause (i.e. act as a perpetrator) or be subject (victim) to drug-drug

interactions, actions should be determined to reduce the risk for harmful consequences. These could include dosage adjustments, therapeutic monitoring, contraindication to simultaneous use with certain drugs, and other treatment recommendations (FDA, 2012, EMA, 2013). The potential for drug-drug interactions should be evaluated for small molecule drugs and also for certain classes of therapeutic proteins (FDA, 2012). Here, a brief overview of the current regulatory guidelines for interactions affecting drug-metabolising enzymes and drug transporters by small molecule drugs is presented.

***In vitro* studies.** Drug-drug interaction studies usually start with *in vitro* experiments to determine if the study drug is a substrate, inhibitor, and/or inducer of metabolising enzymes and transporters (Figure 4). The interaction potential of metabolites present at ≥25% of the parent drug AUC and 10% of the AUC of total drug-related material should also be tested (FDA, 2012, EMA, 2013). If an enzyme contributes to a metabolic pathway estimated to account for more than 25% of the total drug elimination, clinical interaction studies are warranted to study its role *in vivo* (see *in vivo* guidelines section) (FDA, 2012, EMA, 2013). EMA also recommends *in vivo* studies to evaluate the role of enzymes forming active metabolites estimated to contribute to more than 50% of the total therapeutic effect *in vivo*. In some cases, minor elimination pathways (contributing to ≤25% of drug elimination) should also be elucidated, e.g. when the study drug is metabolised by a polymorphic enzyme (FDA, 2012, EMA, 2013). Similarly, the effects on enzymes by the parent drug and its major metabolites should be studied. Drug candidates that do not undergo metabolism should also be tested for inhibition and induction of metabolising enzymes (FDA, 2012).

FDA recommends that all new drugs should be evaluated *in vitro* to determine if they are substrates of P-gp and BCRP. EMA primarily focuses on P-gp, but advises that other transporters involved in drug absorption should be tested when physiochemical properties of the drug or other knowledge indicate that additional transporters could be involved. Both authorities recommend *in vitro* studies of transporters mediating drug disposition when *in vivo* data indicates that the study drug is significantly eliminated by active renal, biliary or gut wall secretion. Studies of the *in vitro* roles of OATPs, such as OATP1B1 and OATP1B3, are recommended when hepatic elimination is ≥25% of the total drug clearance. Furthermore, FDA suggests that drugs that undergo renal elimination through active secretion by ≥25%, should be tested for transport by OAT1, OAT3, and OCT2 (FDA, 2012). Drug candidates and their major metabolites should also be evaluated as possible inhibitors of these transporters mentioned above (FDA, 2012, EMA, 2013). Because validated *in vitro* systems to study transporter induction are lacking, these studies can be carried out using *in vivo* methods (FDA, 2012). Both EMA and FDA acknowledge that the drug transport field is evolving rapidly, so transporters other than those mentioned should be tested when appropriate.

Prediction and modelling guidelines. Together with pharmacokinetic and mass balance data on main elimination routes and knowledge on enzymes and transporters involved in the

disposition of the drug, *in vitro-in vivo* extrapolations are used to predict the clinical interaction risk based on *in vitro* data. Basic static models are suitable as a first screening method to evaluate the need for a clinical study (EMA, 2013). A positive interaction signal from a basic static model may be further examined by use of mechanistic static models and more dynamic models (section 5.2.). The criteria used for assessing bioequivalence (predicted AUC ratio of 0.8-1.25) can be used as a cut-off to determine if *in vivo* studies are needed (FDA, 2012, EMA, 2013). Physiologically based pharmacokinetic (PBPK) modelling is recommended as a useful tool to improve the design of clinical studies (section 5.3.). These models may be used at different stages in drug development to estimate the interaction potential qualitatively and to predict the interaction outcome quantitatively (EMA, 2013). In some cases, PBPK modelling can be used as an alternative to clinical studies, for instance when determining the likelihood of interactions in special populations, such as paediatric or geriatric populations (FDA, 2012). Modelling approaches can also be useful in complex drug-drug interactions involving several mechanisms, for instance, concurrent inhibition and induction of an enzyme or simultaneous enzyme and transporter inhibition. If conventional interaction studies cannot be performed, the interaction potential can also be investigated using population pharmacokinetic analyses (FDA, 2012).

***In vivo* guidelines.** Due to marked species differences, pharmacokinetic interaction studies should generally be conducted in humans (EMA, 2013). *In vivo* drug-drug interaction studies are typically designed to compare drug concentrations with and without a perpetrator drug. Because a specific study can address a number of questions and clinical objectives, many study designs for investigating drug-drug interactions can be considered (section 6.). If a specific enzyme or transporter is involved in the main elimination pathway of a drug, interaction studies generally start by testing the effect of strong inhibitors and inducers on its metabolism. A strong inhibitor is defined as an inhibitor causing an ≥five-fold increase in the AUC of the victim drug, while a strong inducer reduces the victim drug AUC by ≥80% (FDA, 2012, EMA, 2013). If an interaction is observed, studies with less strong inhibitors and inducers can be evaluated (Figure 4). When testing the perpetrator potential of a drug, *in vivo* studies start by testing its effect on sensitive probe drugs. A sensitive substrate is defined as a drug, whose AUC is increased ≥five-fold when taken together with a known CYP inhibitor (FDA, 2012). As an alternative or complement to interaction studies, clinical studies in different polymorphic populations may be carried out (EMA 2013).

4. *In vitro* methods for study of CYP-mediated drug interactions

The *in vitro* characterisation of drug metabolism and interactions must be performed with high quality and consistency, in particular when they influence the design of clinical trials.

This section describes some common methods for studying CYP-mediated drug metabolism and inhibition *in vitro*, while induction will not be discussed.

4.1. Phenotyping of CYP-mediated reactions

In drug metabolism, reaction phenotyping is defined as the process of identifying the enzyme that is responsible for metabolising a drug (Ogilvie *et al.*, 2008). Reaction phenotyping allows an estimation of the victim potential of a drug. Before conducting such studies, however, it is important to first determine the main elimination pathways of the drug, and the most appropriate test systems in which to study the reactions. CYP reaction phenotyping data will be of clinical interest only if oxidative metabolism reactions are estimated to play a significant role in the overall elimination of a drug (Bjornsson *et al.*, 2003).

Table 7. Human enzyme sources used in *in vitro* metabolism and interaction studies (modified from Madan *et al.* (2002) and Pelkonen and Turpeinen (2007)).

Enzyme source	Advantages	Disadvantages
Liver slices	Contain all hepatic enzymes and drug transporters, induction can be studied.	Limited availability, as fresh tissue is needed. Require specific techniques and procedures. Have a barrier to the diffusion of drugs to cells. Limited viability.
Liver homogenates	Contain nearly all hepatic enzymes.	Liver architecture lost.
Primary and cultured hepatocytes	Contain all hepatic enzymes and several transporters cellularly integrated. Induction can be studied.	Requires specific techniques and procedures. Quality and stability may vary. Interpretation of findings may be challenging. For primary hepatocytes, limited availability and relatively healthy tissue needed.
S9 fractions	Contain many enzymes, including CYP, FMO, and UGT enzymes.	Lower enzyme activity than in microsomes and expressed enzymes.
HLM	Contain the most important drug-metabolising enzymes, low in cost and easy to store. Commercially available from several sources.	Contain only phase I and UGT enzymes. Enzyme levels can vary. Contain lipids and proteins that can reduce unbound drug concentrations.
Expressed individual CYPs	Useful for high throughput screening. The importance of an individual enzyme and its variants can easily be studied. No need for CYP-specific substrates. Commercially available from several sources.	Only one enzyme can be studied at a time, and the metabolic contribution of other enzymes is not represented. Cytochrome b5 and POR levels may vary.

CYP, cytochrome P450; FMO, flavin-containing monooxygenase; HLM, human liver microsomes; POR, cytochrome P450 oxidoreductase; UGT, uridine-5'-diphosphate glucuronosyltransferase.

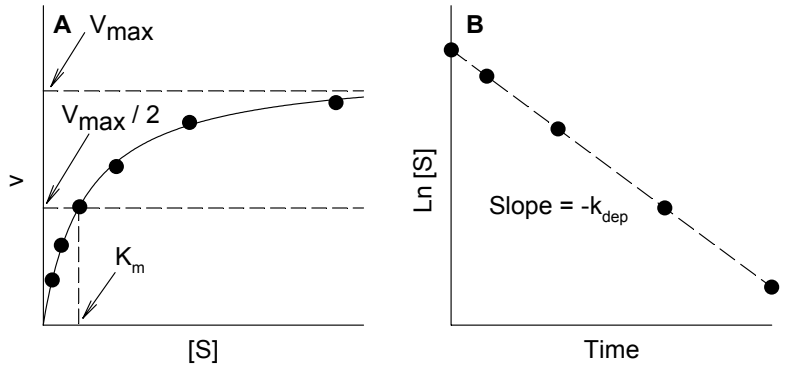

Figure 5. Determination of intrinsic clearance.

A, Enzyme kinetic plot.
B, Substrate depletion.

k_{dep}, depletion rate constant; K_m, Michaelis-Menten constant; [S], substrate concentration; v, reaction velocity; V_{max}, maximum velocity.

Test systems. The *in vitro* metabolism of a drug is studied by measuring the reduction in its concentrations and/or the increase in metabolite concentrations with time (Pelkonen and Turpeinen, 2007). Various enzyme preparations are available for these studies (Table 7). Because all systems have advantages and disadvantages, selection of a given system should be based on the desired endpoint. When preliminary information on the metabolism of the drug is scarce, more advanced test systems such as hepatocytes, liver homogenates and slices can be useful to identify different metabolic pathways. Otherwise, human liver microsomes (HLM) and recombinant enzymes are recommended for phenotyping of CYP-mediated reactions because of their accessibility, and due to the fact that measurements in these reduced systems are not confounded by other metabolic processes or cellular uptake (Bjornsson *et al.*, 2003).

Incubation and reaction conditions. *In vitro* incubation conditions attempt to mimic the chemical environment of the hepatic cytosol. Common reaction conditions for HLM and recombinant enzyme experiments include 100 mM buffer, pH 7.4, 37°C, and possibly a co-factor such as $MgCl_2$ (Madan *et al.*, 2002, Venkatakrishnan *et al.*, 2003). Addition of NADPH initiates the reactions, while protein precipitation by organic solvents or an acid are used to stop them. In the incubations, the lowest microsomal protein concentration possible should be used in order to minimise non-specific binding of the test compounds. Experiments where reaction rates are measured are generally conducted under initial-rate conditions. Here, the formation of the metabolite should be directly proportional to the incubation time and enzyme concentration, to ensure that the enzyme activity remains stable. Furthermore, in order to ensure that accurate substrate concentration information is available and reduce the risk of product inhibition, the consumption of substrate should be held at a minimum (<20%) (Madan *et al.*, 2002).

In contrast, when reduction in substrate concentration with time is monitored (substrate depletion approach), substrate consumption usually exceeds 20%. The substrate concentration should correspond to its clinically relevant unbound concentrations in plasma because

inappropriate concentrations may yield results that are not reflective of the *in vivo* situation. Furthermore, concentrations of organic solvents should be kept low (≤1%) in the incubations, as solvents may inhibit CYPs (Ogilvie *et al.*, 2008).

Experiments. To identify which CYP isoforms contribute to the oxidative metabolism of drugs *in vitro*, three main approaches are generally used, including: 1) use of selective CYP inhibitors (Figure 2) or inhibitory antibodies in HLM, 2) metabolism in recombinant enzymes, and 3) metabolic correlation of the reaction activity with CYP-selective isoform markers reactions in HLM (Lin and Lu, 1998, Bjornsson *et al.*, 2003). Use of at least two approaches is generally recommended. The enzyme kinetics of a specific reaction is determined using initial rate conditions and substrate concentrations ranging from 0.1 K_m to 10 K_m. V_{max} and K_m are determined by non-linear regression of a plot of enzyme activity versus substrate concentration (Figure 5) (Bjornsson *et al.*, 2003). The intrinsic clearance (CL_{int}) of the reaction can be calculated based on these constants (Equation 8), usually assuming that the substrate concentration is much lower than its K_m value and therefore does not need to be considered in the equation. In the substrate depletion approach, the total intrinsic clearance of a substrate in a specific test system can be estimated according to Equation 9 (Obach *et al.*, 1997, Obach, 1999).

$$CL_{int,in\ vitro} = \frac{V_{max}}{K_m + [S]} \rightarrow \frac{V_{max}}{K_m} \qquad \text{(Equation 8.)}$$

$$CL_{int,in\ vitro} = \frac{\ln(2)}{t_{½} \times [M]} = \frac{k_{dep}}{[M]} \qquad \text{(Equation 9.)}$$

where $t_{½}$ is the half-life of the substrate, [M] is the HLM concentration or CYP concentration in the incubation, and k_{dep} is the first-order depletion rate constant.

4.2. Evaluation of drugs as inhibitors of CYP enzymes

The primary purpose of testing drugs as CYP inhibitors *in vitro* is to estimate their interaction potential and evaluate the need for clinical interaction studies. Well-designed inhibition experiments can be an important predictor of the clinical outcome. Inhibition of CYP activity is commonly examined using HLM (Bjornsson *et al.*, 2003). Generally, the incubation and reaction conditions described in section 4.1. can be adopted.

IC_{50} and K_i experiments. To determine if a drug inhibits a particular CYP isoform, changes in the metabolism of a CYP-specific marker substrate (Figure 2) in HLM or recombinant enzymes are monitored. The potency of the inhibitor is assessed by determination of K_i or IC_{50} values (Bjornsson et al., 2003). IC_{50} is an extrinsic constant, defined as the inhibitor

concentration required to cause 50% inhibition under a given set of experimental conditions (substrate type and concentration, protein concentration, *etc*.) (Madan et al., 2002). Because K_i values are intrinsic constants, which in theory should be reproducible from one laboratory to another, it is preferable to determine K_i rather than IC_{50} values. Appropriate K_i experiments require multiple inhibitor concentrations covering several orders of magnitude, as well as multiple substrate concentrations that embrace the K_m of the substrate (Figure 6). The data obtained are used to determine the K_i value and the inhibition mechanism (competitive, non-competitive, uncompetitive, or mixed) (section 2.1.).

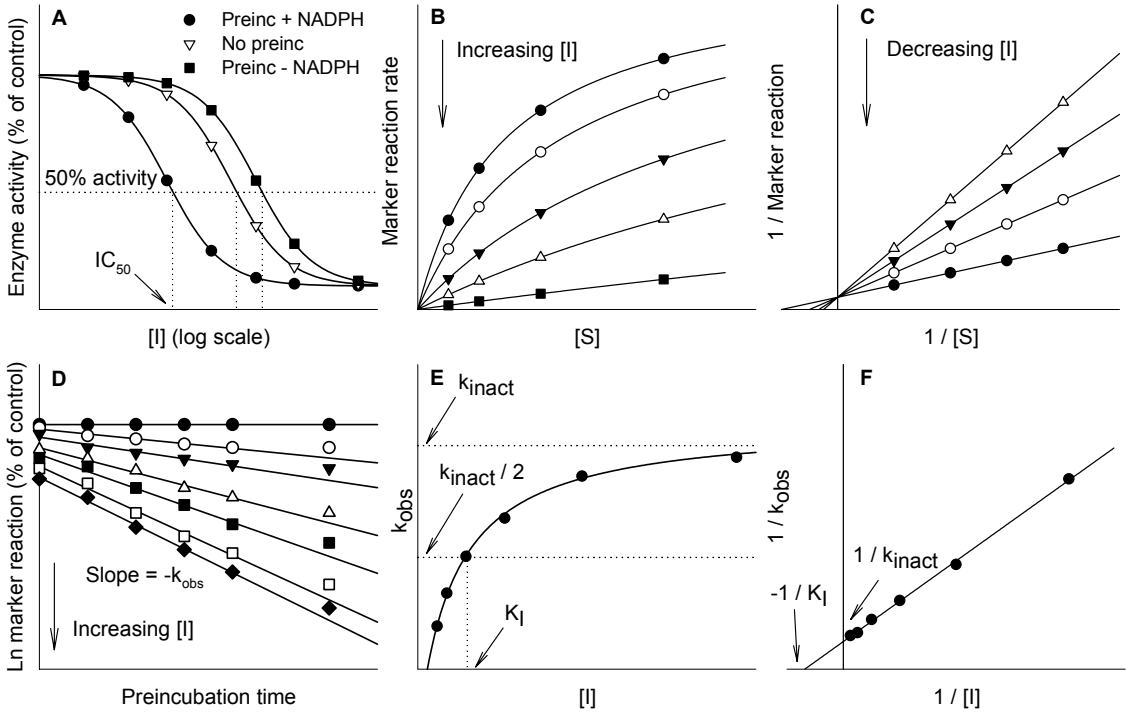

Figure 6. Different types of inhibition plots. **A,** IC_{50}-shift experiment. A ≥1.5-fold lower IC_{50} value following pre-incubation of the inhibitor with NADPH, as compared to no pre-incubation, indicates time- and NADPH-dependent inhibition. **B,** K_i-experiment. In the direct plot, the V_{max} of the substrate does not increase, while its K_m value decreases, thus suggesting a competitive inhibition mechanism. **C,** Lineweaver-Burk plot. The arrangement of lines based on data of the K_i-experiment also suggests competitive inhibition. **D,** Mechanism-based inhibition experiment. The inhibition increases with increasing pre-incubation time and inhibitor concentration. k_{obs} values of each inhibitor concentration are calculated on the basis of *initial* rates of inactivation of the enzyme (slope). **E,** Saturation curve. k_{inact} and K_I can be obtained from a saturation curve where k_{obs} is plotted against inhibitor concentration. **F,** Kitz-Wilson plot. The inactivation constants can also be derived from a reciprocal plot of k_{obs} and inhibitor concentration. [I], inhibitor concentration; IC_{50}, inhibitor concentration producing 50% inhibition; K_I, inhibitor concentration supporting half of the maximal rate of inactivation; k_{inact}, maximal rate of inactivation; k_{obs}, inactivation rate constant for a particular inhibitor concentration; NADPH, nicotinamide adenine dinucleotide phosphate; preinc, pre-incubation; [S], substrate concentration.

However, IC_{50} experiments are less laborious than K_i experiments, and IC_{50} data can be useful to guide the design of K_i and other inhibition experiments (Figure 6). In contrast to K_i experiments, IC_{50} experiments only require a single substrate concentration (at $\leq K_m$), while the inhibitor concentrations vary. The rate of the marker reaction is measured in the presence of various inhibitor concentrations, and the percentage remaining activity with respect to inhibitor concentrations are plotted to derive an IC_{50} value (Figure 6). In IC_{50}-shift experiments, the inhibitor is also tested for NADPH- and time-dependent inhibition. If the IC_{50} value is ≥1.5-fold lower following a 30 min pre-incubation with NADPH as compared to no pre-incubation, the inhibitor should be tested for mechanism-based inhibition (Figure 7) (Grimm et al., 2009).

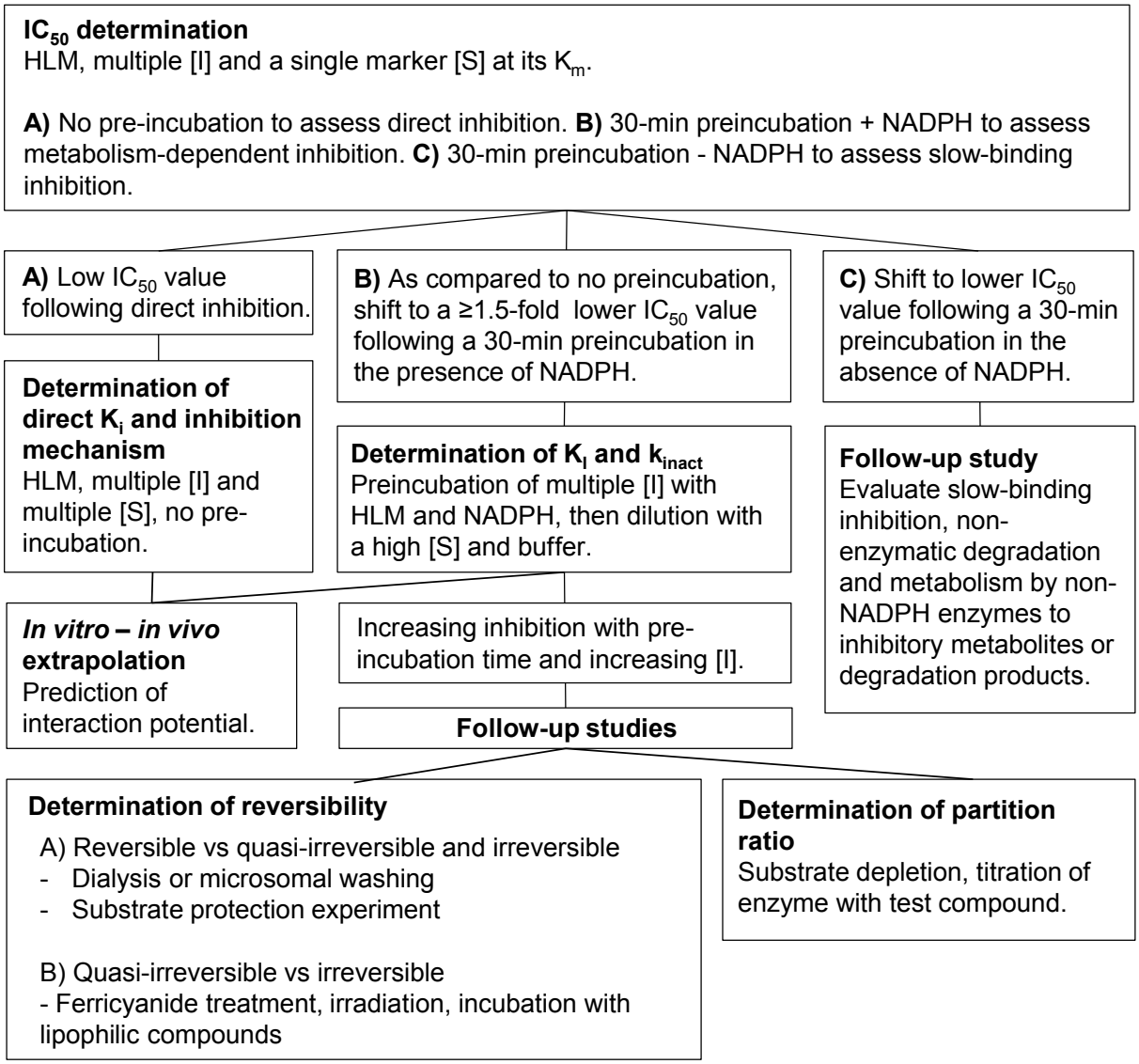

Figure 7. Decision tree for inhibition studies when inhibition is observed (adapted from Grimm *et al.* (2009), Xenotech (2011)). HLM, human liver microsomes; [I], inhibitor concentration; IC_{50}, inhibitor concentration producing 50% inhibition; K_i, reversible inhibition constant; K_I, inhibitor concentration supporting half of the maximal rate of inactivation; k_{inact}, maximal rate of inactivation; K_m, Michaelis-Menten constant; NADPH, nicotinamide adenine dinucleotide phosphate; [S], substrate concentration.

Mechanism-based inhibition. In mechanism-based inhibition experiments, multiple inhibitor concentrations are first pre-incubated with high HLM concentrations and NADPH (Grimm *et al.*, 2009). At determined time points, aliquots are removed and diluted by a factor of 10 or more with buffer and the marker substrate to determine the residual CYP activity. Dilution and a high substrate concentration are used to minimise reversible inhibition by the inhibitor. k_{obs} of each inhibitor concentration are estimated graphically from the initial slope of a graph where the natural log of the remaining enzyme activity is plotted against pre-incubation time (Figure 6). Then, k_{inact} and K_I are estimated using non-linear regression and Equation 7. These values can also be determined from linear regression of a double-reciprocal plot of the k_{obs} versus inhibitor concentrations (Figure 6). Possible follow-up experiments include evaluation of the reversibility and efficacy of the inactivation (determination of partition ratio) (Figure 7) (Grimm *et al.*, 2009).

5. *In vitro-in vivo* extrapolation

Although determination of *in vitro* metabolism and metabolic interactions may be relatively straightforward, a proper interpretation and extrapolation of *in vitro* data to the clinical situation requires a good understanding of pharmacokinetic principles. *In vitro-in vivo* extrapolations are used to interpret the obtained *in vitro* data and translate it to clinical relevance. However, even if a drug is predicted to cause or be subject to interactions, it does not necessary imply that they will be clinically relevant. As described in section 2., several factors need to be considered to estimate the clinical significance of an interaction.

5.1. Prediction of drug clearance

Intrinsic clearance values obtained from *in vitro* experiments ($CL_{int,\ in\ vitro}$) can be scaled to hepatic clearance (CL_H) (Figure 8). Although simplifications and several assumptions must be done, extrapolation of intrinsic clearance obtained from HLM experiments is fairly uncomplicated, while that of data from recombinant enzyme incubations is more complex and several approaches can be used. However, before conducting predictions, it is important that intrinsic clearance values, enzyme kinetic constants, and inhibition constants are corrected for non-specific binding to protein in microsomal incubations (Obach, 1996, Bachmann, 2006).

HLM. Predictions of hepatic clearance from *in vitro* intrinsic clearance obtained from HLM incubations require scaling factors. These include the amount of microsomal protein per gram liver (MPPGL), and the amount liver per kg body weight (Equation 10). Values of 40-50 mg protein/g liver and ~30 g liver/body weight are generally used (Davies and Morris, 1993, Venkatakrishnan *et al.*, 2003, Houston and Galetin, 2008). The most used model in the prediction of hepatic clearance is the well-stirred model (Equation 11):

$$CL_{int,in\ vivo} = CL_{int,in\ vitro} \times MPPGL \times liver\ weight$$ (Equation 10.)

$$CL_H = Q_H \times E_H = Q_H \times \left(\frac{f_{u,B} \times CL_{int,in\ vivo}}{Q_H + f_{u,B} \times CL_{int,in\ vivo}} \right)$$ (Equation 11.)

in which Q_H is the hepatic blood flow (20.7 ml/min/kg) (Houston and Galetin, 2008), E_H is the hepatic extraction ratio, and $f_{u,\ B}$ is the unbound fraction of drug in blood. If a drug is mainly metabolised in the liver, its total clearance can be approximated to equal its hepatic clearance. Drugs can be classified based on their extraction ratio; low-extraction drugs have enzyme-limited hepatic clearance, while high-extraction drugs have a flow-limited hepatic clearance (Wilkinson and Shand, 1975, Wilkinson, 1987, Lin and Lu, 1998). Thus, low-extraction drugs are more sensitive to changes in their intrinsic clearance due to inhibition or induction than high-extraction drugs.

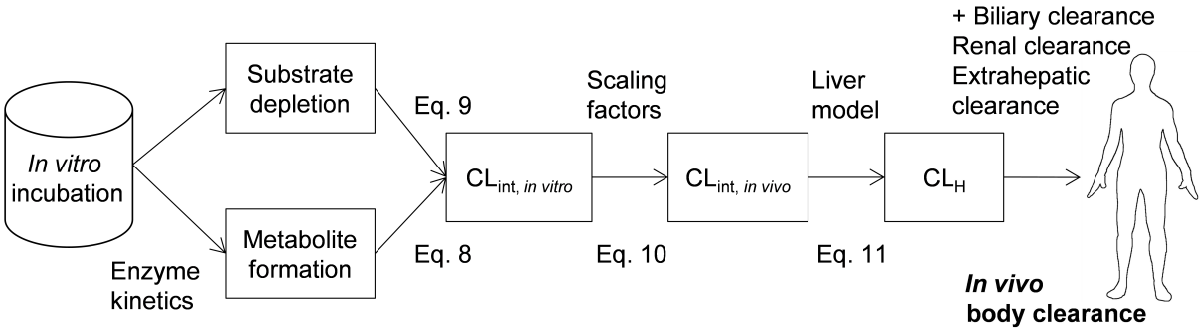

Figure 8. *In vitro-in vivo* extrapolation of clearance (modified from Pelkonen and Turpeinen (2007)). CL_H, hepatic clearance; CL_{int}, intrinsic clearance; Eq, equation.

Recombinant enzymes. When using data from recombinant CYPs, three scaling approaches are available; the relative abundance (RA) method, relative activity factors (RAFs), and intersystem extrapolation factors (ISEFs) (Table 8). In the RA approach, the intrinsic clearance of the substrate in a recombinant CYP incubation is multiplied by the average amount of the specific enzyme per microsomal protein (Becquemont *et al.*, 1998, Stringer *et al.*, 2009). An important limitation of this method, however, is that it does not allow for differences in CYP activities between recombinant enzymes and HLM (Crespi and Miller, 1999). In contrast, the RAF approach accounts for differences in activities between the two test systems, and is considered more reliable than the RA method (Stringer *et al.*, 2009). Here, a CYP-selective marker substrate is first incubated in both recombinant CYPs and HLM. The ratio of its metabolism rate in HLM and recombinant enzymes is then multiplied with the intrinsic clearance of the drug of interest (Table 8) (Crespi and Miller, 1999, Nakajima *et al.*, 1999). The ISEF approach is an extension of the RAF method and also incorporates CYP abundance data (Proctor *et al.*, 2004). The RA-, RAF-, and ISEF-adjusted $CL_{int,\ in\ vitro}$ values are then scaled to hepatic clearance according to Equations 10 and 11.

Table 8. Scaling approaches to predict drug clearance from *in vitro* data from recombinant CYP enzyme incubations.

Method	Definition	Unit	Adjusted $CL_{int,\ in\ vitro}$
RA	CYP_i abundance per microsomal protein	pmol CYP/mg protein	$CL_{int,\ in\ vitro} \times$ RA
RAF	$\frac{CL_{int,HLM}(marker\ reaction)}{CL_{int,CYP,i}\ (marker\ reaction)}$	pmol CYP/mg protein*	$CL_{int,\ in\ vitro} \times$ RAF
ISEF	$\frac{CL_{int,HLM}(marker\ reaction)}{CL_{int,CYP,i}\ (marker\ reaction)} \times \frac{1}{CYP_i\ abundance\ in\ HLM}$	-	$CL_{int,\ in\ vitro} \times$ ISEF $\times$ CYP_i abundance per microsomal protein

* If the CL_{int} values of the marker reactions are expressed in the same units, then RAF will be dimensionless. CL_{int}, intrinsic clearance; CYP, cytochrome P450; HLM, human liver microsomes; $_i$, specific isoform; ISEF, intersystem extrapolation factor; RA, relative abundance; RAF, relative activity factor.

5.2. Evaluation of enzyme inhibition

Prediction of drug-drug interaction studies based on *in vitro* inhibition (and induction) findings may be done using basic static models, mechanistic static models, and dynamic models. Static models compare the measured inhibition constants with a single, clinically relevant inhibitor concentration. Basic static models consider only one interaction mechanism at a time but can be combined to more mechanistic models. Assuming that the clinically observed substrate concentration is far below its K_m value, the degree of inhibition (measured as its ratio of intrinsic clearance in presence and absence of inhibitor, $CL_{int,\ i}/CL_{int}$) can be described by Equations 12 and 13 for direct and mechanism-based inhibition, respectively (Mayhew *et al.*, 2000, Ito *et al.*, 2005).

$$\frac{CL_{int,i}}{CL_{int}} = \frac{1}{1 + \frac{[I]}{K_i}} \qquad \text{(Equation 12.)}$$

$$\frac{CL_{int,i}}{CL_{int}} = \frac{k_{deg}}{k_{deg} + k_{obs}} = \frac{k_{deg}}{k_{deg} + \frac{k_{inact} \times [I]}{K_I + [I]}} \qquad \text{(Equation 13.)}$$

where k_{deg} is the degradation rate constant of the affected enzyme in the absence of inhibitor. Depending on whether inhibition in the liver or intestine is evaluated, enzyme degradation rates and inhibitors concentrations specific for these organs are used. Because of the inverse relationship between AUC and CL_{int}, the change in AUC of the substrate (defined as its ratio of AUC in presence and absence of inhibitor, AUC_i/AUC) can be calculated according to Equation 14 (Mayhew *et al.*, 2000, Wang *et al.*, 2004, Zhang *et al.*, 2007), assuming that the liver is the only organ for clearance.

$$\frac{AUC_i}{AUC} = \frac{1}{\frac{f_m}{CL_{int}/CL_{int,i}} + (1 - f_m)}$$ (Equation 14.)

where f_m is the fraction of the drug metabolised by the affected enzyme. Mechanistic static models combine several interaction processes. For instance, in Equation 15 direct and mechanism-based inhibition (denoted as A and B for Equations 12 and 13, respectively) are combined together with an induction parameter C, in different organs, to estimate the net interaction effect (Fahmi *et al.*, 2008, Fahmi *et al.*, 2009):

$$\frac{AUC_i}{AUC} = \left(\frac{1}{(A_H \times B_H \times C_H) \times f_m + (1 - f_m)}\right) \times \left(\frac{1}{(A_G \times B_G \times C_G) \times (1 - F_G) + F_G}\right)$$ (Equation 15.)

where $_H$ and $_G$ denote the liver and intestine (gut), respectively, and F_G is the fraction available after intestinal metabolism in the absence of inhibitor. In most cases, the inhibitor concentration at the enzyme site is unknown. Based on the hypothesis that only unbound drug diffuses into the hepatocyte, unbound plasma concentrations of the inhibitor are often used in these predictions (Pelkonen *et al.*, 2008). However, the unbound inhibitor concentration in plasma does not always equal the intracellular concentration in the hepatocyte; in particular very lipophilic drugs may accumulate in hepatocytes (von Moltke *et al.*, 1998). Obviously, selection of the inhibitor concentration will greatly affect the outcome of the prediction, and the available literature has not reached a consensus of which inhibitor concentrations to use in predictions. Various alternatives are available, including total and unbound steady state peak plasma concentrations of the inhibitor, average steady-state plasma concentrations, inhibitor concentrations in the portal vein, and estimated inhibitor concentrations in hepatocytes (Yamano *et al.*, 1999, Kanamitsu *et al.*, 2000, Ito *et al.*, 2004, Bachmann, 2006). For prediction of the interaction magnitude at the level of the intestine, the inhibitor concentration in the enterocytes can either be calculated (Rostami-Hodjegan and Tucker, 2004), or estimated by dividing the dose by 250 ml (Zhang *et al.*, 2008, FDA, 2012).

FDA proposes that the likelihood for an interaction should be based on the ratio of intrinsic clearance by the metabolising enzyme in the absence and presence of the inhibitor, labelled as the R value (FDA, 2012). The R values are obtained by inversion of Equations 12 and 13, for reversible and mechanism-based inhibition, respectively. When a basic model generates an R value of >1.1, when using total C_{max} of the inhibitor, a clinical evaluation of the interaction is recommended. EMA recommends clinical studies when $[I]/K_i$ for reversible inhibitors is ≥0.02, and for mechanism-based inhibitors when the R value is ≥1.25, when using the unbound mean C_{max} of the inhibitor (EMA, 2013). For mechanistic and dynamic models, a predicted change in the AUC ratio of the victim substrate of ≥1.25 (or ≤0.8 in case of induction) warrants a clinical study (FDA, 2012, EMA, 2013).

5.3. Physiologically based pharmacokinetic modelling

In silico modelling and simulations are becoming increasingly common in drug development (Rowland *et al.*, 2011). PBPK modelling is an instrument that can be used to predict the *in vivo* pharmacokinetics of drugs, and evaluate the effects of diverse intrinsic and extrinsic factors (such as other drugs) on their concentrations (FDA, 2012). As compared to static models, PBPK models are dynamic, thus simulating changes in drug concentrations over time.

A PBPK model consists of a system-dependent component and a drug-dependent component (Figure 9). The system-dependent module integrates physiological data on body fluid dynamics, tissue composition and sizes, abundance of drug receptors, drug-metabolising enzymes and membrane transporters in different tissues and organs (Zhao *et al.*, 2011). Thus, it forms a 'virtual human', which may range from simplified, truncated models containing only a few tissue/organ compartments to very complex systems comprising multiple compartments. 'Population-based' PBPK models generate different populations of these 'virtual humans', and can provide information related to variability and uncertainty of the pharmacokinetic profiles in different patient and ethnic subgroups (Rowland *et al.*, 2011, Zhao *et al.*, 2011).

The drug-dependent component contains *in vitro* and *in vivo* data of the drug of interest (Figure 9). Physicochemical parameters of the drug can be used to estimate its tissue partition characteristics, microsomal protein binding, and permeability (unless they have been experimentally determined) (Zhao *et al.*, 2011). Metabolism, transport and interaction data from *in vitro* studies are incorporated to the model. When comprehensive drug-dependent *in vivo* parameters are not available, the construction of a PBPK model relies mainly on *in vitro* and *in silico* data. As *in vivo* data is obtained, it is integrated into the model to refine it. Thus, the model is constantly evolving as more information is acquired. Model validation is crucial when developing a PBPK model, and is done by comparing simulated pharmacokinetic profiles with those from available clinical studies (Rowland *et al.*, 2011, Zhao *et al.*, 2011).

Incorporation of *in vitro* data on the intrinsic clearance and identities of the enzymes and transporters involved in the pharmacokinetics of a drug can be used to predict its elimination and liability to drug-drug interactions. Interaction simulations link two or more drug-dependent components (drugs) to the system-dependent component. PBPK simulations can be especially useful for simulating time-dependent events such as mechanism-based inhibition and induction. Except for standard pharmacokinetic and interaction simulations, well-designed PBPK models incorporating inter-individual variability can also be used to optimise clinical study designs, and project pharmacokinetics profiles under different scenarios and in different patient populations (Zhao *et al.*, 2011).

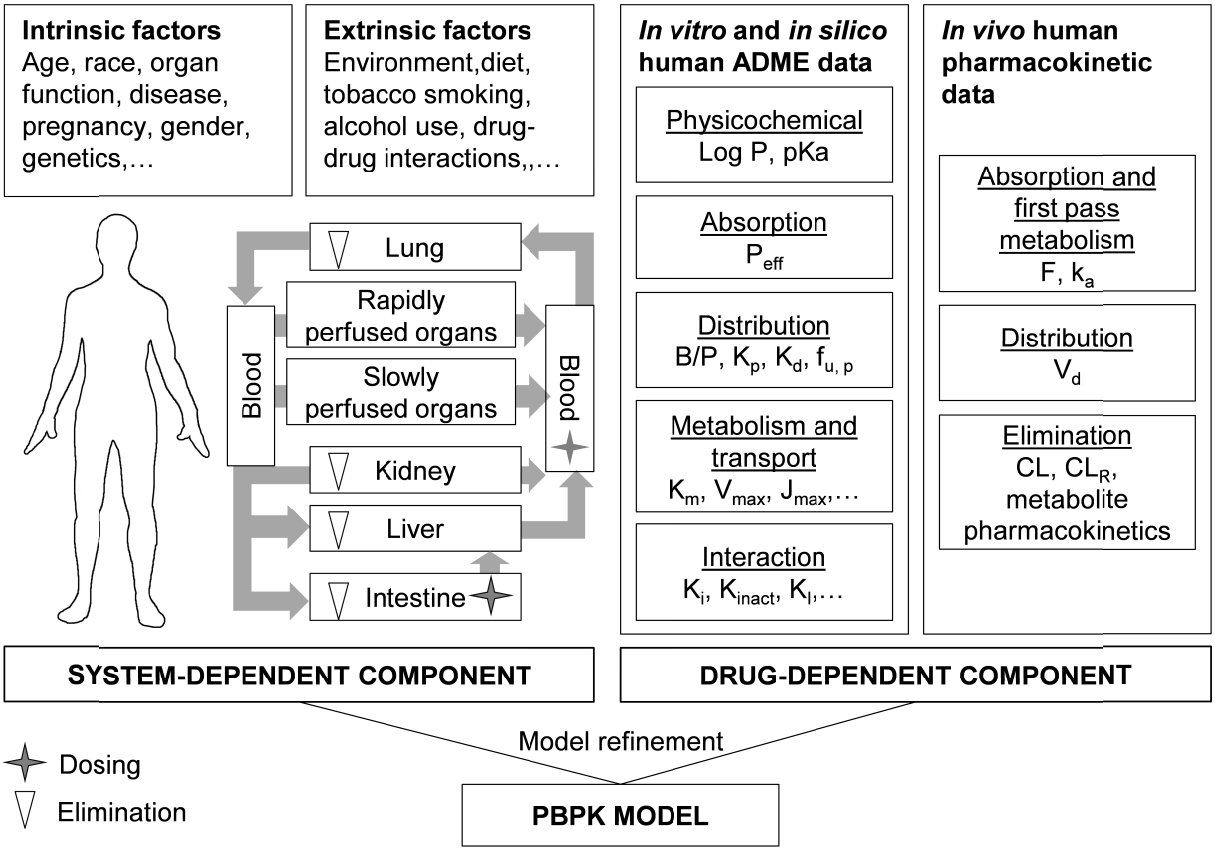

Figure 9. Components of a PBPK model (modified from Zhao *et al.* (2011)). B/P, blood-to-plasma ratio; CL, clearance; CL_R, renal clearance; F, bioavailability; $f_{u,\,p}$, unbound fraction in plasma; J_{max}, maximum transporter-mediated flux; k_a, absorption rate constant; K_d, dissociation constant; K_i, reversible inhibition constant; K_I, inhibitor concentration supporting half of the maximal rate of inactivation; k_{inact}, maximal rate of inactivation; K_m, Michaelis-Menten constant; K_p, tissue-to-plasma partition coefficient; Log P, logarithm of octanol-water partition coefficient; P_{eff}, effective permeability; V_d, distribution volume; V_{max}, maximum velocity.

6. *In vivo* studies of pharmacokinetic drug-drug interactions in drug development

Pharmacokinetic drug-drug interaction studies in humans are generally designed to compare substrate concentrations with and without the perpetrator drug. Because a specific study can address a number of questions and clinical objectives, several study designs for investigating drug-drug interactions can be considered. In drug development, the published guidelines by EMA and FDA assist and direct the pharmaceutical industry when investigating the interaction potential of drug candidates (FDA, 2012, EMA, 2013).

Study design. In general, cross-over designs in which the same subjects receive substrate with and without the perpetrator drug are considered most efficient. Typical study designs include randomised cross-over (victim drug followed by victim drug + perpetrator drug or

victim drug + perpetrator drug followed by victim drug), one-sequence cross-over (victim drug followed by victim drug + perpetrator drug), or parallel (victim drug in one group of subjects and substrate + perpetrator drug in another group) schemes (FDA, 2012, EMA, 2013). The selection of design depends on several factors, including dosing, interaction mechanism, safety considerations *etc*. Due to the risk of confounding inter-individual variability, a parallel group design is usually not preferred. However, it can be useful in cases where it is not possible to perform cross-over or one-sequence studies. Unless pharmacodynamics endpoints are critical to the assessment of the interaction, clinical interaction studies can usually be performed as open studies (FDA, 2012, EMA, 2013).

Substrate and perpetrator drugs. A probe substrate should be used when testing whether the drug candidate inhibits or induces a specific enzyme or transporter. In order to see the largest impact of the interaction potential of the drug candidate, the selected probe should be one whose pharmacokinetics is markedly altered by co-administration of known specific inhibitors/inducers of the affected pathway. Cocktail approaches may be used to investigate the effect on several enzymes and transporters simultaneously. When testing the drug candidate for the possibility that its metabolism is inhibited or induced, known inhibitors/inducers of the pathway studied should be selected. Comparison of drug pharmacokinetics in poor and extensive metabolisers may replace interaction studies for a particular pathway when the drug is metabolised by a polymorphic enzyme (FDA, 2012, EMA, 2013).

Dose. Several dosing regimens of the interacting drugs can be used, including both single and multiple doses of the victim and perpetrator (FDA, 2012, EMA, 2013). When possible, the perpetrator and victim drugs should be dosed so that the exposures of both drugs are relevant to their clinical use, including the highest doses (steady state) likely to be used in clinical practice. For a drug under investigation, the administration route should be the one planned for clinical use, but lower doses can be used if there are safety concerns.

Timing of administration. Additional factors include consideration of the sequence of administration and the time interval between dosing of victim drug and perpetrator (FDA, 2012). A rapid reversible inhibitor may be administered either just before or simultaneously with the substrate to ensure maximum exposure to the two drugs together. An inducer or mechanism-based inhibitor, however, should be administered before the victim drug to maximise the effect. The maximum effect is expected to occur when the affected enzyme has reached a new steady state level. Timing of administration is particularly critical in complex interaction situations, such as concurrent inhibition and induction. Furthermore, it is important to evaluate the duration of the interaction effect after the perpetrator drug has been eliminated (FDA, 2012, EMA, 2013).

Subjects. Pharmacokinetic interaction studies are usually performed in healthy volunteers unless safety considerations preclude their participation (FDA, 2012, EMA, 2013). In some cases, the use of patients offers advantages, such as the opportunity to study pharmacodynamic markers not present in or relevant to healthy subjects. The subject number should be based on considerations taking into account intra-subject variability and the magnitude of the effect considered relevant to detect. Because the extent of drug interactions may vary depending on the genotype for the enzyme or transporter being evaluated, genotyping can be carried out when appropriate. Studies in polymorphic subpopulations are recommended when possible (FDA, 2012).

Endpoints. Changes in pharmacokinetic parameters are generally used to assess the clinical importance of drug-drug interactions (FDA, 2012, EMA, 2013). Pharmacokinetic exposure of the victim drug such as AUC, peak concentration (C_{max}), time to C_{max} (t_{max}), and others as appropriate should always be obtained. In some cases, obtaining the pharmacokinetics of the perpetrator drug may also be of interest, in particular when the study intends to assess possible changes in the disposition of both drugs. In addition, in some cases, measurement of pharmacodynamic endpoints in addition to pharmacokinetic parameters may be useful. The sampling frequency should be adequate to allow accurate determination of the relevant measures and/or parameters for the victim drug and its metabolites (FDA, 2012, EMA, 2013).

7. Drugs studied

7.1. Montelukast

Montelukast (orig. Singulair, MK-0476; Merck), a potent and selective leukotriene receptor antagonist, is widely used in treatment of asthma. It is also indicated for exercise-induced bronchoconstriction and allergic rhinitis (Singulair Label, 2013). Montelukast was approved in 1997 (Young, 2012). Before the patent expiration in 2012, Singulair was among the top ten most prescribed drugs in the United States (Bartholow, 2012). For adults, the recommended dosing of montelukast is 10 mg once daily (Singulair Label, 2013).

The success of montelukast has been attributed to its efficacy and safety (Paggiaro and Bacci, 2011). In clinical studies, montelukast has been administrated at doses up to 200 mg once daily to patients for 22 weeks and up to 900 mg once daily for one week, without clinically important adverse effects (Singulair Label, 2013). The most common adverse reactions reported in trials (with an incidence exceeding 5% and greater than placebo) include upper respiratory infection, fever, headache, pharyngitis, cough, gastrointestinal disorders, otitis media, influenza, rhinorrhoea, sinusitis and otitis (Singulair Label, 2013). However, during post-approval use, several other adverse reactions have been associated with montelukast use,

including hypersensitivity reactions, psychiatric symptoms, and hepatobiliary disorders (Singulair Label, 2013, Calapai *et al.*, 2014).

Pharmacological mechanism. In human airways, montelukast binds to cysteinyl leukotrienes (CysLT) type-1 receptors located in smooth muscle cells and other pro-inflammatory cells such as eosinophils and certain myeloid stem cells (Singulair Label, 2013). Thus, it prevents the effects of cysteinyl leukotrienes, such as airway oedema, smooth muscle contraction and other respiratory inflammation. Montelukast may also inhibit symptoms of allergic rhinitis by binding to receptors in the nasal mucosa.

Montelukast pharmacokinetics. Montelukast has a high molecular weight (586.2 g/mol) and is strongly lipophilic (logarithm of octanol/water partition coefficient of 9.0-9.5) (HSDB, 2008, Mougey *et al.*, 2009). Following oral administration, it is absorbed rapidly, has a bioavailability of 60-70%, is highly bound to plasma proteins, and has an elimination half-life of about 3-7 h (Table 9). In the liver, montelukast is extensively metabolised to one major and several minor metabolites (Figure 10), which are excreted in bile (Balani *et al.*, 1997). Following an oral dose of radiolabelled montelukast, 86% of the radioactivity was recovered in faeces and <1% in urine, within five days (Balani *et al.*, 1997). 36-hydroxy montelukast (diastereomeric; M6a and M6b) is the major metabolite in plasma. M6 binds to the $CysLT_1$ receptor with almost the same potency as montelukast *in vitro* (Singulair Clinical Pharmacology and Biopharmaceutic Review(s), 1998), but its *in vivo* relevance to the therapeutic effect of montelukast is unknown. Other primary metabolites of montelukast include a phenol (M3) and diastereomeric 21-hydroxylated metabolites (M5a and M5b). A diastereomeric dicarboxylic acid (M4), generated from the further metabolism of M6, is the main metabolite found in bile, followed by M3, M6, and M5 (Balani *et al.*, 1997). In addition, small amounts of an acyl glucuronide (M1) and sulfoxides (diastereomeric; M2a and M2b) are found in bile.

Before 2010, CYP2C9 and CYP3A4 were considered to be the most important enzymes involved in the metabolism of montelukast (Figure 10). Early *in vitro* studies concluded that M6 is formed by CYP2C9, while the formation of M5 and M2 was mediated by CYP3A4 (Chiba *et al.*, 1997). CYP2A6 also catalysed M2 formation. However, in this previous study, high montelukast concentrations (100-500 μM) were used, corresponding to more than 20,000-fold its unbound clinically relevant concentrations in plasma. In addition, CYP2C8 and CYP3A5 were not included in the CYP screening, and the enzymes forming M3, M4 and the M1 glucuronide were not investigated. In 2008, an X-ray crystallography study showed that montelukast binds to the active site cavity of CYP2C8, so that its benzyl ring is positioned near the haem iron of CYP2C8 (Schoch *et al.*, 2008). Because the montelukast metabolites M3, M4, and M6 result from the oxidation of its benzyl ring, this finding together with the fact that it is a competitive CYP2C8 inhibitor *in vitro* (Walsky *et al.*, 2005a, Walsky *et al.*, 2005b), suggests that montelukast may actually be a substrate of CYP2C8.

Table 9. Pharmacokinetic profile of montelukast.

Parameter	Value	References
F	0.58-0.67	(Cheng *et al.*, 1996, Zhao *et al.*, 1997, Singulair Clinical Pharmacology and Biopharmaceutic Review(s), 1998)
t_{max}	2-4 h	(Cheng *et al.*, 1996, Zhao *et al.*, 1997, Hegazy *et al.*, 2012)
$V_{d, ss, iv}$	0.14-0.15 l/kg	(Cheng *et al.*, 1996, Zhao *et al.*, 1997, Singulair Clinical Pharmacology and Biopharmaceutic Review(s), 1998)
$f_{u, P}$	0.004	(Singulair Clinical Pharmacology and Biopharmaceutic Review(s), 1998)
B/P	0.65	(Singulair Clinical Pharmacology and Biopharmaceutic Review(s), 1998)
Metabolising enzymes	CYP2C9, CYP3A4	(Chiba *et al.*, 1997)
Elimination	Extensively metabolised, metabolites are excreted into bile and faeces (<1% of the dose is excreted renally)	(Balani *et al.*, 1997)
CL_{iv}	1.8-2.9 l/h	(Cheng *et al.*, 1996, Zhao *et al.*, 1997)
Terminal $t_{½}$	4.4-7.1 h	(Cheng *et al.*, 1996, Zhao *et al.*, 1997, Hegazy *et al.*, 2012)

B/P, blood-to-plasma ratio; CL_{iv}, intravenous clearance; CYP, cytochrome P450; F, bioavailability; $f_{u, P}$, unbound fraction in plasma; $t_{½}$, elimination half-life; t_{max}, time to peak concentration; $V_{d, ss, iv}$, distribution volume at steady state following intravenous doses.

Montelukast has been suggested to be a substrate of the uptake transporter OATP2B1 (Mougey *et al.*, 2009, Mougey *et al.*, 2011), but recent *in vitro* and *in vivo* studies have challenged this finding (Chu *et al.*, 2012, Kim *et al.*, 2013a, Tapaninen *et al.*, 2013, Brännström *et al.*, 2014).

Pharmacokinetic interactions of montelukast. Montelukast is a potent, competitive and selective inhibitor of CYP2C8 *in vitro* (Table 10) (Walsky *et al.*, 2005a, Walsky *et al.*, 2005b). However, it does not affect the pharmacokinetics of the CYP2C8 substrates pioglitazone, repaglinide, and rosiglitazone in healthy subjects (Jaakkola *et al.*, 2006b, Kajosaari *et al.*, 2006, Kim *et al.*, 2007). The lack of an *in vivo* inhibition suggests that the montelukast concentrations in hepatocytes are much lower than its K_i for CYP2C8, consistent with its very small unbound fraction in plasma.

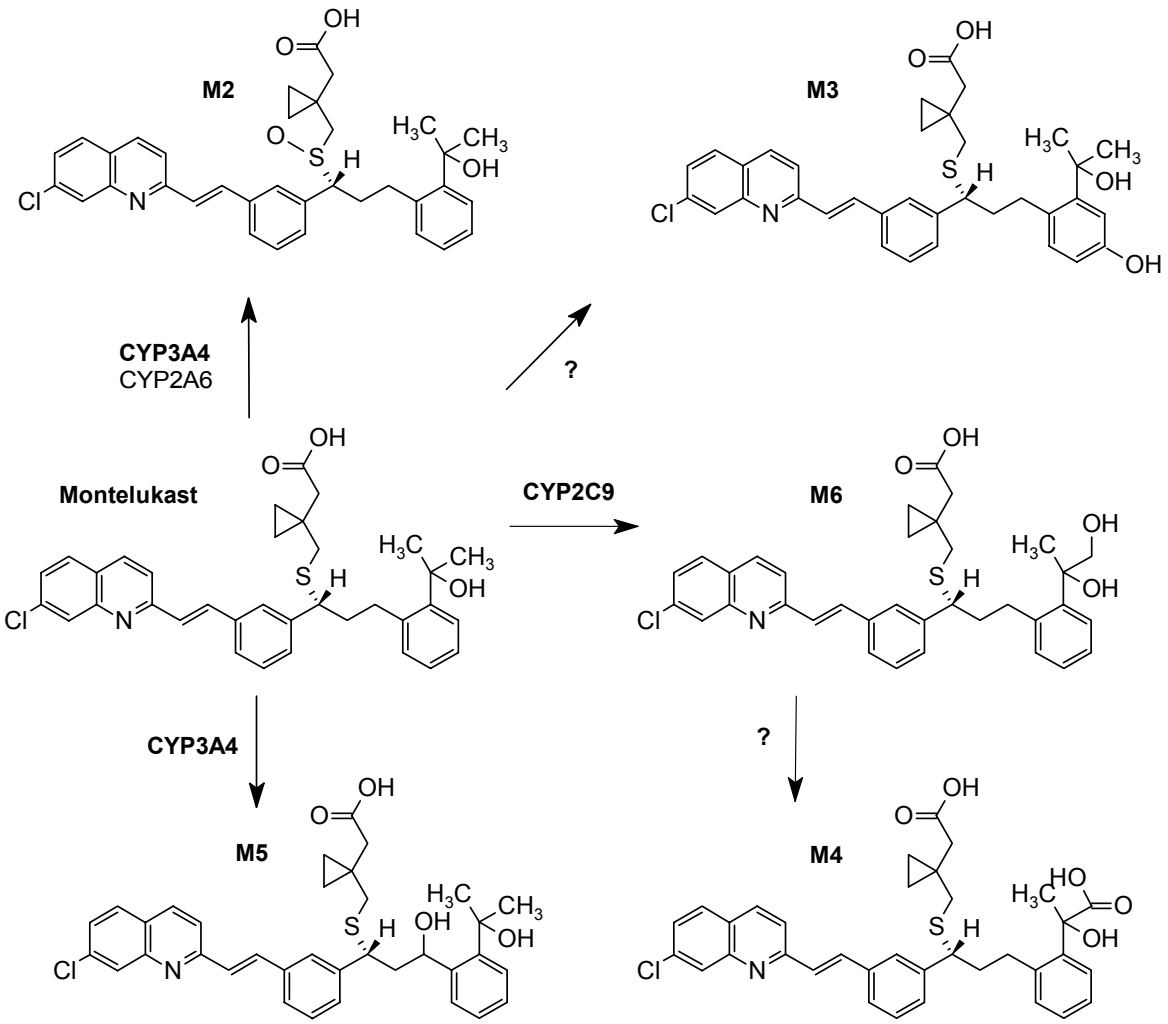

Figure 10. Oxidative metabolism of montelukast according to previous studies (Balani *et al.*, 1997, Chiba *et al.*, 1997, Singulair Clinical Pharmacology and Biopharmaceutic Review(s), 1998). In a mass balance study (Balani *et al.*, 1997), M5 and M6 were found both in plasma and bile, while M1 (an acyl glucuronide; not shown), M2, M3, and M4 were only detected in bile.

In general, montelukast has had only a small or no effect on other drugs. Doses of montelukast 10 mg once daily had no or only a minor effect on the plasma exposure to digoxin, terfenadine, theophylline, and warfarin (Malmstrom *et al.*, 1998, Singulair Clinical Pharmacology and Biopharmaceutic Review(s), 1998, Van Hecken *et al.*, 1999). However, at a very high dose of 600 mg once daily, montelukast reduced the AUC of theophylline by 66% (Malmstrom *et al.*, 1998), possibly due to induction of CYP1A2. Furthermore, high doses of montelukast 200 mg once daily had no effect on prednisolone concentrations, but the AUC of prednisone was reduced by 29% (Singulair Clinical Pharmacology and Biopharmaceutic Review(s), 1998). Montelukast has been routinely administered together with other drugs used in asthma treatment without increased observations of adverse drug reactions (Singulair Label, 2013).

Table 10. Inhibitory effects of montelukast on CYP enzymes *in vitro*. Its inhibition potency on CYPs decreases with increasing protein concentration, due to non-specific binding to proteins (Walsky *et al.*, 2005b).

Inhibited enzyme	IC_{50} (μM)	K_i (μM)	Test system	References
CYP1A2	16	-	HLM	(Walsky *et al.*, 2005b)
	90	-	n/a	(Korzekwa, 2014)
CYP2A6	11	-	HLM	(Walsky *et al.*, 2005b)
CYP2B6	5.95	-	Recombinant CYP	(Walsky *et al.*, 2006)
	11	-	HLM	(Walsky *et al.*, 2005b)
CYP2C8	0.02-2.0	0.014-0.15	HLM	(Walsky *et al.*, 2005a,
	0.0092	0.0092	Recombinant CYP	Walsky *et al.*, 2005b)
	0.02	0.05	Recombinant CYP	(Floyd *et al.*, 2012)
	0.022	0.013	HLM	(Perloff *et al.*, 2009)
	0.27	-	n/a	(Korzekwa, 2014)
CYP2C9	1.2	-	HLM	(Walsky *et al.*, 2005b)
	-	15	HLM	(Chiba *et al.*, 1997)
	12	-	n/a	(Korzekwa, 2014)
CYP2C19	32	-	HLM	(Walsky *et al.*, 2005b)
	>100	-	n/a	(Korzekwa, 2014)
CYP2D6	11	-	HLM	(Walsky *et al.*, 2005b)
	81	-	n/a	(Korzekwa, 2014)
CYP2E1	180	-	HLM	(Walsky *et al.*, 2005b)
CYP3A4	1.2-7.9	-	HLM	(Walsky *et al.*, 2005b)
	-	200	HLM	(Chiba *et al.*, 1997)
	26	-	n/a	(Korzekwa, 2014)

CYP, cytochrome P450; HLM, human liver microsomes; IC_{50}, inhibitor concentration producing 50% inhibition; K_i, reversible inhibition constant; n/a, not available.

With regard to the effect of other drugs on montelukast concentrations, the inducer phenobarbital has decreased the plasma exposure to montelukast by 38% (Singulair Clinical Pharmacology and Biopharmaceutic Review(s), 1998). Roflumilast and desloratadine had no effect on the pharmacokinetics of montelukast (Bohmer *et al.*, 2009, Cingi *et al.*, 2013). Fluconazole at steady state decreased montelukast AUC by 39%, while clarithromycin at a dose of 1000 mg daily for two days, increased montelukast AUC by 2.4-fold (Hegazy *et al.*, 2012). The suggested interaction mechanisms included an interaction of fluconazole with transporters involved in the intestinal absorption of montelukast, mechanism-based inhibition of CYP3A4 by clarithromycin or clarithromycin-induced changes in the transporter-mediated uptake of montelukast into the liver.

Montelukast has been suggested to be a substrate of OATP2B1 *in vitro* and *in vivo* (Mougey *et al.*, 2009). The *SCLO2B1* polymorphism c.935G>A has been associated with a ~30% lower plasma concentration of montelukast and an impaired drug response in patients with the c.935GA genotype, as compared to carriers of the c.935GG genotype (Mougey *et al.*, 2009). In another study, co-administration of grapefruit juice and orange juice did not affect the

plasma exposure to montelukast, as compared to control. On the other hand, when stratified by genotype, orange juice caused a significant reduced montelukast AUC in c.935GG, but not in c.935GA genotypes (Mougey *et al.*, 2011). However, in other studies, c.935G>A and two other *SCLO2B1* polymorphisms, c.1475C>T and c.601G>A, had no effect on montelukast pharmacokinetics in healthy volunteers (Kim *et al.*, 2013a, Tapaninen *et al.*, 2013), thus suggesting that OATP2B1 appears to be a minor determinant of montelukast pharmacokinetics. These findings are supported by recent *in vitro* studies (Chu *et al.*, 2012, Brännström *et al.*, 2014).

7.2. Imatinib

Imatinib (orig. Gleevec, Glivec, CGP57148B, STI-571; Novartis) is a tyrosine kinase inhibitor used in the treatment of chronic myelogenous leukaemia (CML), gastrointestinal tumours (GISTs), and acute lymphoblastic leukaemia (ALL). It is also indicated for the treatment of certain other hematologic and oncologic malignancies, such as aggressive systemic mastocytosis, hypereosinophilic syndrome, and chronic eosinophilic leukaemia (Gleevec label, 2014). The recommended dosing of imatinib is typically 400 or 600 mg once daily.

Imatinib was the first rationally designed protein kinase inhibitor at the time of its approval in 2001. With high response rates and safety, it is one of the first examples of a successful targeted-therapy for cancer. The majority of adverse reactions related to imatinib treatment has been classified as mild or moderate. In patients, the most frequently reported adverse reactions include oedema, nausea, vomiting, muscle cramps, musculoskeletal pain, diarrhoea, rash, fatigue, and abdominal pain (Gleevec label, 2014).

Pharmacological mechanism. The Philadelphia chromosome, found in almost all cases of CML and in about 5-25% of cases of ALL (Clark *et al.*, 1988, Cortes *et al.*, 1995), is formed by a reciprocal translocation between chromosomes 9 and 22. The translocation results in a gene fusion of breakpoint cluster region (BCR) and ABL. Depending on the breakpoint in the BCR-ABL hybrid gene, three different fusion proteins can be generated (Melo, 1996). As compared to the native ABL protein, all three proteins exhibit deregulated tyrosine kinase activity leading to a block of apoptosis, and are associated with CML, BCR-ABL-positive ALL and/or BCR-ABL positive chronic neutrophilic leukaemia to various degrees (Melo, 1996, Pane *et al.*, 1996). Imatinib inhibits the ABL and BCR-ABL tyrosine kinases. It is a competitive antagonist of the ATP binding site; by occupying the binding site of the ABL kinase domain, imatinib prevents a change in the conformation of the protein that would otherwise convert the molecule to its active form (Druker *et al.*, 1996). Binding of imatinib thereby leads to apoptosis of the target cells. Imatinib also interacts with other targets; it inhibits the platelet-derived growth factor receptors α and β (PDGFRα and PDGFRβ), colony

stimulating factor 1 receptor, and c-KIT (Buchdunger *et al.*, 2000, Heinrich *et al.*, 2000, Dewar *et al.*, 2005), important in, e.g. chronic eosinophilic leukaemia and GISTs.

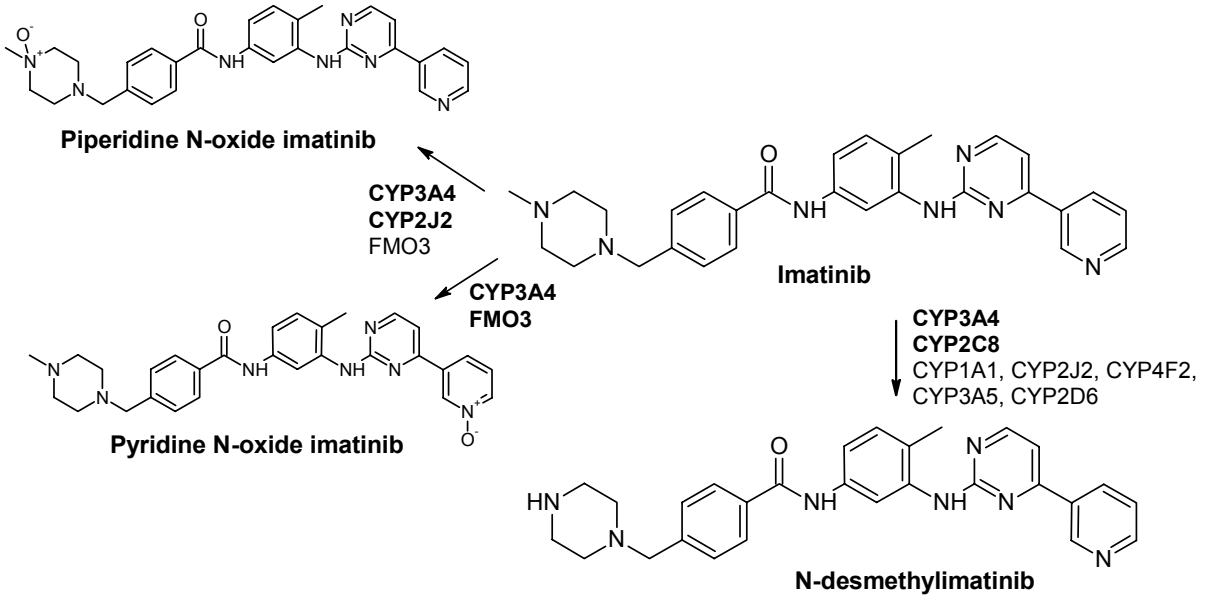

Figure 11. Metabolism of imatinib. Imatinib, its main metabolite N-desmethylimatinib, and two of its minor metabolites, piperidine N-oxide imatinib (M6) and pyridine N-oxide imatinib (M8). Imatinib is considered to primarily undergo metabolism by CYP3A4, but several other enzymes also participate in its biotransformation (Gleevec Clinical Pharmacology and Biopharmaceutic Review(s), 2001, Rochat *et al.*, 2008, Nebot *et al.*, 2010, Narjoz *et al.*, 2014). CYP, cytochrome P450; FMO, flavin-containing monooxygenase.

Imatinib pharmacokinetics. The molecular weight of imatinib is 493.60 g/mol, and its logarithm of octanol/water partition coefficient is 1.99 (Peng *et al.*, 2005). Following oral administration, imatinib is rapidly and completely absorbed (Table 11). It is mainly eliminated via metabolism and biliary-faecal excretion (Gschwind *et al.*, 2005). Following a single radiolabelled imatinib dose, approximately 80% of the dose was excreted within one week in faeces (67% of the dose) and urine (13% of dose). Parent imatinib accounted for 28% of the administered dose (23% faeces, 5% urine), while its main metabolite N-desmethylimatinib (CGP74588) accounted for 13% (11% faeces, 2% urine) (Gschwind *et al.*, 2005). N-desmethylimatinib is pharmacologically active and shows comparable biologic activity *in vitro* as imatinib (Gleevec Clinical Pharmacology and Biopharmaceutic Review(s), 2001). In addition to N-desmethylimatinib, imatinib has several minor metabolites, including oxidative metabolites and their phase II conjugates (Gschwind *et al.*, 2005, Marull and Rochat, 2006, Rochat *et al.*, 2008, Ma *et al.*, 2009). The sum of the excreted fractions of minor metabolites, including piperidine N-oxide imatinib and pyridine N-oxide imatinib (Figure 11), was ~10% of the administered dose (Gschwind *et al.*, 2005).

Imatinib has been considered to principally undergo metabolism by CYP3A4 (Gleevec Clinical Pharmacology and Biopharmaceutic Review(s), 2001, Rochat *et al.*, 2008), but in 2010 an *in vitro* study suggested that CYP2C8 contributes to the formation of N-desmethylimatinib (Figure 11) (Nebot *et al.*, 2010). Other enzymes that have been suggested to participate in its metabolism to a smaller degree include CYP1A2, CYP2C9, CYPC19, CYP2D6, CYP3A5, CYP4F, FMO3, and the extrahepatic enzymes CYP1A1, CYP1B1, and CYP2J2 (Gleevec Clinical Pharmacology and Biopharmaceutic Review(s), 2001, Rochat *et al.*, 2008, Narjoz *et al.*, 2014). *In vitro*, imatinib is a substrate and inhibitor of several transporters, but their *in vivo* significance in imatinib pharmacokinetics has not yet been established, apart from the role of OCT1 in uptake of imatinib to leukocytes and leukaemic cells (Burger *et al.*, 2005, Eechoute *et al.*, 2011b, Wang *et al.*, 2012, Eadie *et al.*, 2014).

Table 11. Pharmacokinetic profile of imatinib.

Parameter	Value	References
F	0.98	(Gleevec Clinical Pharmacology and Biopharmaceutic Review(s), 2001, Peng *et al.*, 2004a, Gleevec label, 2014)
t_{max}	1-4 h	(Bornhauser *et al.*, 2004, le Coutre *et al.*, 2004, Peng *et al.*, 2005, Gleevec label, 2014)
$V_{d, ss}$	1.9-5.7 l/kg	(Gambacorti-Passerini *et al.*, 2003, le Coutre *et al.*, 2004, Bornhauser *et al.*, 2005, Al-Batran *et al.*, 2007, Treiber *et al.*, 2008)
$f_{u, P}$	0.04-0.05	(Kretz *et al.*, 2004, Peng *et al.*, 2005)
B/P	0.73	Estimated from Kretz *et al.* (2004)
Main metabolising enzymes	CYP2C8, CYP3A4, CYP3A5	(Gleevec Clinical Pharmacology and Biopharmaceutic Review(s), 2001, Rochat *et al.*, 2008, Nebot *et al.*, 2010)
Elimination	Metabolism, excreted into faeces (~85%) and urine (~15%) as both unchanged drug and metabolites.	(Gschwind *et al.*, 2005)
CL_{iv}	14 l/h	(Peng *et al.*, 2004a)
Terminal $t_{½}$	8-27 h	(le Coutre *et al.*, 2004, Nikolova *et al.*, 2004, Peng *et al.*, 2005, Treiber *et al.*, 2008)

B/P, blood-to-plasma ratio; CL_{iv}, intravenous clearance; CYP, cytochrome P450; F, bioavailability; $f_{u, P}$, unbound fraction in plasma; $t_{½}$, elimination half-life; t_{max}, time to peak concentration; $V_{d, ss}$, distribution volume at steady state.

Despite its efficacy and favourable pharmacokinetic profile, there is a large inter-individual variability in imatinib plasma concentrations, which may lead to treatment failure and disease progression (Peng *et al.*, 2004b, Schmidli *et al.*, 2005, Picard *et al.*, 2007). It has been estimated that 30-35% of imatinib-treated patients will fail to respond or lose their response (Eadie *et al.*, 2014). Suggested resistance mechanisms include mutations or amplification of

the drug target, epigenetic modification, activation of alternative signalling pathways, poor treatment compliance, and alterations in cellular uptake and efflux of imatinib (Mahon *et al.*, 2003, Thomas *et al.*, 2004, Apperley, 2007). In addition, variability in CYP3A4 expression activity has been proposed to partly explain the observed variations in imatinib concentrations (Peng *et al.*, 2005, Apperley, 2007). Several studies indicate a correlation between imatinib trough levels and efficacy, suggesting that imatinib trough concentrations above 1,000-1,100 ng/ml are associated with a better treatment outcome (Teng *et al.*, 2012, de Wit *et al.*, 2014).

Pharmacokinetic interactions of imatinib. Imatinib inhibits several CYPs competitively *in vitro* (Table 12), such as CYP2D6 and CYP3A4 with K_i values of 7.5 and 8 µM, respectively (Gleevec Clinical Pharmacology and Biopharmaceutic Review(s), 2001). Taking into account that unbound imatinib concentrations in plasma are generally below 0.3 µM, its effects on CYP3A4 *in vivo* seem to be of greater magnitude than what would be predicted based on its *in vitro* inhibition. In healthy volunteers, imatinib has increased the plasma concentrations of the CYP3A4 substrate simvastatin by 3.5-fold, with individual concentrations ranging up to >ten-fold (O'Brien *et al.*, 2003). In another studies, imatinib has reduced the hepatic CYP3A4 activity by 10-70% (Gurney *et al.*, 2007, Connolly *et al.*, 2011). Despite similar K_i values for CYP2D6 and CYP3A4 inhibition, as compared to the interaction study with simvastatin, imatinib had only a small effect on the CYP2D6 substrate metoprolol pharmacokinetics in Chinese patients (AUC increase of 26%) (Wang *et al.*, 2008). In addition, imatinib had no effect on paracetamol pharmacokinetics in Korean patients (Kim *et al.*, 2011).

Table 12. Inhibitory effects of imatinib and N-desmethylimatinib on CYP enzymes in HLM (Gleevec Clinical Pharmacology and Biopharmaceutic Review(s), 2001).

Inhibited enzyme	Imatinib	N-desmethylimatinib
CYP1A2	IC_{50} = 410 µM	n/a
CYP2A6	IC_{50} = 230 µM	n/a
CYP2C8	IC_{50} = 99 µM	n/a
CYP2C9	K_i = 34.7 µM	K_i = 40.3 µM
CYP2C19	IC_{50} = 120 µM	n/a
CYP2D6	K_i = 7.5 µM	K_i = 13.5 µM
CYP3A4	K_i = 8 µM	K_i = 13.7 µM

CYP, cytochrome P450; HLM, human liver microsomes; IC_{50}, inhibitor concentration producing 50% inhibition; K_i, reversible inhibition constant; n/a, not available.

Although CYP3A4 has been suggested to be the main enzyme involved in imatinib metabolism, strong CYP3A4 inhibitors have only had a small or no effect on its pharmacokinetics (Table 13). Following a single dose of the strong CYP3A4 inhibitor ketoconazole, the AUC of imatinib increased by 1.4-fold in healthy volunteers (Dutreix *et al.*, 2004), while ritonavir, another potent CYP3A4 inhibitor, had no effect on imatinib steady state pharmacokinetics in patients (van Erp *et al.*, 2007). Furthermore, in patients, the clearance of the CYP3A4 substrates erythromycin and midazolam correlated with imatinib

clearance at the beginning of imatinib therapy, but no longer at steady state (Gurney *et al.*, 2007). An interaction study with Japanese patients was terminated early when the results indicated no effect on grapefruit juice on imatinib pharmacokinetics (Kimura *et al.*, 2011). The lack of effect was explained by the fact that grapefruit juice primarily inhibits intestinal CYP3A4, and because the bioavailability of imatinib is nearly 100%, no effect on the concentrations of imatinib was observed. The effect of ketoconazole on imatinib pharmacokinetics suggests that CYP3A4 contributes to about 30% of the total clearance of imatinib, following a single imatinib dose.

In patients, CYP enzyme-inducing anti-epileptic drugs such as carbamazepine, phenytoin, and oxcarbazepine reduced the trough plasma concentrations of imatinib by up to 70% as compared to controls (Pursche *et al.*, 2008). In other studies, omeprazole, aluminium hydroxide, magnesium, and tobacco smoking did not affect imatinib pharmacokinetics (van Erp *et al.*, 2008, Egorin *et al.*, 2009, Sparano *et al.*, 2009), thus suggesting that CYP1A1, CYP1A2, and CYP2C19 do not contribute to the metabolism of imatinib *in vivo*, and that elevation of gastric pH does not affect its absorption.

Table 13. Effects of other drugs on imatinib pharmacokinetics *in vivo*.

Parameter	Ketoconazole	Rifampicin	Ritonavir	St John's Wort
Perpetrator dose	400 mg, sd	600 mg, od for eleven days	600 mg, od for three days	300 mg, td for two weeks
Imatinib dose	200 mg, sd	400 mg, sd	400 - 800 mg, od	400 mg, sd
Change in imatinib				
C_{max}	↑ 1.3-fold	↓ 54%	↔	↓ 15-29%
AUC	↑ 1.4-fold	↓ 74%	↔	↓ 30-32%
$t_{½}$	↔	↓ 47%	n/d	↓ 21-30%
Change in N-desmethylimatinib				
C_{max}	↓ 23%	↑ 1.9-fold	↔	↑ 1.1-fold
AUC	↔	↓ 12%	↑ 1.4-fold	↔
$t_{½}$	↔	↓ 10%	n/d	n/d
References	(Dutreix *et al.*, 2004)	(Bolton *et al.*, 2004)	(van Erp *et al.*, 2007)	(Frye *et al.*, 2004, Smith *et al.*, 2004a, Smith *et al.*, 2004b)

AUC, area under concentration-time curve; C_{max}, peak concentration; n/d, not determined; od, once daily; sd, single dose; $t_{½}$, elimination half-life; td, thrice daily.

7.3. Gemfibrozil

Gemfibrozil (Lopid; Pfizer) is a lipid-regulating agent that shares many properties with fibric acid derivates (Miller and Spence, 1998). It has been used in the treatment of hyperlipidaemia and hypertriglyceridemia for more than 30 years.

Pharmacological mechanism. The pharmacological mechanism of action of gemfibrozil is not fully understood (Miller and Spence, 1998). It is an activator of peroxisome proliferator-activated receptor alpha (PPARα), a nuclear receptor involved in metabolism of carbohydrates and fats, and adipose tissue differentiation. Activation of PPARα by gemfibrozil has several effects, including increase in the synthesis of lipoprotein protease, increase in the clearance of triglycerides, stimulation of mobilisation of cholesterol towards the cell membrane, and stimulation of high-density lipoprotein (HDL) production (Miller and Spence, 1998, Roy and Pahan, 2009).

Gemfibrozil is usually administered as 600 mg twice daily, while some patients will respond to 900 mg daily (Todd and Ward, 1988). Gemfibrozil is in general well-tolerated (Todd and Ward, 1988). However, it has a complex interaction profile, which makes it not suitable to use concomitantly with certain drugs.

Gemfibrozil pharmacokinetics. Following oral administration, gemfibrozil is completely and rapidly absorbed, reaching peak plasma concentrations at 1-2 h (Okerholm *et al.*, 1976, Miller and Spence, 1998). It is extensively bound to plasma proteins (>97%), and its distribution volume is ~0.2 l/kg (Todd and Ward, 1988). Gemfibrozil is mainly metabolised by UGT2B7 to gemfibrozil 1-*O*-β glucuronide (Figure 12) (Mano *et al.*, 2007), but also undergoes oxidation, resulting in hydroxymethyl and carboxymethyl metabolites (Miller and Spence, 1998, Lopid Label, 2013). Approximately 70% of the dose is excreted renally, with <2% as unchanged drug (Okerholm *et al.*, 1976, Lopid Label, 2013). The plasma half-life of gemfibrozil is ~1.5 h following multiple doses, but a value of 7.6 h has also been reported (Okerholm *et al.*, 1976, Todd and Ward, 1988, Miller and Spence, 1998, Lopid Label, 2013).

Pharmacokinetic interactions. Gemfibrozil and gemfibrozil 1-*O*-β glucuronide inhibit several enzymes and transporters. Most importantly, gemfibrozil inhibits CYP2C9 and CYP2C8 *in vitro* with K_i values of 5.8-18.6 μM and 55.4 μM, respectively (Wen *et al.*, 2001, Fujino *et al.*, 2003), while its glucuronide metabolite is a potent, irreversible mechanism-based inhibitor of CYP2C8 with k_{inact} and K_I values of 0.21 1/min and 20-52 μM, respectively (Ogilvie *et al.*, 2006, Baer *et al.*, 2009, Jenkins *et al.*, 2011). Inhibition of CYP2C8 by gemfibrozil 1-*O*-β glucuronide explains the strong effects of gemfibrozil on the plasma exposure to many drugs *in vivo* (Table 14). While gemfibrozil markedly affects the pharmacokinetics of CYP2C8 substrates *in vivo*, its effect on the CYP2C9 substrate warfarin is weak (Lilja *et al.*, 2005). The combination of gemfibrozil and itraconazole increased the

AUC of the CYP2C9 and CYP3A4 substrate nateglinide by 47% (Niemi *et al.*, 2005a). The effect of gemfibrozil on pravastatin, rosuvastatin, and simvastatin (Table 14), which are not at all, or only partly, metabolised by CYP2C8, is likely due to inhibition of OATP1B1. Gemfibrozil inhibits this transporter competitively *in vitro* with IC_{50} and K_i values in the range of 4-32 µM, and gemfibrozil 1-*O*-β glucuronide inhibits it with IC_{50} and K_i values of 16-23 µM (Schneck *et al.*, 2004, Shitara *et al.*, 2004, Yamazaki *et al.*, 2005, Hirano *et al.*, 2006, Nakagomi-Hagihara *et al.*, 2007b). In addition, gemfibrozil inhibits OAT3 (IC_{50} 6.8 µM) and OAT2B1 (IC_{50} 8 µM), and its glucuronide inhibits OAT3 with an IC_{50} of 20 µM (Ho *et al.*, 2006, Nakagomi-Hagihara *et al.*, 2007a).

Furthermore, gemfibrozil has been reported to induce CYP2C8, CYP3A4, and UGT1A1 *in vitro* (Prueksaritanont *et al.*, 2005), but the *in vivo* relevance of the induction is not known. No effect of gemfibrozil on brivaracetam, fluvastatin, zafirlukast, and zopiclone has been observed (Spence *et al.*, 1995, Tornio *et al.*, 2006, Karonen *et al.*, 2011, Nicolas *et al.*, 2012).

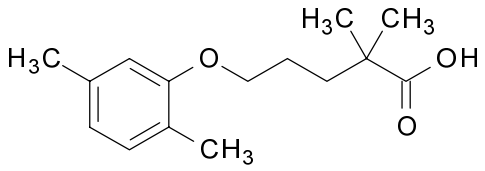

Gemfibrozil

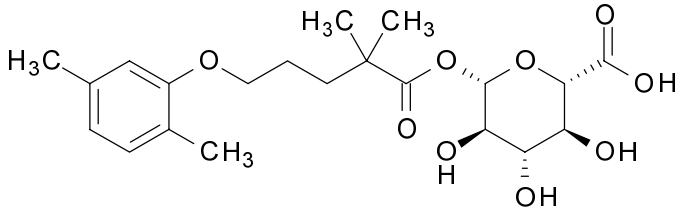

Gemfibrozil 1-*O*-β glucuronide

Figure 12. Chemical structures of gemfibrozil and gemfibrozil 1-*O*-β glucuronide.

Table 14. Effect of gemfibrozil on the pharmacokinetics of other drugs in healthy subjects. Gemfibrozil 600 mg twice daily for three or more days was used as pretreatment in the studies.

Victim drug	Dose	Change in C_{max}	AUC	$t_{½}$	References
Atorvastatin acid	20 mg	↑ 1.2-fold	↑ 1.2-fold	↓ 16%	(Backman *et al.*, 2005)
Cerivastatin acid	0.3 mg	↑ 3.1-fold	↑ 5.6-fold	↑ 2.7-fold	(Backman *et al.*, 2002)
Dabrafenib*	75 mg**	n/a	↑ 1.5-fold	n/a	(Tafinlar label, 2014)
Enzalutamide	160 mg	↓ 18%	↑ 4.3-fold	n/a	(Xtandi Clinical Pharmacology and Biopharmaceutic Review(s), 2012)
Ezetimibe*	10 mg**	↑ 1.3-fold	↑ 1.4-fold	n/a	(Zetia Clinical Pharmacology and Biopharmaceutic Review(s), 2001)
Glimepiride	0.5 mg	↔	↑ 1.2-fold	↑ 1.1-fold	(Niemi *et al.*, 2001)
R-ibuprofen	400 mg***	↔	↑ 1.3-fold	↑ 1.5-fold	(Tornio *et al.*, 2007)
Loperamide	4 mg	↑ 1.6-fold	↑ 2.2-fold	↑ 1.4-fold	(Niemi *et al.*, 2006)
Lovastatin acid	40 mg	↑ 2.8-fold	↑ 2.8-fold	n/d	(Kyrklund *et al.*, 2001)
Pioglitazone	15 mg	↔	↑ 4.3-fold	↑ 3.1-fold	(Aquilante *et al.*, 2013a)
	15 mg	↔	↑ 3.2-fold	↑ 2.7-fold	(Jaakkola *et al.*, 2005)
	30 mg	↔	↑ 3.4-fold	↑ 2.2-fold	(Deng *et al.*, 2005)
Pitavastatin (acid)	4 mg**	↑ 1.3-fold	↑ 1.5-fold	n/a	(Mathew *et al.*, 2004)
Pravastatin	40 mg	↑ 1.8-fold	↑ 2.0-fold	↔	(Kyrklund *et al.*, 2003)
Repaglinide	0.25 mg	↑ 2.0-fold	↑ 7.0-fold	↑ 1.9-fold	(Honkalammi *et al.*, 2012)
		↑ 2.7-fold	↑ 7.6-fold	↑ 2.0-fold	(Backman *et al.*, 2009)
		↑ 2.2-fold	↑ 7.0-fold	↑ 2.6-fold	(Tornio *et al.*, 2008)
		↑ 2.4-fold	↑ 8.1-fold	↑ 2.9-fold	(Niemi *et al.*, 2003b)
Rosiglitazone	4 mg	↑ 1.2-fold	↑ 2.3-fold	↑ 2.1-fold	(Niemi *et al.*, 2003a)
Rosuvastatin	80 mg	↑ 2.2-fold	↑ 1.9-fold	↔	(Schneck *et al.*, 2004)
Simvastatin acid	40 mg	↑ 2.1-fold	↑ 2.9-fold	↑ 1.5-fold	(Backman *et al.*, 2000)
Sitagliptin	100 mg	↑ 1.2-fold	↑ 1.6-fold	↑ 1.3-fold	(Arun *et al.*, 2012)
R-warfarin	10 mg***	↔	↓ 6%	↔	(Lilja *et al.*, 2005)
S-warfarin	10 mg***	↔	↓ 11%	↔	(Lilja *et al.*, 2005)

* Unclear whether the study was performed in healthy volunteers. ** Multiple doses. *** Administered as racemic drug. AUC, area under concentration-time curve; C_{max}, peak concentration; n/a, not available; n/d, not determined; od, once daily; sd, single dose; $t_{½}$, elimination half-life; td, thrice daily.

AIMS OF THE STUDY

The aim of this thesis was to determine the role of CYP2C8 in the *in vitro* and *in vivo* metabolism of montelukast and imatinib.

The specific aims of the studies were:

I To establish the importance of CYP2C8 in the *in vitro* metabolism of montelukast using human liver microsomes and recombinant CYP enzymes.

II To determine the effects of the CYP2C8 inhibitor gemfibrozil on the pharmacokinetics of montelukast in healthy subjects. In addition, to investigate the effects of gemfibrozil and gemfibrozil 1-*O*-β glucuronide on the *in vitro* metabolism of montelukast in human liver microsomes.

III To determine the inhibitory effects of imatinib on CYP2C8 and CYP3A4 activities in human liver microsomes.

IV To establish the importance of CYP2C8 in the *in vitro* metabolism of imatinib using human liver microsomes and recombinant CYP enzymes. In addition, to construct a physiologically based pharmacokinetic model for imatinib in order to translate *in vitro* findings to clinical relevance.

V To determine the effects of the CYP2C8 inhibitor gemfibrozil on the pharmacokinetics of imatinib in healthy subjects. In addition, to apply the physiologically based pharmacokinetic model to these data in order to predict the contribution of CYP2C8 to imatinib metabolism during multiple-dose administration.

MATERIALS AND METHODS

The work consisted of *in vitro*, *in silico*, and *in vivo* studies according to Figure 13.

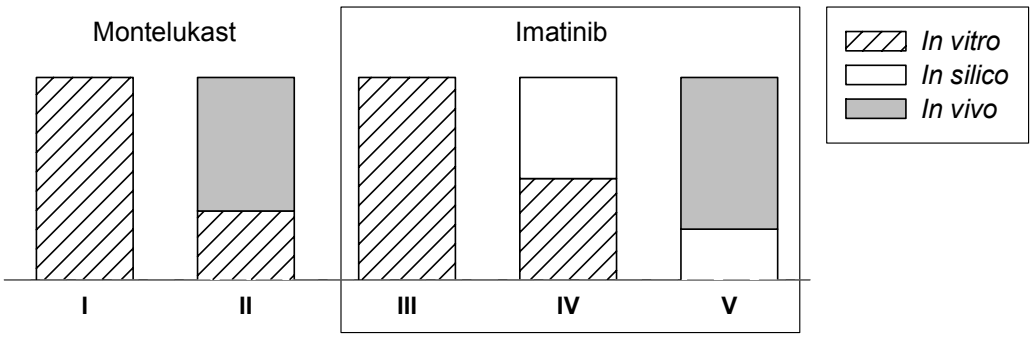

Figure 13. Overview of the content of studies **I**-**V**.

8. *In vitro* studies (Studies I-IV)

In vitro experiments were carried out in studies **I**-**IV**. The *in vitro* metabolism of montelukast was investigated in study **I**. Study **II** included an *in vitro* assessment of the inhibitory effects of gemfibrozil and gemfibrozil 1-*O*-β glucuronide on the main metabolic pathway of montelukast. In study **III**, the inhibitory effects of imatinib and N-desmethylimatinib on CYP2C8 and CYP3A4/5 activities were evaluated. Finally, in study **IV**, the *in vitro* metabolism of imatinib was investigated. Detailed descriptions of chemicals, microsomes, and experiments are presented in the respective publications. This section briefly summarises the most important methods used in these studies.

8.1. Microsomes and chemicals

Pooled HLM and recombinant CYPs (CYP1A2, CYP2A6, CYP2B6, CYP2C8, CYP2C9, CYP2C19, CYP2D6, CYP2E1, CYP3A4, and CYP3A5) were purchased from BD Biosciences (BD Gentest; Woburn, MA, USA). The study drugs, their metabolites, inhibitors, and other chemicals were obtained from commercial sources.

8.2. *In vitro* conditions and assays

Incubation conditions. All incubations contained sodium phosphate buffer (0.1 M, pH 7.4), microsomes, and substrate. Addition of 1.0 mM NADPH initiated the reactions. Incubations in studies **I** and **II** also contained 5.0 mM $MgCl_2$. With the exception of some experiments,

the incubations generally contained a protein concentration of 0.1, 0.05, 0.1, and 0.5 mg/ml in studies **I**, **II**, **III**, and **IV**, respectively. The equal protein concentration in recombinant enzyme incubations resulted in variable CYP isoform contents. Compounds were dissolved in acetonitrile, ethanol, or methanol, and the final solvent concentration was 1% in all incubations (including controls). As appropriate, the incubation time was optimised within the linear range for metabolite formation depending on the turnover conditions of each specific experiment. Incubations were carried out in Eppendorf tubes as duplicates or triplicates in a shaking water bath (37ºC). Samples were taken at determined time points, added to a solvent solution containing internal standard, and put on ice to stop the reactions.

Table 15. CYP-selective inhibitors used in inhibition experiments in studies **I** and **IV**.

Inhibitor	Inhibited CYP	Inhibitor concentration (μM)	References
Furafylline*	CYP1A2	20	(Newton *et al.*, 1995, Eagling *et al.*, 1998)
8-methoxy-psoralen*	CYP2A6	0.5	(Draper *et al.*, 1997, Koenigs *et al.*, 1997)
Clopidogrel*	CYP2B6	1	(Richter *et al.*, 2004)
Gemfibrozil 1-*O*-β glucuronide*	CYP2C8	60	(Ogilvie *et al.*, 2006)
Montelukast	CYP2C8	5 (**IV**)	(Walsky *et al.*, 2005b)
Trimethoprim	CYP2C8	100 (**I**)	(Wen *et al.*, 2002)
Sulfaphenazole	CYP2C9	10	(Baldwin *et al.*, 1995, Newton *et al.*, 1995, Eagling *et al.*, 1998)
Omeprazole	CYP2C19	10	(Ko *et al.*, 1997)
Quinidine	CYP2D6	10	(Newton *et al.*, 1995, Bourrie *et al.*, 1996)
Diethyldithio-carbamate*	CYP2E1	100	(Guengerich *et al.*, 1991, Newton *et al.*, 1995, Eagling *et al.*, 1998)
Ketoconazole	CYP3A4/5	1	(Baldwin *et al.*, 1995, Eagling *et al.*, 1998)
Troleandomycin*	CYP3A4/5	50 (**IV**), 100 (**I**)	(Newton *et al.*, 1995)

* Mechanism-based inhibitors. Compared to direct inhibition experiments, where substrate and inhibitor were simultaneously added to the incubation, mechanism-based inhibitors were first pre-incubated for 15 min with HLM and NADPH before addition of substrate. In the case of gemfibrozil 1-*O*-β glucuronide, the inhibitor was first pre-incubated for 30 min with a high HLM concentration (2 and 10 mg/ml in studies **I** and **IV**, respectively) and NADPH before a 20-fold dilution to another tube containing substrate and NADPH. CYP, cytochrome P450.

Metabolism of montelukast. In study **I**, inhibition of the metabolism of montelukast was investigated by incubating montelukast at concentrations of 0.02-0.4 μM and CYP-selective inhibitors (Table 15) with HLM. Thereafter, the metabolism of montelukast at a high concentration (1 μM) was first studied in a recombinant CYP screening containing each of the ten CYPs individually. Based on the results, lower, clinically more relevant montelukast concentrations (0.02-0.1 μM) were further incubated with CYP2A6, CYP2C8, CYP2C9, CYP3A4, and CYP3A5. In addition, the enzyme kinetics of M6 formation from montelukast (0.03-30 μM) by CYP2C8 and CYP2C9 was investigated. As CYP2A6 has previously been reported to participate in montelukast metabolism, it was also tested with a high montelukast

concentration of 10 μM. Finally, further metabolism of M6 (0.02-1 μM) was studied using recombinant CYPs.

In study **II**, the effects of gemfibrozil (1-320 μM) and gemfibrozil 1-O-β glucuronide (0.2-3240 μM) on the formation of M6 from montelukast (0.05 μM) and that of M4 from M6 (0.2 μM) in HLM were tested in an IC_{50} experiment. Gemfibrozil 1-O-β glucuronide was first pre-incubated for 30 min with a high HLM concentration (2 mg/ml) and NADPH, before dilution (40-fold) to another tube containing substrate and NADPH.

CYP2C8 and CYP3A4/5 inhibition by imatinib and N-desmethylimatinib. In study **III**, amodiaquine N-deethylation and midazolam 1′-hydroxylation were used as marker reactions for CYP2C8 and CYP3A4/5 activities, respectively. First, IC_{50}-shift experiments in HLM were carried out with imatinib (0.25-500 μM) and N-desmethylimatinib (0.25-500 μM), using substrate concentrations of 2 μM. In addition, the effects of piperidine N-oxide imatinib and pyridine N-oxide imatinib (0.1-10 μM) on CYP2C8 and CYP3A4/5 were studied. To evaluate time-dependent inhibition of CYP3A4 by imatinib, imatinib (2-128 μM) was pre-incubated with NADPH and HLM (0.5 mg/ml) for up to 30 min, before a 20-fold dilution to another tube containing midazolam (8 μM) and NADPH. Follow-up experiments included an experiment with ketoconazole (0.01-1 μM) and dialysis with sodium phosphate buffer, as well as testing of mechanism-based inhibition potential of imatinib in recombinant CYP3A4 and CYP3A5 incubations. Direct K_i experiments were also carried out for imatinib (5-30 μM) and N-desmethylimatinib (5-30 μM) using substrate concentrations of 0.6-20 μM in HLM.

Metabolism of imatinib. In study **IV**, the depletion of imatinib (0.1 μM) and metabolite formation from imatinib (1 μM) was first investigated using recombinant CYP screening. Then, the kinetics of N-desmethylimatinib formation from imatinib (0.10-320 μM) in CYP2C8, CYP3A4, and CYP3A5 incubations was determined. Next, inhibition of imatinib metabolism (1 or 0.1 μM) by CYP-selective inhibitors was studied in HLM (Table 15). Finally, the further metabolism of N-desmethylimatinib (0.05-1 μM) was studied using HLM and recombinant CYPs.

8.3. Determination of drug concentrations

After sample preparation (protein precipitation or protein precipitation and solid phase extraction), the concentrations of the study drugs and their metabolites were determined using liquid chromatography-tandem mass spectrometry (LC-MS/MS) (MDS Sciex, Concord, ON, Canada) (Table 16). No authentic reference compounds were available for montelukast metabolites M3, M4, and M5a/b in studies **I** and **II**, nor for piperidine N-oxide imatinib, pyridine N-oxide imatinib, and hydroxyl benzylic imatinib (M5) in study **IV**. Their concentrations were therefore measured as arbitrary units based on the ratio of the peak height

of each metabolite to that of the internal standard in the chromatogram. A signal/noise ratio of 10:1 was used as the limit of quantification of these metabolites.

Table 16. Quantification of analytes in *in vitro* studies.

Study	Analytes quantified	Lower limit of quantification	Interday CV
I	Montelukast	2 nM	<14%
	M6	2.5 nM	<19%
II	Montelukast	3.8 nM (2.2 ng/ml)	<17%
	M6	3.7 nM (2.2 ng/ml)	<10%
III	N-desethylamodiaquine	1 nM	<18%
	1'-hydroxymidazolam	2 nM	<13%
IV	Imatinib	5 nM	<15%
	N-desmethylimatinib	10 nM	<15%

CV, coefficient of variation.

8.4. Data analysis

Mean values of duplicate or triplicate incubations were used in calculations.

Enzyme kinetics and substrate depletion. In studies **I** and **IV**, the enzyme kinetics of montelukast 36-hydroxylation (M6 formation) and imatinib N-demethylation were analysed using SigmaPlot version 9.01 (Systat Software Inc., San Jose, CA, USA). Selection of the best model was based on the Akaike information criterion (AIC), on r^2, and on the examination of Michaelis-Menten plots. SigmaPlot was also used to calculate k_{dep} values of the depletion of montelukast, montelukast M6, imatinib, and N-desmethylimatinib concentrations. $CL_{int,\ in\ vitro}$ values were calculated according to Equations 8 and 9.

Enzyme inhibition. In CYP-selective inhibition experiments in studies **I** and **IV**, per cent inhibition of montelukast and imatinib depletion was calculated by comparing k_{dep} values of incubations containing inhibitor with those of control incubations. In studies **II** and **III**, IC_{50} values were determined by non-linear regression analysis with SigmaPlot. For determination of direct inhibition K_i values in study **III**, selection of the best-fit enzyme inhibition model in SigmaPlot was based on AIC and on r^2 (primary criteria), and on the visual examination of different inhibition plots (secondary criterion when AIC and r^2 of different models were similar or when these values were conflicting with each other). In study **III**, imatinib was investigated for time-dependent inhibition of CYP3A4. For estimation of its metabolism-dependent inactivation constants, pre-incubation time dependent loss of CYP3A4 activity in the absence of imatinib was accounted for by adjusting the observed rate of metabolism with reference to the respective control incubation at each pre-incubation time. k_{obs} was determined by linear regression analysis of the natural logarithm of the percentage of remaining activity versus pre-incubation time. Initial estimates of K_I and k_{inact} were obtained from the Kitz-

Wilson plot (Kitz and Wilson, 1962), while final K_I and k_{inact} values were estimated by non-linear regression using Equation 7.

9. *In vitro-in vivo* predictions (Studies I and III-V)

9.1. Static models

Metabolism of montelukast. To estimate the relative contributions of different CYPs to the metabolism of montelukast in study **I**, RAF values were calculated for CYP2C8, CYP2C9 and CYP3A4 using activity information provided by the manufacturer for the recombinant CYP and HLM batches used. For comparison, the relative contributions of CYP2C8, CYP2C9, CYP3A4, and CYP3A5 to montelukast metabolism were also estimated using the RA approach. RAF and RA adjusted $CL_{int,\ in\ vitro}$ values and HLM $CL_{int,\ in\ vitro}$ were converted to hepatic clearance using standard *in vitro-in vivo* scaling parameters and the well-stirred model (Equation 11). Blood clearance (CL_B) of montelukast was calculated according to Equation 16:

$$CL_B = CL_P \times \frac{1}{C_B/C_P} \quad \text{(Equation 16.)}$$

where CL_P is the *in vivo* plasma clearance of montelukast (0.578 ml/min) (Singulair Pharmacology Review(s), 2002), and C_B/C_P is the blood/plasma concentration ratio of montelukast (0.65) (Singulair Clinical Pharmacology and Biopharmaceutic Review(s), 1998). The unbound fraction of montelukast in blood was assumed to correspond to that in plasma (0.004) (Singulair Pharmacology Review(s), 2002),

CYP2C8 and CYP3A4/5 inhibition by imatinib. In study **III**, the potential clinical impact of the inhibition of CYP2C8 and CYP3A4/5 by imatinib was predicted by use of static models considering the f_m and F_G of the substrates. In the calculations, K_i and K_I were adjusted for non-specific binding to microsomes. Hepatic CYP3A4 half-lives of 36 and 72 h were used in the predictions (Yang *et al.*, 2008, Rowland Yeo *et al.*, 2011), which were carried out for clinically relevant unbound plasma concentrations of imatinib.

Metabolism of imatinib. In study **IV**, to estimate the relative contributions of different CYPs to imatinib and N-desmethylimatinib metabolism, $CL_{int,\ in\ vitro}$ values, adjusted for non-specific binding in microsomes, were multiplied with ISEFs of each CYP isoform and with average CYP isoform abundance per microsomal protein. The obtained values were scaled to *in vivo* CL_H using standard scaling factors and the well-stirred model (Equation 11).

9.2. Physiologically based pharmacokinetic simulations

In study **IV**, *in vitro* inhibition and metabolism data from studies **III** and **IV** were combined with literature data to create the drug-dependent component of a PBPK model for imatinib and N-desmethylimatinib. The model was created within the Simcyp Population-Based Simulator (version 11.00; Simcyp Ltd., Sheffield, UK). PBPK simulations were carried out to predict the importance of CYP2C8 and CYP3A4 in imatinib pharmacokinetics. After completion of the clinical trial in study **V**, the models of imatinib and N-desmethylimatinib were refined in Simcyp version 12.00 to better match the obtained clinical findings (Figure 14). Simulations were subsequently conducted to estimate the contribution of CYP2C8 to imatinib metabolism during multiple-dose administration, and to provide a possible explanation for the unexpected effect of gemfibrozil on imatinib absorption observed *in vivo*. Detailed descriptions of the models and simulations are presented in the respective publications. Here, an overview of these dynamic predictions is given.

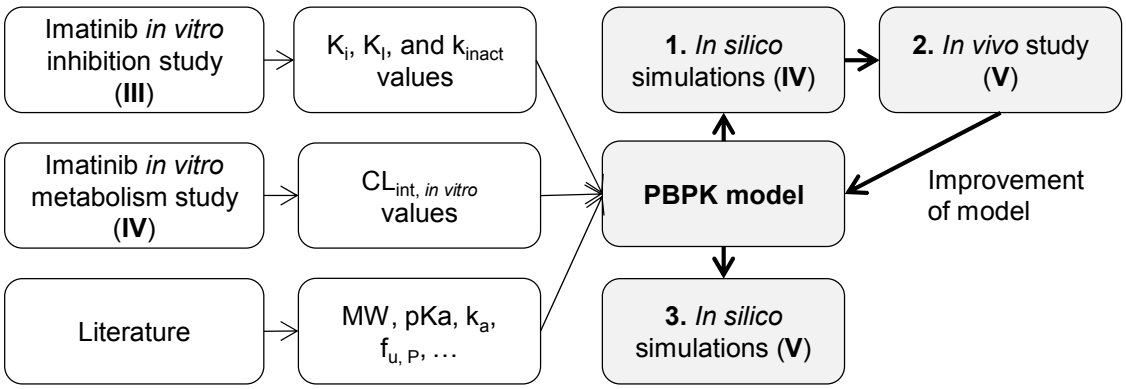

Figure 14. Construction of the PBPK model for imatinib and N-desmethylimatinib. Data from two *in vitro* studies (**III** and **IV**) was combined with literature data to create the drug-dependent component of a PBPK model for imatinib and its metabolite. After the clinical study (**V**) in healthy volunteers, the PBPK model was refined to better match the obtained clinical data. CL_{int}, intrinsic clearance; $f_{u,\ p}$, fraction unbound in plasma; k_a, absorption rate constant; K_i, inhibition constant; K_I, inactivation constant; k_{inact}, maximal inactivation rate; MW, molecular weight; PBPK, physiologically based pharmacokinetic.

PBPK simulations in study IV. Initial PBPK models for imatinib and N-desmethylimatinib comprised first-order oral absorption of imatinib from the intestine, intestinal metabolism, a minimal physiologically based distribution model including a single adjusting compartment, and elimination by hepatic CYP-mediated metabolism, and by renal excretion. Hepatic elimination input parameters were obtained from the *in vitro* data of study **IV**. ISEF factors for CYP2C8, CYP3A4, and CYP3A5 were experimentally determined, while ISEFs for CYP1A2, CYP2B6, and CYP2D6 were provided by the software. ISEFs and other software-generated parameters were then used to scale $CL_{int,\ in\ vitro}$ to CL_H with the well-stirred model. Hepatic and renal clearances were combined with additional systemic clearance to derive the total clearance. When literature and experimental values had been entered into the drug-dependent component, the model was refined by modifying the single adjusting compartment,

so that published single-dose pharmacokinetic data could be described accurately (Nikolova *et al.*, 2004). Thereafter, the model was validated by comparing simulations to published multiple-dose pharmacokinetic studies and interaction studies (Bolton *et al.*, 2004, Dutreix *et al.*, 2004, van Erp *et al.*, 2007). In addition, PBPK models for gemfibrozil and gemfibrozil 1-*O*-β glucuronide were constructed to allow interaction simulations with a CYP2C8 inhibitor. Final simulations were conducted aiming to estimate the roles of CYP2C8 and CYP3A4 in the *in vivo* pharmacokinetics of imatinib (Table 17).

PBPK simulations in study V. Based upon the findings of the clinical study, the initial models for imatinib and N-desmethylimatinib were slightly modified: imatinib additional clearance was increased to better match the proportion excreted as unchanged imatinib in faeces (~25%), the unbound fraction of imatinib in plasma was reduced, and an advanced absorption and dissolution model was chosen to simulate imatinib absorption so that an apical uptake transport mechanism could be included. In addition, the additional compartment of N-desmethylimatinib was modified. The refined model was validated by comparing the simulated time-concentration profile with that of the clinical study (**V**), and with previous studies (Bolton *et al.*, 2004, Dutreix *et al.*, 2004, van Erp *et al.*, 2007).

In Simcyp version 12.00, default PBPK models for gemfibrozil and gemfibrozil 1-*O*-β glucuronide were included in the software. However, to better match the clinical data of study **V**, they were slightly adjusted, and a transporter inhibition constant was included so that inhibition of an apical transporter involved in imatinib absorption by gemfibrozil could be tested. Simulations were conducted to estimate the role of CYP2C8 to imatinib metabolism during multiple-dose administration, and to provide a potential explanation for the unexpected effect of gemfibrozil on imatinib absorption observed *in vivo* (Table 17).

Table 17. Main PBPK simulations of studies **IV** and **V**.

Study		Description
IV	1	Multiple dose simulation with imatinib 100 or 400 mg once daily or 400 mg twice daily.
	2	Interaction simulations with gemfibrozil (600 mg twice daily), itraconazole (100 mg twice daily), or their combination on imatinib pharmacokinetics after a single or multiple doses of imatinib 400 mg.
	3	Simulation of the effects of CYP2C8 polymorphisms on imatinib pharmacokinetics after multiple doses of imatinib 400 mg.
V	1	Interaction simulation with gemfibrozil (600 mg twice daily) on the pharmacokinetics of a single dose of imatinib 200 mg, when inhibition of an intestinal uptake transporter by gemfibrozil was included in or excluded from the model.
	2	Interaction simulation with gemfibrozil (600 mg twice daily) on imatinib pharmacokinetics after multiple doses of imatinib 200 mg or 400 mg once daily.

10. *In vivo* studies in humans (Studies II and V)

Two clinical drug-drug interaction studies (**II** and **V**) were carried out at the Department of Clinical Pharmacology, University of Helsinki. The study protocols were approved by the Coordinating Ethics Committee of the Helsinki and Uusimaa Hospital District, by the Helsinki University Central Hospital (HUSLAB), and by the Finnish Medicines Agency (Fimea).

10.1. Subjects

The subjects in the clinical studies were healthy volunteers. Before entering the studies, they had been given both oral and written information, and they had given a written informed consent. The number of subjects in the studies was estimated to be sufficient to detect a 30% difference between the phases in the $AUC_{0-\infty}$ of montelukast and imatinib with a power of >80% (α-level 5%). Ten subjects were chosen for the studies.

The subjects (Table 18) were ascertained to be healthy by medical history, physical examination and routine laboratory tests. None of them used continuous medication such as oral contraceptives and none was a tobacco smoker. Female subjects gave a negative pregnancy test before entering the studies. Participation in other studies and blood donation were prohibited two months before and during the studies. Use of alcohol, grapefruit, and any medications was not allowed one week prior to each study day.

Table 18. Characteristics of the subjects in studies **II** and **V**.

	II	**V**
Subjects n (female/male)	10 (4/6)	10 (2/8)
Age (y)	23 ± 2	24 ± 3
Weight (kg)	69 ± 11	72 ± 13
BMI (kg/m2)	23 ± 3	22 ± 2
*CYP2C8*1/*1* genotype	7/10	8/10
*CYP2C8*1/*3* genotype	2/10	1/10
*CYP2C8*1/*4* genotype	1/10	1/10
*CYP3A5*1/*3* genotype	1/10	n/d
*CYP3A5*3/*3* genotype	9/10	n/d

Age, weight, and body mass index are presented as mean ± standard deviation. BMI, body mass index; n/d, not determined.

10.2. Study design

Both studies had a randomised, placebo-controlled cross-over (all subjects completing both phases) design (Table 19). The studies consisted of two phases, which included a pre-

treatment period with gemfibrozil or placebo, followed by ingestion of a single oral dose of the study drug on the study day (day 3). Gemfibrozil, placebo, and the study drugs (montelukast/imatinib) were supplied, packed, and labelled according to a randomisation list for each subject by the Helsinki University Central Hospital Pharmacy.

Table 19. Designs of *in vivo* studies **II** and **V**.

Study	Pre-treatment	Pre-treatment (days)	Wash-out period (weeks)	Study drug
II	1. Gemfibrozil 600 mg × 2 2. Placebo ×2	3	4	Montelukast 10 mg, single dose, on day 3 at 09:00
V	1. Gemfibrozil 600 mg × 2 2. Placebo × 2	6	2	Imatinib 200 mg, single dose, on day 3 at 09:00

After an overnight fast, the study drugs were administered orally with water at 09:00 on the study day, one hour after the morning dose of gemfibrozil. The subjects received a standardised warm meal three hours after the study drug intake. In study **II**, standardised light meals were served seven and 11 hours after montelukast intake. In study **V**, light meals were served six and nine hours after the intake of imatinib. The subjects were under medical supervision for 12 hours after administration of the study drug.

10.3. Blood sampling and determination of drug concentrations in plasma

Timed blood samples (5 or 10 ml in study **II**, 9 ml in study **V**), were drawn from a cannulated forearm vein before administration of the study drug and at determined time points. Samples were collected into ethylenediaminetetraacetic acid (EDTA) containing tubes. Plasma was separated within 30 min and stored at -70°C until analysis.

Plasma samples were spiked with internal standards. Montelukast and M6 concentrations and the metabolite-to-internal standard peak height ratios (M4, M5a, and M5b) were measured using a SCIEX API 2000 LC-MS/MS system (MDS Sciex, Toronto, ON, Canada), after protein precipitation (montelukast) or solid-phase extraction (metabolites). Imatinib plasma samples were spiked with internal standards, extracted to methyl tert-butyl ether and centrifuged at 2,500g for 10 min. The concentrations of imatinib and N-desmethylimatinib were measured using an Agilent 1100 series LC system (Agilent Technologies, Waldbronn, Germany) coupled to an API 3000 MS/MS system (MDS Sciex) (Table 20). The plasma concentrations of gemfibrozil and gemfibrozil 1-*O*-β glucuronide in studies **II** and **V** were determined using an API 2000 QTRAP LC-MS/MS system (MDS Sciex).

Table 20. Quantification of analytes in the two clinical studies.

Study	Analytes quantified	Lower limit of quantification	Interday CV
II	Montelukast	3.8 nM (2.2 ng/ml)	<17%
	M6	3.7 nM (2.2 ng/ml)	<10%
	Gemfibrozil	10 nM (0.0025 mg/l)	<4%
	Gemfibrozil 1-*O*-β glucuronide	5.9 nM (0.0025 mg/l)	<8%
V	Imatinib	6.1 nM (3 ng/ml)	<5%
	N-desmethylimatinib	6.3 nM (3 ng/ml)	<15%
	Gemfibrozil	1.0 µM (0.25 mg/l)	<4%
	Gemfibrozil 1-*O*-β glucuronide	0.59 µM (0.25 mg/l)	<7%

CV, coefficient of variation

10.4. Pharmacokinetic calculations

The pharmacokinetics of the study drugs, gemfibrozil, and metabolites were characterised by C_{max}, t_{max}, $t_{½}$, and AUC. C_{max} and t_{max} values were obtained directly from original data. The terminal log-linear part of each plasma concentration-time curve was identified visually. The elimination rate constant (k_e) was determined by linear regression analysis of the log-linear part of the plasma concentration-time curve. $t_{½}$ was calculated according to $t_{½} = \ln(2)/k_e$. AUC values were calculated using a combination of the linear and the log-linear trapezoidal rules, with extrapolation to infinity, when appropriate, by dividing the last measured concentration by k_e. The pharmacokinetics was calculated by non-compartmental analysis using MK-Model, version 5.0 (Biosoft, Cambridge, UK).

10.5. Statistical analysis

In study **II**, results were expressed as mean ± standard deviation. Due to updated journal guidelines, in study **V**, results were expressed as geometric mean values and coefficients of variation (or 95% confidence intervals; or 90% confidence intervals in figures). t_{max} was expressed as median (range) in both studies. In study **V**, logarithmic transformation was performed for pharmacokinetic variables (except for t_{max}) before statistical analysis. Statistical comparisons between the phases were made with the paired t-test or, in the case of t_{max}, with the Wilcoxon signed-rank test. Differences were considered statistically significant at $P < 0.05$. Statistical analyses were carried out using SPSS for Windows, version 17.0 (SPSS, Chicago, IL, USA) and PASW for Windows, version 18.0 (SPSS), in studies **II** and **V**, respectively.

RESULTS

11. Montelukast studies (I and II)

11.1. *In vitro* metabolism of montelukast

In studies **I** and **II**, CYP2C8 was found to play a major role in the metabolism of montelukast.

Montelukast. Among the ten recombinant CYPs tested, CYP2C8, CYP2C9, and CYP3A4 metabolised montelukast most extensively. The relative importance of CYP2C8 in its *in vitro* metabolism increased from about 14 to 68% as the concentration of montelukast was reduced from 1 μM to a more clinically relevant concentration of 0.02 μM (Figure 15). At 0.02 μM, CYP2C8 inhibitors and CYP3A4 inhibitors inhibited montelukast depletion in HLM by ~40-60%, while the CYP2C9 inhibitor did not affect it at all. CYP2A6 did not metabolise montelukast.

M6 and M4. In study **I**, M6 was formed by CYP2C8 (by ~75%) and CYP2C9 (by ~22%). Recombinant CYP2C8 formed M6 at a six-fold higher intrinsic clearance (V_{max}/K_m) than CYP2C9 (Figure 15). At montelukast 0.05 μM, M6 formation was inhibited by gemfibrozil 1-*O*-β glucuronide by 78%, while the inhibition by sulfaphenazole was weak (7%). Furthermore, while other CYPs did not form M4, CYP2C8 catalysed its formation. In study **II**, gemfibrozil 1-*O*-β glucuronide was 36-fold more potent than gemfibrozil as an inhibitor of M6 formation in HLM (Figure 15). Gemfibrozil 1-*O*-β glucuronide also inhibited the further metabolism of M6 to M4 more potently than did gemfibrozil.

M3. In study **I**, several CYP isoforms formed M3 from montelukast, 1 μM, but at 0.1 μM only CYP2C8 formed detectable M3 amounts. Among the CYP-selective inhibitors, gemfibrozil 1-*O*-β glucuronide inhibited M3 formation most strongly (by 49%).

M5a/b and M2. In study **I**, M5a/b was formed in recombinant CYP3A4 (by ~90%) and CYP3A5 (by ~10%) incubations, and the CYP3A4/5 inhibitors almost completely inhibited (>90%) the formation of these metabolites in HLM. Similarly, initial experiments indicated that CYP3A4 and CYP3A5 formed M2. However, the metabolite was not quantified because montelukast sulfoxide (M2) was found as an impurity (~1%) in montelukast sodium. This impurity inhibited CYP2C8 but not CYP2C9 at high montelukast concentrations, as evident from HLM and CYP incubations of M2 with montelukast. Montelukast sulfoxide 0.1 μM inhibited M6 formation by ~55 and 73% in HLM and CYP2C8 incubations, respectively. In study **II**, M5b formation was unaffected by gemfibrozil and its glucuronide, while M5a was not detectable at the montelukast concentration used.

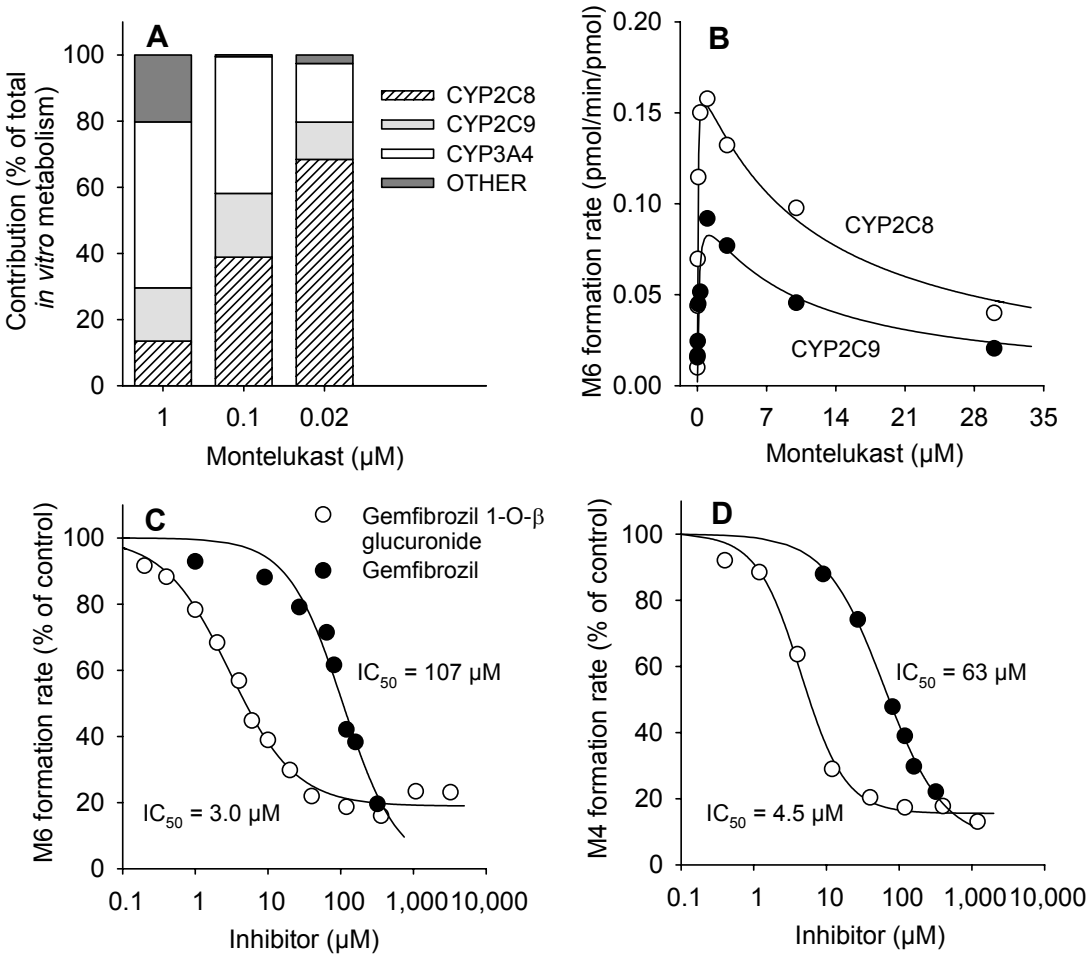

Figure 15. Main findings from montelukast experiments. **A,** the (RAF-adjusted) relative importance of CYP2C8 in the *in vitro* metabolism of montelukast increased with decreasing montelukast concentrations. **B,** the enzyme kinetics of M6 formation was best described by an uncompetitive substrate inhibition model for both CYP2C8 and CYP2C9. V_{max}, K_m, and K_i for M6 formation by CYP2C8 were 0.18 pmol/min/pmol, 0.050 μM, and 11 μM, respectively, and by CYP2C9 0.11 pmol/min/pmol, 0.19 μM, and 7.4 μM, respectively. **C, D,** the inhibitory effect of gemfibrozil 1-*O*-β glucuronide on M6 and M4 formation (from montelukast and M6, respectively) in HLM incubations was greater than that of gemfibrozil. CYP, cytochrome P450; IC_{50}, inhibitor concentration producing 50% inhibition.

Table 21. Intrinsic and predicted hepatic clearance values of montelukast, calculated based on the depletion of montelukast in recombinant CYP2C8, CYP2C9, and CYP3A4 incubations.

Enzyme	$CL_{int,\ in\ vitro}$ (ml/min/nmol)	$CL_{int,\ RAF}$ (ml/min/mg)	CL_H (ml/min/kg)	% total CL_H*
CYP2C8	3.6	0.25	0.97	72
CYP2C9	0.48	0.040	0.16	12
CYP3A4	1.8	0.053	0.22	16

* Total CL_H (1.35 ml/min/kg) calculated as the sum of predicted CL_H values. CL_H, hepatic clearance; $CL_{int,\ RAF}$, RAF-adjusted intrinsic clearance; CYP, cytochrome P450.

11.2. Prediction of the role of CYP2C8 in montelukast pharmacokinetics

The $CL_{int,\ in\ vitro}$ based on montelukast depletion (0.02 μM) in HLM was 0.14 ml/min/mg. This value yields a scaled montelukast *in vivo* CL_H of 0.54 ml/min/kg, which is approximately 60% of the estimated CL_B (0.89 ml/min/kg) in humans. Based on depletion of montelukast 0.02 μM in recombinant CYP incubations, the contribution of CYP2C8 to the total *in vivo* metabolism of montelukast was estimated to average 72% using the RAF approach (Table 21). The RA approach resulted in a higher predicted role for CYP3A4 (60%) and a lower one for CYP2C8 (27%), with 11 and 2.3% contributions for CYP2C9 and CYP3A5. Both approaches slightly overestimated the *in vivo* CL_B: the sum of CL_H of CYP2C8, CYP2C9, CYP3A4, and CYP3A5 was ~1.4 ml/min/kg (Table 21).

11.3. Effect of gemfibrozil on montelukast *in vivo*

In study **II**, gemfibrozil markedly affected the concentrations of montelukast and its metabolites M6, M4 and M5a/b in humans.

Montelukast and its metabolites. Compared to placebo, gemfibrozil increased the mean $AUC_{0-\infty}$ of montelukast 4.5-fold ($P < 0.001$) and mean C_{max} 1.5-fold ($P < 0.001$) (Figure 16). Montelukast $t_{½}$ was prolonged three-fold to 13.5 h ($P < 0.001$). Compared to placebo, the formation rate of M6 was reduced by gemfibrozil. M6 median t_{max} was prolonged three-fold and its mean AUC_{0-7} was reduced to 60% of control (Figure 16), while its AUC_{0-24} was increased by 86% ($P = 0.005$) by gemfibrozil. In addition, gemfibrozil markedly reduced the plasma exposure to M4 to about 10% of control ($P < 0.001$). Furthermore, gemfibrozil increased the C_{max} of M5a and M5b five-fold and 2.5-fold ($P \leq 0.001$), respectively, and their AUC_{0-24} by 9.3-fold and 4.8-fold ($P < 0.001$), respectively. Based upon the effect of gemfibrozil on the $AUC_{0-\infty}$ of montelukast, it can be estimated that total clearance of montelukast was reduced by almost 80% by gemfibrozil.

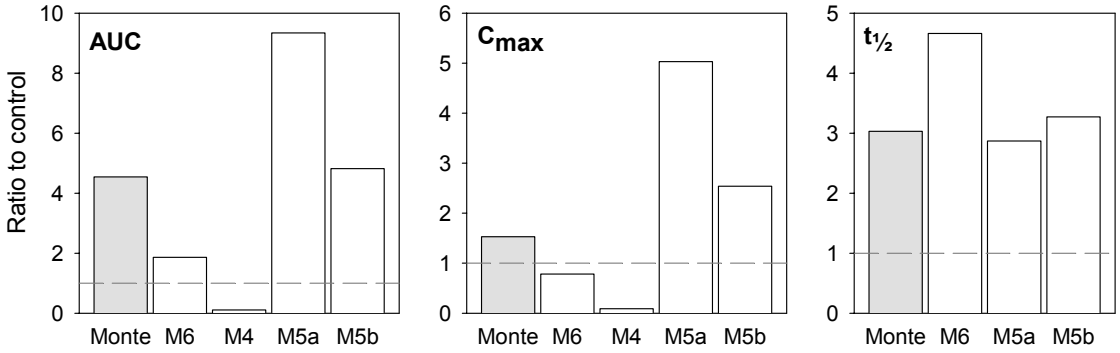

Figure 16. Effects of gemfibrozil on the pharmacokinetics of montelukast (Monte) and its metabolites M6, M4, M5a, and M5b. Bars represent ratios of mean values during the gemfibrozil phase to those during the control (placebo) phase (n = 10). AUC, area under concentration-time curve; C_{max}, peak concentration; $t_{½}$, elimination half-life.

Effects of genotype. Two of 10 subjects had the *CYP2C8*1/*3* genotype and one had the *CYP2C8*1/*4* genotype (Table 18). One of the subjects had the *CYP3A5*1/*3* (CYP3A5 expressor) genotype, while the other subjects had the *CYP3A5*3/*3* non-expressor genotype. Pharmacokinetic variables of montelukast in *CYP2C8*3*, *CYP2C8*4*, and *CYP3A5*1* carriers were similar to those in non-carriers.

12. Imatinib studies (III-V)

12.1. Effect of imatinib on CYP2C8 and CYP3A4/5 activities *in vitro*

In study **III**, imatinib affected CYP3A4 by mechanism-based inhibition.

Time-dependent inhibition. Compared to no pre-incubation, a 30-min pre-incubation of imatinib in the presence of NADPH increased its CYP3A4/5 inhibitory effect, leading to an eight-fold reduction in its (unadjusted) IC_{50} value to 7.1 μM (Table 22). Pre-incubation of imatinib with NADPH increased its inhibition of midazolam 1'-hydroxylation in recombinant CYP3A4 incubations but not in CYP3A5 incubations, suggesting that imatinib inhibits only CYP3A4 time-dependently. Its (unadjusted) K_I and k_{inact} in HLM were 14.3 μM and 0.072 1/min. Ketoconazole reduced the inactivation of CYP3A4 by imatinib in a concentration-dependent manner, and dialysis did not abolish the inhibitory effect of imatinib on midazolam 1'-hydroxylation, suggesting that the imatinib-induced inactivation of CYP3A4 is irreversible or quasi-irreversible. Imatinib did not affect amodiaquine N-deethylation (CYP2C8 activity) by time-dependent inhibition. In addition, N-desmethylimatinib, piperidine N-oxide imatinib, and pyridine N-oxide imatinib were not time-dependent inhibitors of CYP2C8 or CYP3A4/5.

Table 22. Inhibition of CYP2C8 and CYP3A4 by imatinib and N-desmethylimatinib in HLM. The values have been corrected for non-specific binding to microsomal proteins.

Inhibitor	Enzyme inhibited	IC_{50} (μM), no pre-incubation	IC_{50} (μM), pre-incubation with NADPH	K_i (μM)	K_I (μM)	k_{inact} (1/min)
Imatinib	CYP2C8	14	23	7.6	-	-
	CYP3A4/5	48	6.4	21	11	0.07
N-desmethyl-imatinib	CYP2C8	28	40	12	-	-
	CYP3A4/5	32	26	16	-	-

CYP, cytochrome P450; IC_{50}, inhibitor concentration producing 50% inhibition; K_i, reversible inhibition constant; K_I, inhibitor concentration supporting half of the maximal rate of inactivation; k_{inact}, maximal rate of inactivation; NADPH, nicotinamide adenine dinucleotide phosphate.

Direct inhibition. Direct inhibition of CYP2C8 activity by imatinib and N-desmethylimatinib was best described by a mixed full inhibition model for both inhibitors. Direct inhibition of

midazolam 1′-hydroxylation by imatinib was also best described by the mixed full inhibition model, while N-desmethylimatinib inhibited CYP3A4/5 activity in a competitive manner.

12.2. *In vitro* metabolism of imatinib

In study **IV**, CYP2C8 and CYP3A4 metabolised imatinib extensively, while other isoforms had minor effect on imatinib concentrations.

Table 23. Intrinsic and predicted hepatic clearance values of imatinib, calculated based on the depletion of imatinib and formation of N-desmethylimatinib in recombinant enzyme incubations. The values have been corrected for non-specific binding to microsomal proteins.

Enzyme	Metabolic pathway	$CL_{int,\ in\ vitro}$ (µl/min/pmol)	$CL_{int,\ ISEF}$ (µl/min/mg)	$CL_{int,\ scaled}$ (l/h)	CL_H (l/h)	% total CL_H*
CYP1A2	M	0.03	0.84	3.6	0.14	1.1
CYP2B6	M	0.07	0.66	2.9	0.11	0.83
CYP2C8	N-DMI	1.06	29	127	4.8	40
	OM	0.14	3.9	17	0.66	
CYP2D6	M	0.05	0.34	1.5	0.059	0.43
CYP3A4	N-DMI	1.03	13	56	2.2	57
	OM	2.75	35	151	5.7	
CYP3A5	N-DMI	0.07	0.47	2.0	0.081	0.79
	OM	0.02	0.16	0.67	0.027	

* Total CL_H (13.75 l/h) calculated as the sum of predicted CL_H values from recombinant incubations. CL_{int}, intrinsic clearance; $CL_{int,\ ISEF}$, ISEF-adjusted intrinsic clearance; CL_H, hepatic clearance; CYP, cytochrome P450; M, metabolites (intrinsic clearance calculated using the substrate depletion approach); N-DMI, N-desmethylimatinib (intrinsic clearance calculated on the basis of N-desmethylimatinib formation kinetics); OM, other metabolites (intrinsic clearance calculated as substrate depletion $CL_{int,\ in\ vitro}$ - N-desmethylimatinib formation $CL_{int,\ in\ vitro}$).

Imatinib. Recombinant CYP2C8 and CYP3A4 metabolised imatinib rapidly (<15% of the parent drug remained at 30 min), while other CYPs had a minor effect on its concentrations (>78% imatinib left). CYP2C8 inhibitors inhibited the depletion of imatinib (0.1 µM) by ~45%, while CYP3A4 inhibitors inhibited it by almost 80%.

N-desmethylimatinib. At imatinib 1 µM, the formation of N-desmethylimatinib was mediated by CYP2C8, CYP3A4 and CYP3A5, but small amounts were formed also by CYP2D6, CYP2C19, and CYP2C9. However, at imatinib 0.1 µM, only CYP2C8, CYP3A4, and CYP3A5 formed detectable N-desmethylimatinib amounts. CYP2C8 inhibitors and CYP3A4 inhibitors inhibited its formation by ≥50%. The further metabolism of N-desmethylimatinib was mainly catalysed by CYP3A4, with a smaller contribution by CYP2C8, and minor involvement by CYP1A2, CYP2D6 and CYP3A5. Comparison of CL_{int} values obtained from the depletion (total metabolism) of imatinib 0.1 µM with those calculated based on the kinetics of N-desmethylimatinib formation indicated that N-

desmethylation accounts for the majority (88%) of imatinib metabolism by CYP2C8, while the metabolite accounts for 27 and 75% of imatinib metabolism by CYP3A4 and CYP3A5, respectively (Table 23).

12.3. *In vitro-in vivo* predictions

In study **III**, the mechanism-based inhibition of CYP3A4 by imatinib was predicted to cause clinically relevant interactions. In study **IV**, the static prediction and PBPK simulations estimated a marked role for CYP2C8 in imatinib metabolism. In study **V**, PBPK simulations estimated that the importance of CYP2C8 in imatinib pharmacokinetics increases with time during multiple dosing, while that of CYP3A4 decreases.

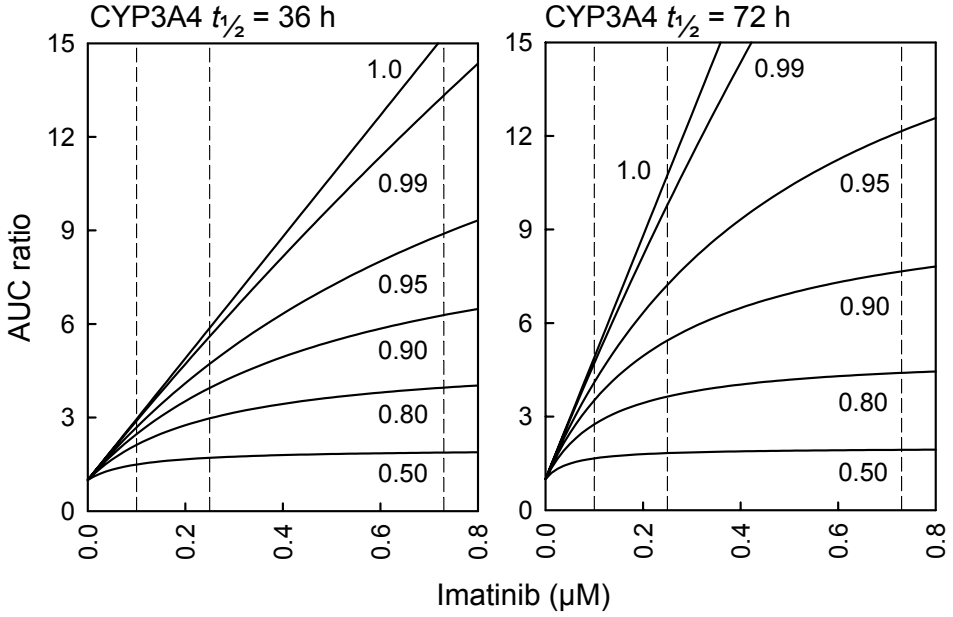

Figure 17. Predicted effect of imatinib on the pharmacokinetics of CYP3A4 substrates *in vivo*, assuming that the intestinal bioavailability is unaffected. The substrate AUC depends on several factors: imatinib concentration, the fraction of the substrate metabolised by CYP3A4, and on CYP3A4 half-life. During treatment with imatinib 400 mg once daily, its average unbound trough concentration (C_{trough}) and C_{max} in plasma approximates 0.1 and 0.25 μM, respectively, while the unbound imatinib C_{max} in the portal vein was estimated at 0.73 μM (indicated by the dashed lines). AUC, area under concentration-time curve; $t_{½}$, turnover half-life.

Prediction of *in vivo* drug interactions with imatinib as the inhibitor drug. In study **III**, interaction predictions based on inhibition of hepatic CYP3A4 by imatinib using the obtained mechanism-based inhibition values yielded a maximal AUC increase of 5.9-fold for a drug completely metabolised by hepatic CYP3A4, when using unbound imatinib C_{max} (0.25 μM) during steady state administration of 400 mg imatinib daily and the CYP3A4 half-life of 36 h (Figure 17) (Gleevec Clinical Pharmacology and Biopharmaceutic Review(s), 2001, le Coutre *et al.*, 2004, Peng *et al.*, 2004b, Bornhauser *et al.*, 2005). The interaction magnitude was even

higher when inhibition of intestinal CYP3A4 was included in the prediction. The direct inhibitory effects of CYP2C8 and CYP3A4 by imatinib and N-desmethylimatinib were predicted to be clinically insignificant. For instance, the predicted increase in the plasma exposure to simvastatin was 1.1-fold, when assuming direct inhibition only of hepatic CYP3A4 by imatinib. When predicting the effect of mechanism-based inhibition of both hepatic and intestinal CYP3A4 on simvastatin concentrations, the corresponding increase was 5.9-fold.

Imatinib metabolism using the ISEF approach. In study **IV**, with use of the ISEF approach, CYP2C8 and CYP3A4 were estimated to be the most important enzymes in imatinib metabolism *in vivo* (contributions of 40 and 57%, respectively, following a single imatinib dose) (Table 23). The total CL_H (13.8 l/h) calculated as the sum of predicted CL_H values of recombinant CYP incubations corresponded to 72% of the estimated *in vivo* CL_B (19.2 l/h). The calculated CL_H based on imatinib depletion in HLM equalled 14.8 l/h.

Imatinib metabolism using PBPK simulations. In study **IV**, simulated concentration-time curves, as well as mean pharmacokinetic parameters of imatinib and N-desmethylimatinib, matched well with published data on imatinib single-dose and multiple dose pharmacokinetics (Figure 18). Compared with when direct inhibition only of CYP3A4 by imatinib was considered, a model which included mechanism-based autoinhibition of CYP3A4 matched better with observed imatinib plasma concentrations during treatment with imatinib 400 mg once daily. This model predicted a 2.1-2.3-fold accumulation of imatinib, imatinib trough levels of 900-950 ng/ml, and peak concentrations of ~2,800 ng/ml following multiple dosing with imatinib 400 mg once daily, in line with clinical data (Gleevec Clinical Pharmacology and Biopharmaceutic Review(s), 2001, Peng *et al.*, 2004b, van Erp *et al.*, 2007, Larson *et al.*, 2008, Demetri *et al.*, 2009).

Similarly, the simulations predicted well the effects of ketoconazole, rifampicin, and ritonavir on the pharmacokinetics of imatinib. In drug-drug interaction simulations, gemfibrozil was predicted to increase the $AUC_{0-\infty}$ of a single dose of imatinib 400 mg by 1.8-fold and reduce that of N-desmethylimatinib by 59%. Following multiple doses of imatinib, gemfibrozil was predicted to increase its $AUC_{0-\tau}$ by 2.3-fold and reduce that of the metabolite by ~85%. Furthermore, simulations of a low activity CYP2C8 genotype (50% reduction in its activity) resulted in a reduced imatinib metabolism, leading to increased imatinib and decreased N-desmethylimatinib concentrations. In contrast, a high CYP2C8 activity (two-fold increase in activity) was predicted to cause markedly increased imatinib metabolism. The results of the simulations with the refined PBPK model in study **V** are described in section 12.4.

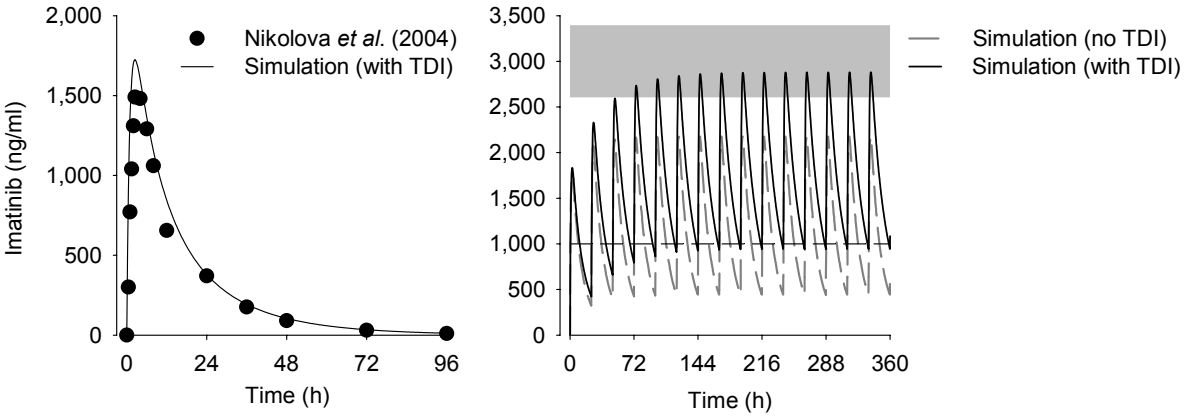

Figure 18. Pharmacokinetic simulations of the concentrations of imatinib following a single dose (left) and multiple doses (right) of imatinib 400 mg in study **IV**. The circles refer to clinical data from Nikolova et al. (2004). The grey area in the right figure depicts the range of reported peak concentrations of imatinib following treatment with imatinib 400 mg once daily (Gleevec Clinical Pharmacology and Biopharmaceutic Review(s), 2001, Peng *et al.*, 2004b, van Erp *et al.*, 2007, Demetri *et al.*, 2009). The dashed line defines the suggested target trough concentration for imatinib treatment (1,000 ng/ml) (Teng *et al.*, 2012). TDI, time-dependent inhibition.

12.4. Effect of gemfibrozil on imatinib *in vivo*

In study **V**, gemfibrozil unexpectedly reduced the peak concentration of imatinib. In line with the simulations of study **IV**, however, gemfibrozil markedly reduced the CYP2C8-mediated formation of N-desmethylimatinib from imatinib.

Imatinib. Compared to placebo, gemfibrozil 600 mg twice daily reduced the geometric mean C_{max} and $AUC_{0–12\ h}$ of imatinib by 35 and 23% ($P < 0.001$), respectively (Figure 19, Figure 20). During the gemfibrozil phase, impaired absorption of imatinib was seen in all ten subjects, and six subjects had a double peak of imatinib plasma concentrations. In the placebo phase, only one subject had a double peak. The imatinib peak plasma concentration/plasma concentration at 24 h ($C_{max}/C_{24\ h}$) ratio was reduced by 44% during co-administration with gemfibrozil ($P < 0.001$). Gemfibrozil prolonged imatinib $t_{½}$ by 8% ($P = 0.003$), while its $AUC_{0–96\ h}$ and $AUC_{0–\infty}$ were unaffected by gemfibrozil (Figure 19). Gemfibrozil did not alter imatinib $f_{u,\ P}$ measured in 2-h and 12-h samples.

N-desmethylimatinib. Gemfibrozil reduced N-desmethylimatinib C_{max} and $AUC_{0–\infty}$ by 56 and 48% ($P < 0.001$), respectively, as compared with placebo. Thus, gemfibrozil markedly reduced the N-desmethylimatinib/imatinib plasma concentration ratio in all subjects. On average, the N-desmethylimatinib/imatinib $AUC_{0–\infty}$ ratio was reduced by 45% by gemfibrozil ($P < 0.001$), but N-desmethylimatinib half-life was unaffected. Furthermore, gemfibrozil reduced the $C_{max}/C_{24\ h}$ ratio of N-desmethylimatinib by 17% ($P = 0.022$). Moreover,

gemfibrozil reduced the $AUC_{0-\infty}$ of the sum of imatinib and N-desmethylimatinib by 14% only ($P = 0.015$). N-desmethylimatinib $f_{u,\,P}$ in 2-h samples was increased 1.3-fold ($P = 0.017$) by gemfibrozil co-administration, but no change was observed in 12-h samples.

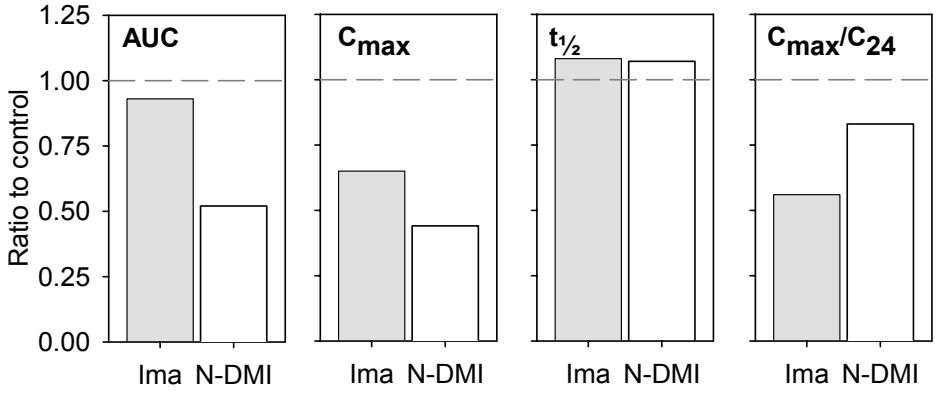

Figure 19. Effects of gemfibrozil on the pharmacokinetics of imatinib (Ima) and N-desmethylimatinib (N-DMI) in the clinical study (**V**). Bars represent ratios of geometric mean values during the gemfibrozil phase to those during the control (placebo) phase (n = 10). AUC, area under concentration-time curve; C_{24}, concentration at 24 h; C_{max}, peak concentration; $t_{½}$, elimination half-life.

Effect of genotype. One subject was heterozygous for the *CYP2C8*3* allele, and one was heterozygous for *CYP2C8*4*. The other eight subjects had the *CYP2C8*1/*1* genotype (Table 18). The *CYP2C8*3* carrier had the largest N-desmethylimatinib $AUC_{0-\infty}$ during both study phases. Otherwise, the pharmacokinetic variables of imatinib and N-desmethylimatinib in *CYP2C8*3* and *CYP2C8*4* carriers were similar to those in non-carriers.

PBPK simulations. In study **V**, the effect of gemfibrozil on imatinib pharmacokinetics could be well simulated when the PBPK model considered inhibition of both CYP2C8-mediated metabolism and active intestinal uptake transport by gemfibrozil (Figure 20). Gemfibrozil was predicted to decrease the AUC_{0-12} of a single imatinib dose of 200 mg by 20% and to increase its $AUC_{0-\infty}$ by 14%. The model over-predicted the effect of gemfibrozil on N-desmethylimatinib pharmacokinetics, and steady state simulations of N-desmethylimatinib concentrations were therefore not conducted. Interaction simulations with multiple imatinib doses suggested that gemfibrozil can increase its dosing interval AUC 1.3-fold after imatinib doses of 200 mg once daily and 1.5-fold after doses of 400 mg once daily. The simulations also suggested that gemfibrozil can increase its trough concentrations more than two-fold. During multiple dosing of imatinib 400 mg once daily, the contribution of CYP2C8 to imatinib metabolism was predicted to increase from ~40 to 70%, and consequently, gemfibrozil was predicted to increase imatinib trough concentrations to ~1,700 ng/ml (Figure 20). At steady state, the peak/trough fluctuation of the simulated imatinib concentrations was smaller during co-administration with gemfibrozil ($C_{max}/C_{24\ h}$ ratio: ~2/1) than during the placebo phase ($C_{max}/C_{24\ h}$ ratio: ~4/1–5/1). Compared to simulations including gemfibrozil-mediated inhibition of an uptake transporter in the intestine, other alternatives such as enzyme

induction and displacement of imatinib from plasma protein by gemfibrozil did not reflect the observed interaction as accurately.

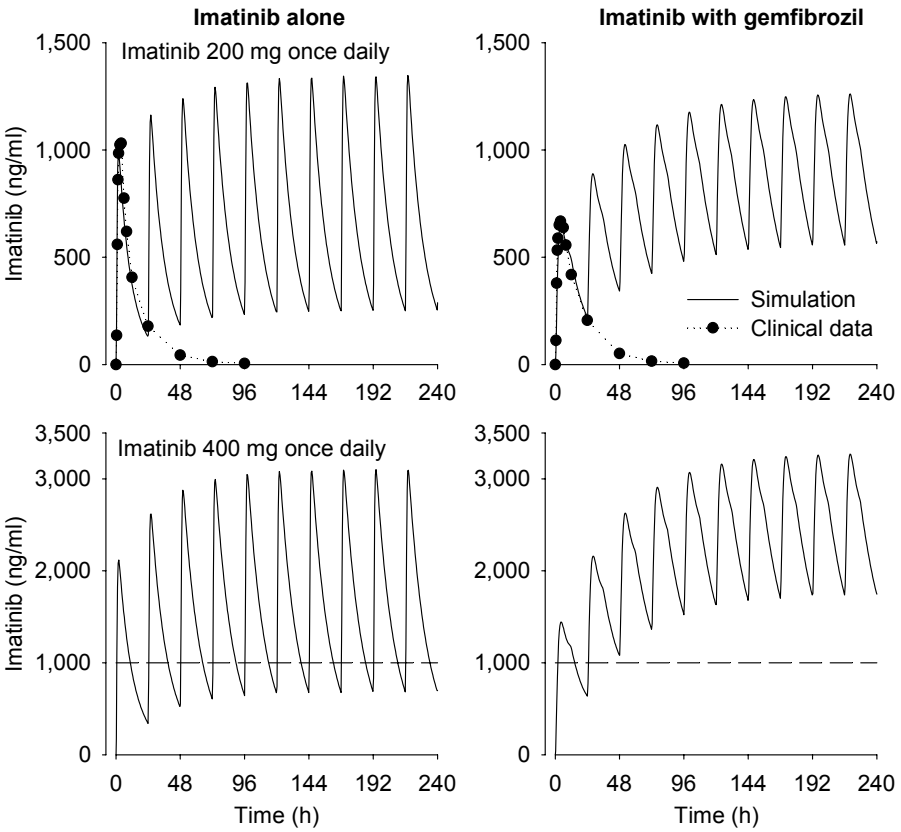

Figure 20. Simulations of the gemfibrozil-imatinib interaction with the refined PBPK model in study **V**. Simulated effects of gemfibrozil (600 mg twice daily) on multiple dose pharmacokinetics of imatinib, when imatinib treatment was started on day 3 of the gemfibrozil treatment. The full lines represent the simulations, while circles refer to the clinical data of study **V**. The dashed lines in the lower figures define the suggested target C_{trough} for imatinib treatment (1,000 ng/ml) (Teng *et al.*, 2012).

DISCUSSION

13. Methodological considerations

13.1. *In vitro* studies

Pooled HLM and recombinant CYPs were used in the *in vitro* studies as they are recommended systems for *in vitro* phenotyping of CYP-mediated metabolism and inhibition (FDA, 2012). To mimic physiological conditions, sodium phosphate buffer (0.1 M, pH 7.4) was used as the incubation medium, and incubations were conducted at 37ºC. In studies **I** and **II**, $MgCl_2$ was added to the incubation mixtures to support binding of NADPH to POR (Ogilvie *et al.*, 2008). However, it was excluded from incubations in **III** and **IV**, following preliminary experiments where exclusion of $MgCl_2$ in the incubations did not alter the metabolism of the tested drugs, as compared to when $MgCl_2$ was included. Furthermore, $MgCl_2$ was not mentioned in the incubation condition recommendations of the manufacturer. Because organic solvents affect the activities of CYPs, their concentrations were kept low in the incubations (1%). In order to keep non-specific binding of drugs equal in the experiments, and to enable precise comparisons of results with different CYP isoforms, an equal protein concentration was used in parallel experiments.

In study **I**, the CYP-mediated metabolism of montelukast *in vitro* was re-evaluated. Low montelukast concentrations were incubated with recombinant CYPs or HLM and CYP-selective inhibitors. Following a single oral dose of montelukast 10 mg, its peak concentrations in plasma approximate to 500 ng/ml (Zhao *et al.*, 1997), which corresponds to an unbound concentration of 0.003 μM. Using LC-MS/MS, a montelukast concentration of 0.02 μM could be incubated and accurately quantified. This concentration is reasonably close to its unbound plasma concentration. Studies have suggested that the intracellular concentrations of montelukast in hepatocytes might be higher than its unbound plasma concentrations due to uptake transport by OATP2B1, however, recent findings indicate that montelukast is not a OAT2B1 substrate (Chu *et al.*, 2012, Kim *et al.*, 2013a, Tapaninen *et al.*, 2013, Brännström *et al.*, 2014, Korzekwa, 2014).

Because montelukast binds non-specifically to protein (Walsky *et al.*, 2005b), low protein concentrations were used. Unfortunately, similarly as in a previous study (Walsky *et al.*, 2005b), it was not possible to determine the unbound fraction of montelukast in the microsomal incubations. Equilibrium dialysis and ultrafiltration were used in attempts to determine its non-specific binding, while ultracentrifugation was not tested. This method has been shown to accurately determine the unbound fraction of very lipophilic compounds (MacKichan, 2006). Using the Simcyp *in silico* fumic prediction calculator

(http://www.simcyp.com), the unbound fraction of montelukast in microsomal incubations can retrospectively be predicted to have equalled 0.70 and 0.82 at protein concentrations of 0.1 and 0.05 mg/ml, respectively. The implications of adjusting the obtained enzyme kinetic parameters for these values are discussed in section 13.2.

Another limitation of study **I** was the montelukast sulfoxide (M2) impurity (1%) found in montelukast sodium from two commercial vendors. Montelukast sulfoxide inhibited CYP2C8 *in vitro*. However, the inhibition is likely to be negligible at the low montelukast concentrations (≤1 μM) used in the study; although it could have affected the enzyme kinetics of M6 formation by CYP2C8, where the highest montelukast concentration tested was 30 μM. An additional limitation is the lack of reference compounds for M3, M4, and M5. In particular, quantification of M4 would have been of interest, as it is the main metabolite in bile (Balani *et al.*, 1997).

In study **III**, the inhibitory effects of imatinib on CYP2C8 and CYP3A4 activities in HLM were studied. In accordance with recommendations (FDA, 2011, EMA, 2013), amodiaquine deethylation and midazolam 1-hydroxylation were used as marker reactions for CYP2C8 and CYP3A4, respectively. The study could have been improved by use of a second marker reaction for CYP3A4 (FDA, 2011, EMA, 2013). In addition, more extensive follow-up experiments could have been conducted, including incubations with ferricyanide to discriminate between quasi-irreversible and irreversible inhibition, or determination of the partition ratio of imatinib to evaluate its inactivation potency (Grimm *et al.*, 2009). Furthermore, it would also have been of interest to identify and determine the structure of the inactivating agent.

In study **IV**, the importance of CYP2C8 in the *in vitro* metabolism of imatinib was investigated. Similarly as in study **I**, low drug concentrations were incubated with HLM or with recombinant enzymes. The imatinib concentrations used corresponded to clinically relevant unbound peak concentrations of imatinib in plasma during treatment with imatinib 400 mg once daily (generally around 0.2-0.3 μM) (Gleevec Clinical Pharmacology and Biopharmaceutic Review(s), 2001, le Coutre *et al.*, 2004, Peng *et al.*, 2004b, Bornhauser *et al.*, 2005). In order to overcome mechanism-based inhibition of its own CYP3A4-mediated metabolism, very short incubation times were used. No other metabolites than N-desmethylimatinib were quantified, although M5, piperidine N-oxide imatinib, and pyridine N-oxide imatinib were monitored.

13.2. *In vitro-in vivo* predictions

In study **I**, montelukast intrinsic clearance obtained from recombinant enzyme incubations was scaled to *in vivo* hepatic clearance using the RA and RAF approaches. The estimated

relative contributions of CYP2C8 and CYP3A4 to the hepatic clearance of montelukast varied markedly depending on the method used. The RAF approach takes CYP activity into account and has been considered more reliable than the RA method (Stringer *et al.*, 2009). With the RAF approach, the contribution of CYP2C8 was estimated to equal 72%, which is in good agreement with the *in vivo* results of study **II**. However, activity data provided by the manufacturer for the microsomal lots was used to calculate RAFs. Because the activities of CYP3A4 and CYP3A5 had not been differentiated, it was not possible to determine the contribution of CYP3A5 using RAFs. Theoretically, assuming that some of the donors of the HLM pool used were CYP3A5 expressors, and that CYP3A5 thus contributed to the CYP3A activity as measured by the manufacturer, it can be estimated that the role of CYP3A4 in montelukast metabolism is in fact smaller than predicted. Thus, a possible contribution by CYP3A5 alters the predicted role of CYP3A4 but affects those of CYP2C8 and CYP2C9 very little. The contribution of CYP3A5 might have been possible to estimate by use of HLM from single donors expressing CYP3A5.

One limitation of the *in vitro-in vivo* extrapolations was the fact that it was not possible to correct the obtained enzyme kinetic values for non-specific binding at the time of the study. However, as described in section 13.1., by use of an *in silico* predictor it is possible to retrospectively adjust the intrinsic clearance values obtained from montelukast depletion in recombinant enzymes (Table 21) and HLM. Using an unbound fraction of 0.70, the calculated intrinsic clearance values of montelukast in different microsomal incubations will increase by 43%. The sum of the scaled hepatic clearance from recombinant enzyme experiments can then be estimated to equal 1.89 ml/min/kg, which is ~two-fold of the calculated blood clearance of montelukast. However, the estimated percentage contributions of the different CYPs involved in the metabolism of montelukast are not altered by adjusting for non-specific binding (Table 21). Furthermore, when adjusting for non-specific binding, the hepatic clearance calculated based on the depletion of montelukast in HLM can then be estimated to 0.76 ml/min/kg, corresponding to 85% of the blood clearance of montelukast.

In study **III**, static models were used to predict the effects of imatinib and N-desmethylimatinib on the plasma exposure to CYP2C8 and CYP3A4 substrate drugs. The predictions were carried out using different inhibitor concentrations, since no consensus has been reached on which inhibitor concentration to use (Yamano *et al.*, 1999, Kanamitsu *et al.*, 2000, Ito *et al.*, 2004, Bachmann, 2006). Because several values for the hepatic CYP3A4 turnover half-life have been reported in the literature (Yang *et al.*, 2008), the predictions based on mechanism-based inhibition by imatinib were carried out using 36 and 72 h, of which 36 h has been considered to be more accurate (Rowland Yeo *et al.*, 2011). Similarly, at least two different F_G values (0.14 and 0.66) of simvastatin have been reported (Obach *et al.*, 2006, Gertz *et al.*, 2008). The F_G value of 0.14 led to over-predictions of the effect of imatinib on simvastatin concentrations, while that of 0.66 was predicted to cause a 5.9-fold increase in simvastatin AUC, when using a steady-state unbound imatinib C_{max} of 0.25 μM. This value is

somewhat higher than that observed *in vivo* (average AUC increase of 3.5-fold), however, the individual AUC ratios ranged from no change to >ten-fold increase (O'Brien *et al.*, 2003). It is, however, common that interaction predictions based on time-dependent inhibition of CYP3A4 in HLM experiments leads to over-predictions, possibly due to inaccuracies in prediction parameters, such as the turnover half-life of CYP3A4 (Chen *et al.*, 2011).

In study **III**, one source of error in the predictions was that an imatinib dose of 335 mg was used in the calculation of imatinib unbound $C_{max,\ portal}$ and inhibitor concentration in the enterocytes. This dose would have corresponded to 400 mg of imatinib mesilate. However, using an imatinib dose of 400 mg, the corrected values for these concentrations generate interaction magnitudes that are <13% higher than those predicted based on the original values. Thus, this miscalculation does not alter findings and conclusions reported in the study **III** publication.

In study **IV**, ISEFs were used to adjust imatinib clearance. One potential source of error might have been the fact that ISEFs were obtained from different sources. For CYP2C8, CYP3A4, and CYP3A5 it was possible to experimentally determine the ISEFs, while those of CYP1A2, CYP2B6, and CYP2D6 were obtained from Simcyp. However, because CYP2C8 and CYP3A4 are the most important CYPs in imatinib metabolism, the ISEFs of the other enzymes are not crucial to the predictions.

In studies **IV** and **V**, PBPK simulations with Simcyp were conducted. The PBPK models make several assumptions and simplifications. In study **IV**, the model comprised first-order oral absorption, assuming that the administered drug is in solution, and that the driving concentration at the level of the intestine is that of the portal vein $\times$ $f_{u,\ G}$. $f_{u,\ G}$ of imatinib was chosen to correspond to that in plasma. Because the elimination of imatinib has not been fully reported, it was assumed that <5% was eliminated renally and that ~10-15% was excreted as unchanged imatinib. A single adjusting compartment, which represents a lump tissue, was included to adjust the concentration-time profile of imatinib. The model seemed to predict imatinib pharmacokinetics after a single dose and multiple doses, as well as the effects of CYP3A4 inhibitors on imatinib and N-desmethylimatinib pharmacokinetics well. However, as evident after completion of the clinical study in **V**, the model had over-predicted the effect of gemfibrozil on imatinib pharmacokinetics. The model was therefore refined so that the additional clearance was increased to correspond to ~25%, and the unbound fraction of imatinib in plasma was reduced. In addition, an advanced absorption and dissolution model was selected to simulate its absorption so that an intestinal uptake transporter could be included in the model.

13.3. *In vivo* studies

The two clinical studies **II** and **V** performed in healthy volunteers had a randomised, placebo-controlled cross-over design. Thus, the subjects served as their own controls, limiting the effects of inter-individual variability. In addition, it reduced the number of subjects needed to find a possible clinically significant interaction. The wash-out periods were chosen to minimise the risk of possible carry-over effects. The wash-out time intervals were chosen according to the pharmacokinetic properties of the drugs studied, and taking into account the time necessary for the synthesis of new CYP enzyme in the case of irreversible inhibition.

In both studies, the pre-treatment dose was administered one hour before the victim drug on the study day. This was done to ensure adequate absorption of the pre-treatment drug by the time the study drug was ingested. In order to decrease variability in drug absorption, the subjects fasted overnight and received standardised meals during the study days. Gemfibrozil was used as the inhibitor drug of CYP2C8. The subjects were given gemfibrozil 600 mg twice daily for three days as pre-treatment since this dosing has been shown to cause an almost complete inhibition of CYP2C8 in healthy volunteers (Backman *et al.*, 2009). The concentrations of gemfibrozil and its glucuronide were monitored during the study days and ascertained to be at therapeutic levels. In study **V**, gemfibrozil was given to the end of the sampling period, while in study **II**, gemfibrozil was administered to the end of the study day. Because full recovery of CYP2C8 occurs first after four days (Backman *et al.*, 2009), it can be assumed that the inhibition of CYP2C8 lasted over the whole sampling period.

In study **II**, a montelukast dose of 10 mg was used, which corresponds to its normal, therapeutic dose. The drug is relatively safe as doses up to 900 mg have been administered without clinically relevant adverse effects (Singulair Label, 2013). In study **V**, a low dose of imatinib (200 mg) was chosen for safety reasons.

14. Role of CYP2C8 in the metabolism of montelukast (Studies I and II)

Before the initiation of study **I**, several studies indicated that montelukast interacts with CYP2C8 (Walsky *et al.*, 2005a, Walsky *et al.*, 2005b, Schoch *et al.*, 2008). However, the role of CYP2C8 in the pharmacokinetics of montelukast had not been examined. Early *in vitro* studies demonstrated that the oxidative metabolism of montelukast was exclusively mediated by CYPs, in particular by CYP2C9 and CYP3A4 (Chiba *et al.*, 1997). These experiments were conducted using supra-therapeutic montelukast concentrations exceeding more than 20,000-fold its clinically relevant unbound concentrations in plasma. In addition, very high protein concentrations were used, the enzymes forming M3 and M4 were not studied, and the contributions by CYP2C8 and CYP3A5 were not examined. Thus, because of data suggesting

an interaction between montelukast and CYP2C8, studies **I** and **II** were carried out aiming to determine the importance of CYP2C8 in the metabolism of montelukast *in vitro* and *in vivo*.

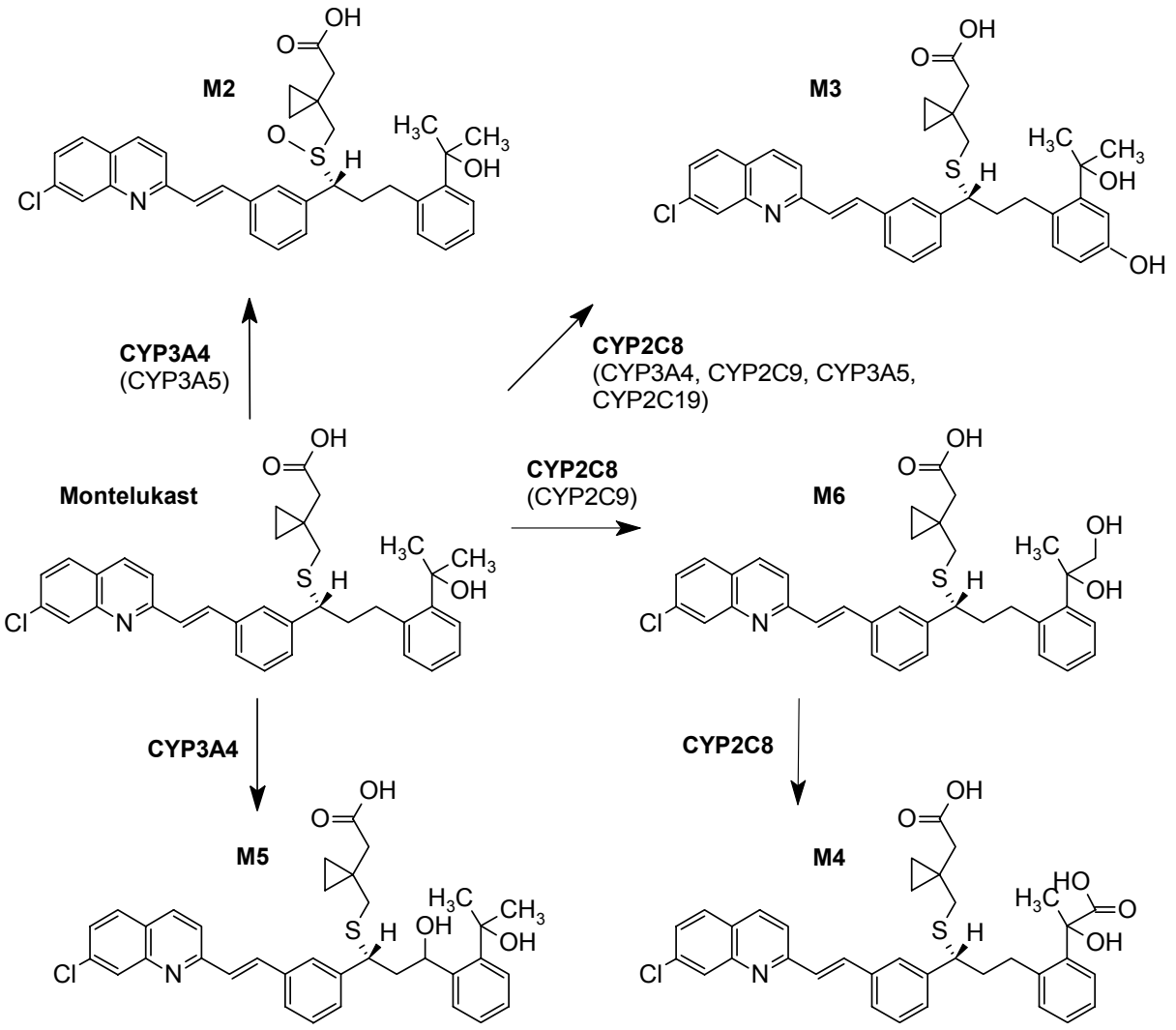

Figure 21. Oxidative metabolism of montelukast according to studies **I** and **II**, and recent literature (VandenBrink *et al.*, 2011, Karonen *et al.*, 2012).

In study **I**, CYP2C8-selective inhibitors inhibited the main metabolic pathway (formation of M6) of montelukast more potently than did inhibitors of the other CYPs. Recombinant CYP2C8 and CYP2C9 were the only CYP isoforms forming M6 at low montelukast concentrations; however, CYP2C8 catalysed its formation at a six-fold higher intrinsic clearance rate than did CYP2C9. Moreover, CYP2C8 mediated montelukast depletion and the further metabolism of M6 more actively than did any of the other CYP forms. The findings of study **I** further suggested that M3 is mainly formed by CYP2C8, whereas M4 formation from M6 is mediated almost exclusively by CYP2C8 (Figure 21). It should be noted, however, that the formation of M4 from M6 is a two-step reaction, where enzymes other than CYPs might

participate. The RAF approach estimated a >70% contribution of CYP2C8 in the *in vivo* metabolism of montelukast, and contributions of 12 and 16% for CYP2C9 and CYP3A4, respectively.

In study **II**, in almost exact accordance with the estimation, the strong CYP2C8 inhibitor gemfibrozil increased the plasma exposure to montelukast by 4.5-fold. Thus, the observed effect on montelukast concentrations by gemfibrozil is smaller than that on cerivastatin and repaglinide, but larger than the effect on other CYP2C8 substrates, such as pioglitazone and rosiglitazone (Table 14). Furthermore, in study **II**, the formation of M6 was delayed by gemfibrozil and the formation of the secondary metabolite M4 was reduced by over 90%. In the *in vitro* study, gemfibrozil and gemfibrozil 1-*O*-β glucuronide inhibited the formation of M4 and M6, but not of M5.

In addition to the mechanism-based inhibition of CYP2C8, gemfibrozil also inhibits several membrane transporters, including OATP2B1 *in vitro* (Ho et al., 2006). This transporter has been suggested to be involved in the pharmacokinetics of montelukast (Mougey *et al.*, 2009, Mougey *et al.*, 2011). However, a possible inhibition of OATP2B1-mediated uptake of montelukast in the intestine by gemfibrozil would have resulted in a decreased plasma exposure to montelukast. In contrast, if hepatic OATP2B1 had been inhibited by gemfibrozil, it could have contributed to the observed interaction, due to inhibited hepatic uptake and thus decreased hepatic clearance of montelukast. However, a possible inhibitory effect of OATP2B1 by gemfibrozil is likely to be weak and of short duration; gemfibrozil has a short half-life and its inhibition of OATP2B1 was only as strong as that of CYP2C9 *in vitro* (Wen *et al.*, 2001, Ho *et al.*, 2006). In addition, recent *in vitro* and *in vivo* findings suggest that the role of OATP2B1 in montelukast disposition is not important (Chu *et al.*, 2012, Kim *et al.*, 2013a, Tapaninen *et al.*, 2013, Brännström *et al.*, 2014).

Altogether, the findings of studies **I** and **II** strongly suggest that CYP2C8 plays a major role (~80%) in the metabolism of montelukast. After the publication of studies **I** and **II**, this conclusion has been confirmed by other reports. In an *in vitro* study using a low montelukast concentration of 0.01 μM, M6 was mainly formed by CYP2C8 (by almost 75%) and CYP2C9 (~20%), M2 was formed by CYP3A4 (~70%), and M5 by CYP3A4 (almost 80%) (VandenBrink *et al.*, 2011). The V_{max} and K_m of M6 formation by recombinant CYP2C8 at an enzyme concentration of 0.05 μM corresponded to ~23 pmol/min/pmol and 0.014 μM, respectively, which is in good agreement with the enzyme kinetic results of study **I**. In addition, paclitaxel 6α-hydroxylation (CYP2C8 marker reaction) was highly correlated (r^2=0.89) with M6 formation. In a clinical study, the CYP3A4 inhibitor itraconazole had no effect on the total elimination of montelukast (Karonen *et al.*, 2012), nor did it affect the concentrations of M6 and M4. However, itraconazole markedly reduced those of M5a and M5b, thus confirming *in vitro* findings indicating that CYP3A4 forms M5. In addition, this study also investigated the effects of gemfibrozil on montelukast exposure, and similar results

as in study **II** were obtained; gemfibrozil increased montelukast $AUC_{0-\infty}$ by 4.3-fold and prolonged its elimination $t_{½}$ by 2.1-fold (Karonen *et al.*, 2012).

Given the findings of studies **I** and **II** and literature data, the high $f_{m,\ CYP2C8}$ of montelukast (0.8), and its beneficial safety profile, montelukast is a good candidate for use as a CYP2C8 probe in both *in vitro* and in humans. The suitability of montelukast as a marker substrate is further discussed in section 16.

15. Roles of CYP2C8 and CYP3A4 in the metabolism of imatinib (Studies III-V)

At the time of study **III**, a discrepancy between *in vitro* and *in vivo* data on CYP3A4/5 inhibition by imatinib was evident. In clinical studies, imatinib was a relatively strong inhibitor of CYP3A4/5; imatinib at steady state increased the plasma exposure to the CYP3A4/5 substrate simvastatin by 3.5-fold (O'Brien *et al.*, 2003), and reduced hepatic CYP3A4/5 activity by up to 70% (Gurney *et al.*, 2007, Connolly *et al.*, 2011). However, the unbound concentrations of imatinib and its main metabolite N-desmethylimatinib in plasma (<1 and <0.1 μM, respectively) were much lower than their reported direct K_i values for CYP3A4/5 inhibition in HLM (8 and 14 μM, respectively) (Gleevec Clinical Pharmacology and Biopharmaceutic Review(s), 2001, Gleevec label, 2014). Because of these inconsistencies, and because CYP2C8 was reported to be involved in the metabolism of imatinib (Nebot *et al.*, 2010), study **III** aiming to elucidate the inhibitory effects of imatinib on CYP2C8 and CYP3A4 in HLM was carried out.

In study **III**, both imatinib and N-desmethylimatinib were found to be moderately potent direct inhibitors of CYP2C8 and CYP3A4/5. In addition, inhibition of CYP3A4 (but not of CYP3A5) by imatinib was concentration-, NADPH-, and time-dependent; the presence of a competitive CYP3A4 inhibitor decreased the inhibition; and dialysis was unable to restore CYP3A4 activity. Thus, these findings suggested that imatinib affects CYP3A4 by mechanism-based inhibition *in vitro*. Its K_I and k_{inact} values were 11 μM (after adjusting for non-specific binding) and 0.072 1/min, respectively. The direct inhibitory effects of imatinib on CYP2C8 and CYP3A4/5 were predicted to be of negligible clinical relevance, while mechanism-based inhibition by imatinib was estimated to cause several-fold increases in the plasma concentrations of CYP3A4 substrates.

CYP3A4 has been described to be the main enzyme in imatinib metabolism (Marull and Rochat, 2006, Rochat *et al.*, 2008, Gleevec label, 2014). However, imatinib-mediated mechanism-based inhibition of this enzyme suggests that imatinib could time- and concentration-dependently inhibit its own metabolism, leading to a decreasing importance of CYP3A4 in its pharmacokinetics with time. This hypothesis could explain why strong

CYP3A4 inhibitors have had only a small or no effect on imatinib concentrations *in vivo* (Dutreix *et al.*, 2004, Widmer *et al.*, 2006, van Erp *et al.*, 2007), and why the clearances of CYP3A4 substrates correlated with imatinib clearance in the beginning of imatinib treatment but no longer at steady state (Gurney *et al.*, 2007). Based on this theory and the fact that CYP2C8 was suggested to play a key role in imatinib metabolism (Nebot *et al.*, 2010), studies **IV** and **V** were undertaken to investigate the importance of CYP2C8 in the pharmacokinetics of imatinib by use of an integrated *in vitro*, *in silico*, and *in vivo* approach.

In study **IV**, both CYP2C8 and CYP3A4 inhibitors inhibited the depletion of imatinib by >40%, and the main metabolic pathway of imatinib by >50%. Likewise, recombinant CYP2C8 and CYP3A4 metabolised imatinib extensively, while other CYP isoforms had minor effect on its concentrations. Using the ISEF approach, the fractions of the hepatic clearance of imatinib mediated by CYP2C8 and CYP3A4 were predicted to approximate 40 and 60%, respectively. PBPK simulations predicted that the autoinhibition of CYP3A4 by imatinib could increase the role of CYP2C8 in imatinib pharmacokinetics time-dependently, and that a strong CYP2C8 inhibitor like gemfibrozil could increase its plasma exposure by 1.8-fold following a single imatinib dose of 400 mg.

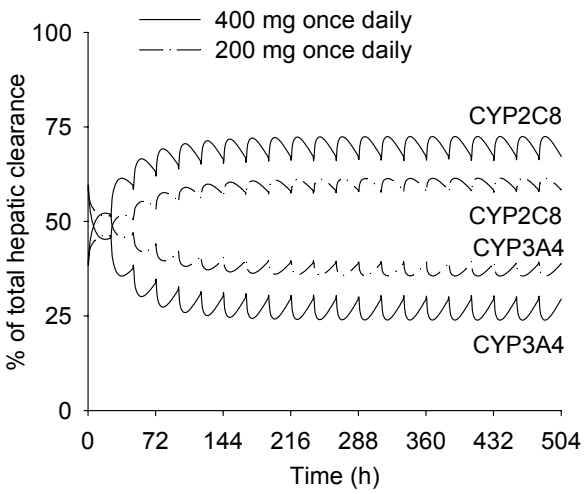

Figure 22. Simulated importance of CYP2C8 and CYP3A4 in imatinib metabolism during treatment with imatinib 200 or 400 mg once daily (**V**). Curves for CYP1A2, CYP2B6, CYP2D6, and CYP3A5 were omitted for clarity because their roles were negligible (<5% of total hepatic clearance) (Filppula *et al.* (2013), unpublished results).

In study **V**, gemfibrozil unexpectedly reduced the absorption of imatinib; its C_{max} decreased by 35%, while its total AUC was unaffected by gemfibrozil coadministration. Gemfibrozil also reduced the C_{max} and total AUC of N-desmethylimatinib by 56 and 48%, respectively, and the C_{max}/C_{24} ratios of imatinib and N-desmethylimatinib by 44 and 17%, respectively. Simulations with the refined PBPK model predicted well the effect of gemfibrozil on imatinib pharmacokinetics, when inhibition of both CYP2C8-mediated metabolism and active intestinal uptake transport were included in the model. Based upon these simulations, the contribution of CYP2C8 to imatinib metabolism was predicted to increase from ~40 to 70% during multiple dosing with imatinib 400 mg once daily because of time-dependent autoinhibition of CYP3A4 by imatinib (Figure 22). Interaction simulations with gemfibrozil

600 mg twice daily and imatinib 200 or 400 mg once daily suggested that the interaction magnitude increases with higher imatinib doses and during multiple dosing.

The effect of gemfibrozil on the absorption of imatinib had not been anticipated. Initially, the absorption rate of imatinib appeared to follow that observed in the placebo phase, but it successively declined, resulting in reduced peak concentrations and double peaks in the gemfibrozil phase. Due to the similar absorption profiles of imatinib in the beginning of the placebo and gemfibrozil phases, its altered absorption is unlikely due to gemfibrozil-induced changes in the emptying rate of the stomach or dissolution of imatinib. Previously, markedly reduced itraconazole concentrations and a reduced C_{max} of enzalutamide have been observed during gemfibrozil coadministration (Niemi *et al.*, 2003b, Jaakkola *et al.*, 2005, Niemi *et al.*, 2006, Xtandi Clinical Pharmacology and Biopharmaceutic Review(s), 2012). One of the proposed explanations for the finding with itraconazole is displacement of it from plasma proteins by gemfibrozil, leading to an increased clearance or volume of distribution. In a previous study, displacement of imatinib from α1-acid glycoprotein has been suggested to explain why clindamycin reduced the plasma exposure to imatinib by 70% (Gambacorti-Passerini *et al.*, 2003). However, in study **V**, gemfibrozil had no effect on the unbound fraction of imatinib in 2 and 12-h plasma, making displacement of imatinib from plasma proteins an unlikely cause of interaction.

Induction of CYPs or other enzymes involved in imatinib pharmacokinetics could possibly explain the observed effect on imatinib absorption by gemfibrozil. Previously, the CYP2C8 and CYP3A4 inducers rifampicin and St John's Wort have reduced imatinib C_{max} and AUC by 15-54% and 30-74%, respectively, and increased N-desmethylimatinib C_{max} by 13-89%, but had little or no effect on its AUC (Bolton *et al.*, 2004, Frye *et al.*, 2004, Smith *et al.*, 2004a, Smith *et al.*, 2004b). Gemfibrozil is a mild inducer of CYP2C8 and CYP3A4 *in vitro* (Prueksaritanont *et al.*, 2005), but there is no evidence for such an effect *in vivo*. *In vitro*, imatinib is also a substrate of other CYPs, FMO3, and the extrahepatic enzymes CYP1A1, CYP1B1, and CYP2J2 (Rochat *et al.*, 2008, Narjoz *et al.*, 2014). In theory, gemfibrozil-mediated induction of other enzymes than CYP2C8 and CYP3A4 could also be one putative explanation, but no such effect has been described in the literature. Regardless, strong mechanism-based inhibition of CYP2C8 is most likely the dominating mechanism in the metabolism-mediated interaction. Furthermore, induction of imatinib-transporting efflux proteins is also unlikely; no such mechanism has been demonstrated for gemfibrozil. Because of the high absolute availability of imatinib (98%), the role of uptake proteins is probably more important than that of efflux transporters.

Based on early *in vitro* transport studies, imatinib was initially classified as a low permeability drug (Gleevec Clinical Pharmacology and Biopharmaceutic Review(s), 2001). However, following a clinical study showing that its bioavailability is very high (Peng *et al.*, 2004a), imatinib was classified as a high permeability drug, thus suggesting that it might be a

substrate of uptake transporters. Gemfibrozil inhibits OATP1B1 both *in vitro* and *in vivo* (Kyrklund *et al.*, 2003, Schneck *et al.*, 2004). As the AUC of imatinib did not increase following gemfibrozil co-administration, it is unlikely that OATP1B1 inhibition by gemfibrozil contributed to the interaction. The transporters OATP1A2 and OCTN have been suggested to participate in the intestinal absorption of imatinib (Hu *et al.*, 2008, Eechoute *et al.*, 2011a, Eechoute *et al.*, 2011b); however, it is not known whether gemfibrozil or its metabolites can affect these proteins. *In vitro* studies are therefore needed to identify the transporter possibly affected by gemfibrozil.

Thus, the findings of study **III** suggest that imatinib is a mechanism-based inhibitor of CYP3A4, while those of studies **IV** and **V** indicate that CYP2C8 forms N-desmethylimatinib from imatinib. Simultaneously with the publication of study **III**, another study also proposed that imatinib is a mechanism-based inhibitor of CYP3A4 (Kenny *et al.*, 2012). Here, its K_I and k_{inact} values were determined to 4.4 μM and 0.028 1/min, respectively. In addition, a recent publication studied the reactive intermediates of imatinib, and found that they could be imine and imine-carbonyl conjugate structures on the piperazine ring, and imine-methide on the p-toluidine partial structure of imatinib (Li *et al.*, 2014). Altogether, the findings of studies **III**, **IV**, and **V**, and recent literature propose that it is likely that imatinib inhibits its own CYP3A4-mediated pharmacokinetics, and this may lead to an increasing role for CYP2C8 in its clinical use.

16. General discussion and clinical implications

Montelukast was developed before CYP2C8 was recognised as a major drug-metabolising enzyme. Therefore it was not included in the early *in vitro* screening studies. However, had CYP2C8 been included, it would likely have been saturated due to the high montelukast concentrations tested. In addition, high protein concentrations were used in the incubations in the previous study. Because montelukast is highly lipophilic, and binds non-specifically to microsomal proteins, low HLM concentrations were used in studies **I** and **II**. In addition, very low montelukast concentrations were tested, corresponding to its unbound peak concentrations in plasma. Results obtained using low montelukast and HLM concentrations together with carefully validated *in vitro* conditions, indicated that CYP2C8 is the main enzyme in the metabolism of montelukast.

The *in vitro* finding was confirmed in the clinical interaction study with gemfibrozil. Together, the findings of studies **I** and **II** propose that CYP2C8 contributes to about 80% of the elimination of montelukast. Because no differences in montelukast pharmacokinetics between healthy volunteers and asthma patients have been reported (Singulair Clinical Pharmacology and Biopharmaceutic Review(s), 1998, Singulair Label, 2013), it is likely that the gemfibrozil-mediated increase in montelukast AUC in healthy subjects could also occur in

patients. Because montelukast has a very wide safety margin, however, the increase in montelukast exposure is probably not clinically significant in most cases. On the other hand, an increased risk for concentration-dependent adverse effects cannot be excluded, in particular for patients with impaired hepatic function. Therefore, a dose reduction of 50-80% could be considered for montelukast when given in combination with CYP2C8 inhibitors.

As compared to other CYP2C8 substrate drugs (Table 14), only the effects of gemfibrozil on the pharmacokinetics of repaglinide and cerivastatin have been larger than that observed on montelukast. Cerivastatin was early withdrawn from the market, partly due to harmful interactions with gemfibrozil (Backman *et al.*, 2002, Huang *et al.*, 2008), while repaglinide is commonly used as a CYP2C8 probe in clinical interaction studies. Although sensitive to CYP2C8 inhibition *in vivo* (Niemi *et al.*, 2003b, Tornio *et al.*, 2008, Backman *et al.*, 2009, Honkalammi *et al.*, 2012), repaglinide is, like cerivastatin, also a substrate of OATP1B1 (Niemi et al., 2005b), which confounds the interpretation of interaction data. Furthermore, repaglinide, an antidiabetic drug, easily causes hypoglycaemia in healthy volunteers, whereby monitoring of blood glucose levels is necessary in interaction studies. Another CYP2C8 probe is the antimalarial agent amodiaquine (EMA, 2013). However, although available in Africa, it is not on the market in the European Union and United States. Therefore, given its availability, beneficial safety profile, high $f_{m,\ CYP2C8}$ (0.8), linear pharmacokinetics, and the fact that it does not seem to be a substrate of clinically relevant drug transporters, montelukast could be used as sensitive CYP2C8 probe in clinical interaction studies. In addition, because CYP2C8 forms the main metabolite of montelukast, M6, almost exclusively *in vitro*, montelukast 36-hydroyxylation (M6 formation) could also serve as a CYP2C8 marker reaction *in vitro*.

The results obtained for imatinib in study **III** indicate that it is a mechanism-based CYP3A4 inhibitor, which suggest that concomitant use of imatinib with CYP3A4 substrates may increase the risk of concentration-dependent adverse drug reactions. Its estimated R value for mechanism based inhibition of CYP3A4 (section 5.2), calculated based on its steady state unbound C_{max}, equals ~6, suggesting a >two-fold change in AUC of CYP3A4 substrates (Fujioka *et al.*, 2012). Hence, its R value is smaller than those observed for other mechanism-based inhibitors of CYP3A4, such as erythromycin (12), nelfinavir (77), and verapamil (21) (Fujioka *et al.*, 2012), which have increase the AUC of simvastatin by 4.6-6.2-fold (Kantola *et al.*, 1998, Hsyu *et al.*, 2001). The finding that imatinib affects CYP3A4 by mechanism-based inhibition explains its interaction with simvastatin, but also the previously mentioned inconsistencies related to its own pharmacokinetics. Therefore, in order to reliably determine the role of CYP2C8 in its metabolism, it was necessary to first characterise the inhibitory effect of imatinib on CYP3A4 (**III**), and then conduct the *in vitro* metabolism studies (**IV**). Furthermore, use of static models to predict the *in vivo* contribution of CYP2C8 was not sufficient as the mechanism-based autoinhibition of its metabolism proceeds with increasing

time and concentrations. Consequently, dynamic PBPK simulations were carried out to model the contributions by CYP2C8 and CYP3A4 with time.

In the clinical study (**V**), gemfibrozil reduced the CYP2C8-mediated formation of N-desmethylimatinib from imatinib, in line with the *in vitro* findings of study **IV**. However, the CYP2C8 inhibitory effect of gemfibrozil was possibly counteracted by a simultaneous inhibition of the absorption of imatinib. The impaired absorption may be a result of inhibition of a transporter involved in imatinib uptake. Further studies are needed to elucidate the exact mechanism by which gemfibrozil affects imatinib absorption. It is thus likely that at least three different processes participated in the findings; mechanism-based inhibition of CYP2C8 by gemfibrozil, impairment of imatinib absorption by gemfibrozil, and mechanism-based inhibition of CYP3A4 by imatinib. However, the effect of imatinib on CYP3A4 was probably small following the single imatinib dose administrated. With use of a PBPK model, it was possible to simulate this complex interaction following repeated dosing of both gemfibrozil and imatinib. According to the simulations, the interaction magnitude increases as imatinib approaches steady state. Due to a cumulating effect of the CYP3A4-mediated autoinhibition by imatinib, the role of CYP3A4 in its metabolism becomes less important with time, while that of CYP2C8 increases. According to the final simulations, the elimination of imatinib relies more on CYP2C8 than on CYP3A4 during long-term treatment. Clinical studies with multiple doses of imatinib are needed to further evaluate the roles of CYP3A4 and CYP2C8 in imatinib pharmacokinetics during steady state. Given that the efficacy and adverse effects of imatinib are concentration-dependent, care is warranted when CYP2C8 inhibitors are given in combination with imatinib.

In this work, the role of CYP2C8 in the metabolism of two structurally unrelated drugs from two different therapeutic classes was investigated. The finding that CYP2C8 was able to metabolise both drugs is in line with its capability to accommodate molecules of diverse sizes and structures. Together, these studies strengthen the role of CYP2C8 as an important drug-metabolising enzyme, and suggest that the number of drugs metabolised by CYP2C8 might actually be higher than previously thought. In addition, they highlight the importance of carefully validated *in vitro* experiments, and demonstrate the advantages of PBPK simulations to explain complex drug-drug interactions.

CONCLUSIONS

The following conclusions can be made based on the studies in this thesis:

1. In contrast to previous information, CYP2C8 is the principal enzyme involved in the metabolism of montelukast. CYP2C8 catalyses the main metabolic pathway of montelukast; the formation of M6 and its further metabolism to M4.

2. Montelukast could serve as a safe and sensitive CYP2C8 marker substrate in drug-drug interaction studies during drug development.

3. Imatinib is a mechanism-based inhibitor of CYP3A4 *in vitro*, which explains its previously observed interaction with simvastatin. Imatinib may also increase the plasma exposure to other CYP3A4 substrate drugs. Autoinhibition of CYP3A4 by imatinib provides an explanation to previously documented inconsistencies regarding the role of CYP3A4 in its pharmacokinetics.

4. The formation of the active metabolite of imatinib, N-desmethylimatinib, is catalysed by CYP2C8 and CYP3A4. During multiple dosing, the elimination of imatinib is likely to rely more on CYP2C8 than on CYP3A4, due to the concentration- and time-dependent CYP3A4 autoinhibition by imatinib.

ACKNOWLEDGEMENTS

This work was carried out at the Department of Clinical Pharmacology, University of Helsinki, between the years 2009 and 2014. I am most grateful to all who have helped, assisted and accompanied me during this period in time.

First, I would like to express my deepest gratitude to my supervisors **Professor Janne Backman** and **Professor *Emeritus* Pertti Neuvonen** for giving me the opportunity to conduct research at the Department of Clinical Pharmacology. Thank you for your invaluable guidance, motivation, and enthusiasm. Janne is especially acknowledged for his time, endless patience and for his remarkable ability to always find new perspectives. I want to thank Pertti for his generosity; for unselfish sharing of his notable expertise and experience, and for help with both challenging and small issues. I am also grateful for all the opportunities I have been given to attend miscellaneous courses and meetings, both in Finland and abroad.

I thank **Associate Professor Nina Isoherranen** and **Adjunct Professor Mikko Koskinen** for reviewing and improving this thesis; for constructive comments and helpful suggestions.

I am thankful to **Dr Jennifer Rowland** for revising the language of this thesis.

I am most grateful to **Professor Mikko Niemi** for his significant input to studies **II** and **V**, and also for his generous help and insightful comments during these years. **Jouko Laitila** and **Mikko Neuvonen** are acknowledged for their vast expertise and invaluable collaboration in the laboratory. I would especially like to thank Jouko for patiently guiding me through *in vitro* experiments in 2009. **Eija Mäkinen-Pulli** and **Lisbet Partanen** are warmly recognised for their skilful technical assistance and most delightful company.

I wish to sincerely thank all other of my present and former colleagues at the Department of Clinical Pharmacology for their encouragement, company and collaboration: **Katja Halme**, **Päivi Hirvensalo**, **Mikko Holmberg**, **Johanna Honkalammi**, **Matti Itkonen**, **Tuija Itkonen**, **Jenni Keskitalo**, **Kaisa Kurkinen**, **Outi Lapatto-Reiniluoto**, **Terhi Launiainen**, **Maria Paile-Hyvärinen**, **Helmi Pett**, **Päivi Ruokoniemi**, **Tuija Tapaninen**, **Juha Vakkilainen**, and **Xiaoqiang Xiang**. Especially, I want to thank **Katriina Tarkiainen** for her friendship, support, and for being my *logistiikkapäällikkö*; **Tiina Karonen** is warmly acknowledged for the collaboration in study **II** and **Aleksi Tornio** for the collaboration in study **V**.

I would like to thank all students who have been involved in various research projects at the department for cheerful company, in particular **Ollipekka Kailari**, **Outi Koskela**, **Tiffany Mustonen**, and **Paavo Pietarinen**.

I wish to thank all healthy volunteers who kindly participated in the clinical studies.

The HUS Pharmacy is acknowledged for excellent collaboration.

This work was financially supported by the Helsinki University Central Hospital Research Fund, the Sigrid Jusélius Foundation, the Clinical Drug Research Graduate School, Carin och Gustaf Arppes fond, the Finnish Pharmaceutical Society, and the Orion-Farmos Research Foundation, all of which are gratefully acknowledged.

I would like to thank all my friends, near and far, for their friendship. I especially wish to acknowledge **Sofie** at the HUS Pharmacy for her input to study **V** and for pleasant company during our tea breaks. I thank **Sarah**, **Catarina**, **Jonna**, and **Jessica** for reminding me of the importance of leisure time with yoga, power walks, and brunches. My dear friends **Hanna** and **Rebecka** from the years in Uppsala are acknowledged for encouraging and entertaining Internet conversations. Furthermore, I would like to thank the **Högnabba** family, my relatives, and my grandmother **Helena** for composing a strong support network around me.

I wish to thank my parents, **Britt** and **Seppo**, my brothers **Kim** and **Sami**, and Sami's fiancée **Johanna** for their unconditional love, support, and encouragement. I would also like to thank my sweet niece **Isabella** for bringing sunshine and joy to our family.

Finally, I would like to thank **Sebastian** for helping me in so many ways, for fresh perspectives, inspiration, and for making me laugh. Thank you for your love and for helping me to stay positive and motivated.

Moffa, nu e ja en skald.

Helsinki, October 2014

Anne Filppula

REFERENCES

Achour, B., Barber, J. and Rostami-Hodjegan, A. Expression of Hepatic Drug-Metabolizing Cytochrome P450 Enzymes and Their Inter-Correlations: A Meta-Analysis. *Drug Metab Dispos* doi: 10.1124/dmd.114.058834 (2014).

Al-Batran, S. E., Atmaca, A., Schleyer, E., Pauligk, C., Hosius, C., Ehninger, G. and Jager, E. Imatinib mesylate for targeting the platelet-derived growth factor beta receptor in combination with fluorouracil and leucovorin in patients with refractory pancreatic, bile duct, colorectal, or gastric cancer--a dose-escalation Phase I trial. *Cancer* 109: 1897-1904 (2007).

Alessandrini, M., Asfaha, S., Dodgen, T. M., Warnich, L. and Pepper, M. S. Cytochrome P450 pharmacogenetics in African populations. *Drug Metab Rev* 45: 253-275 (2013).

Apperley, J. F. Part I: mechanisms of resistance to imatinib in chronic myeloid leukaemia. *Lancet Oncol* 8: 1018-1029 (2007).

Aquilante, C. L., Kosmiski, L. A., Bourne, D. W., Bushman, L. R., Daily, E. B., Hammond, K. P., Hopley, C. W., Kadam, R. S., Kanack, A. T., Kompella, U. B., Le, M., Predhomme, J. A., Rower, J. E. and Sidhom, M. S. Impact of the CYP2C8 *3 polymorphism on the drug-drug interaction between gemfibrozil and pioglitazone. *Br J Clin Pharmacol* 75: 217-226 (2013a).

Aquilante, C. L., Niemi, M., Gong, L., Altman, R. B. and Klein, T. E. PharmGKB summary: very important pharmacogene information for cytochrome P450, family 2, subfamily C, polypeptide 8. *Pharmacogenet Genomics* 23: 721-728 (2013b).

Aquilante, C. L., Wempe, M. F., Spencer, S. H., Kosmiski, L. A., Predhomme, J. A. and Sidhom, M. S. Influence of CYP2C8*2 on the pharmacokinetics of pioglitazone in healthy African-American volunteers. *Pharmacotherapy* 33: 1000-1007 (2013c).

Arun, K. P., Meda, V. S., Kucherlapati, V. S. P. R., Dubala, A., Deepalakshmi, M., Anand VijayaKumar, P. R., Elango, K. and Suresh, B. Pharmacokinetic drug interaction between gemfibrozil and sitagliptin in healthy Indian male volunteers. *Eur J Clin Pharmacol* 68: 709-714 (2012).

Attar, M., Dong, D., Ling, K. H. and Tang-Liu, D. D. Cytochrome P450 2C8 and flavin-containing monooxygenases are involved in the metabolism of tazarotenic acid in humans. *Drug Metab Dispos* 31: 476-481 (2003).

Baca, Q. J. and Golan, D. E. Pharmacodynamics. *Principles of pharmacology: the pathophysiologic basis of drug therapy*. Golan, D. E. and Tashjian, A. H. Wolters Kluwer Health/Lippincott Williams & Wilkins, Philadelphia (2012). 17-26.

Bachmann, K. A. Inhibition constants, inhibitor concentrations and the prediction of inhibitory drug drug interactions: pitfalls, progress and promise. *Curr Drug Metab* 7: 1-14 (2006).

Backman, J. T., Honkalammi, J., Neuvonen, M., Kurkinen, K. J., Tornio, A., Niemi, M. and Neuvonen, P. J. CYP2C8 activity recovers within 96 hours after gemfibrozil dosing: estimation of CYP2C8 half-life using repaglinide as an in vivo probe. *Drug Metab Dispos* 37: 2359-2366 (2009).

Backman, J. T., Kivisto, K. T., Olkkola, K. T. and Neuvonen, P. J. The area under the plasma concentration-time curve for oral midazolam is 400-fold larger during treatment with itraconazole than with rifampicin. *Eur J Clin Pharmacol* 54: 53-58 (1998).

Backman, J. T., Kyrklund, C., Kivisto, K. T., Wang, J. S. and Neuvonen, P. J. Plasma concentrations of active simvastatin acid are increased by gemfibrozil. *Clin Pharmacol Ther* 68: 122-129 (2000).

Backman, J. T., Kyrklund, C., Neuvonen, M. and Neuvonen, P. J. Gemfibrozil greatly increases plasma concentrations of cerivastatin. *Clin Pharmacol Ther* 72: 685-691 (2002).

Backman, J. T., Luurila, H., Neuvonen, M. and Neuvonen, P. J. Rifampin markedly decreases and gemfibrozil increases the plasma concentrations of atorvastatin and its metabolites. *Clin Pharmacol Ther* 78: 154-167 (2005).

Backman, J. T., Wang, J. S., Wen, X., Kivisto, K. T. and Neuvonen, P. J. Mibefradil but not isradipine substantially elevates the plasma concentrations of the CYP3A4 substrate triazolam. *Clin Pharmacol Ther* 66: 401-407 (1999).

Baer, B. R., DeLisle, R. K. and Allen, A. Benzylic oxidation of gemfibrozil-1-O-beta-glucuronide by P450 2C8 leads to heme alkylation and irreversible inhibition. *Chem Res Toxicol* 22: 1298-1309 (2009).

Bahadur, N., Leathart, J. B., Mutch, E., Steimel-Crespi, D., Dunn, S. A., Gilissen, R., Houdt, J. V., Hendrickx, J., Mannens, G., Bohets, H., Williams, F. M., Armstrong, M., Crespi, C. L. and Daly, A. K. CYP2C8 polymorphisms in Caucasians and their relationship with paclitaxel 6alpha-hydroxylase activity in human liver microsomes. *Biochem Pharmacol* 64: 1579-1589 (2002).

Balani, S. K., Xu, X., Pratha, V., Koss, M. A., Amin, R. D., Dufresne, C., Miller, R. R., Arison, B. H., Doss, G. A., Chiba, M., Freeman, A., Holland, S. D., Schwartz, J. I., Lasseter, K. C., Gertz, B. J., Isenberg, J. I., Rogers, J. D., Lin, J. H. and Baillie, T. A. Metabolic profiles of montelukast sodium (Singulair), a potent cysteinyl leukotriene1 receptor antagonist, in human plasma and bile. *Drug Metab Dispos* 25: 1282-1287 (1997).

Baldwin, S. J., Bloomer, J. C., Smith, G. J., Ayrton, A. D., Clarke, S. E. and Chenery, R. J. Ketoconazole and sulphaphenazole as the respective selective inhibitors of P4503A and 2C9. *Xenobiotica* 25: 261-270 (1995).

Baldwin, S. J., Clarke, S. E. and Chenery, R. J. Characterization of the cytochrome P450 enzymes involved in the in vitro metabolism of rosiglitazone. *Br J Clin Pharmacol* 48: 424-432 (1999).

Bartholow, M. Top 200 Drugs of 2011. *Pharmacy Times. URL: http://www.pharmacytimes.com/publications/issue/2012/July2012/Top-200-Drugs-of-2011 (Accessed 2014, May 12)* (2012).

Becquemont, L., Le Bot, M. A., Riche, C., Funck-Brentano, C., Jaillon, P. and Beaune, P. Use of heterologously expressed human cytochrome P450 1A2 to predict tacrine-fluvoxamine drug interaction in man. *Pharmacogenetics* 8: 101-108 (1998).

Becquemont, L., Mouajjah, S., Escaffre, O., Beaune, P., Funck-Brentano, C. and Jaillon, P. Cytochrome P-450 3A4 and 2C8 are involved in zopiclone metabolism. *Drug Metab Dispos* 27: 1068-1073 (1999).

Bertilsson, L., Hojer, B., Tybring, G., Osterloh, J. and Rane, A. Autoinduction of carbamazepine metabolism in children examined by a stable isotope technique. *Clin Pharmacol Ther* 27: 83-88 (1980).

Bidstrup, T. B., Bjornsdottir, I., Sidelmann, U. G., Thomsen, M. S. and Hansen, K. T. CYP2C8 and CYP3A4 are the principal enzymes involved in the human in vitro biotransformation of the insulin secretagogue repaglinide. *Br J Clin Pharmacol* 56: 305-314 (2003).

Bidstrup, T. B., Damkier, P., Olsen, A. K., Ekblom, M., Karlsson, A. and Brosen, K. The impact of CYP2C8 polymorphism and grapefruit juice on the pharmacokinetics of repaglinide. *Br J Clin Pharmacol* 61: 49-57 (2006).

Bidstrup, T. B., Stilling, N., Damkier, P., Scharling, B., Thomsen, M. S. and Brosen, K. Rifampicin seems to act as both an inducer and an inhibitor of the metabolism of repaglinide. *Eur J Clin Pharmacol* 60: 109-114 (2004).

Bjornsson, T. D., Callaghan, J. T., Einolf, H. J., Fischer, V., Gan, L., Grimm, S., Kao, J., King, S. P., Miwa, G., Ni, L., Kumar, G., McLeod, J., Obach, R. S., Roberts, S., Roe, A., Shah, A., Snikeris, F., Sullivan, J. T., Tweedie, D., Vega, J. M., Walsh, J., Wrighton, S. A., Pharmaceutical, R., Manufacturers of America Drug Metabolism/Clinical Pharmacology Technical Working, G., Evaluation, F. D. A. C. f. D. and Research. The conduct of in vitro and in vivo drug-drug interaction studies: a Pharmaceutical Research and Manufacturers of America (PhRMA) perspective. *Drug Metab Dispos* 31: 815-832 (2003).

Bohmer, G. M., Nassr, N., Wenger, M., Hunnemeyer, A., Lahu, G., Templin, S., Gleiter, C. H. and Hermann, R. The targeted oral, once-daily phosphodiesterase 4 inhibitor roflumilast and the leukotriene receptor antagonist montelukast do not exhibit significant pharmacokinetic interactions. *J Clin Pharmacol* 49: 389-397 (2009).

Bolton, A. E., Peng, B., Hubert, M., Krebs-Brown, A., Capdeville, R., Keller, U. and Seiberling, M. Effect of rifampicin on the pharmacokinetics of imatinib mesylate (Gleevec, STI571) in healthy subjects. *Cancer Chemother Pharmacol* 53: 102-106 (2004).

Bornhauser, M., Illmer, T., Le Coutre, P., Pursche, J., von Bonin, M., Freiberg-Richter, J., Schaich, M., Platzbecker, U., Thiede, C., Ottmann, O. G., Kohne, C., Braess, J., Ehninger, G. and Schleyer, E. Imatinib mesylate selectively influences the cellular metabolism of cytarabine in BCR/ABL negative leukemia cell lines and normal CD34+ progenitor cells. *Ann Hematol* 83 Suppl 1: S61-64 (2004).

Bornhauser, M., Pursche, S., Bonin, M., Freiberg-Richter, J., Jenke, A., Illmer, T., Ehninger, G. and Schleyer, E. Elimination of imatinib mesylate and its metabolite N-desmethyl-imatinib. *J Clin Oncol* 23: 3855-3856; author reply 3857-3858 (2005).

Bourrie, M., Meunier, V., Berger, Y. and Fabre, G. Cytochrome P450 isoform inhibitors as a tool for the investigation of metabolic reactions catalyzed by human liver microsomes. *J Pharmacol Exp Ther* 277: 321-332 (1996).

Brown, R. R., Miller, J. A. and Miller, E. C. The metabolism of methylated aminoazo dyes. IV. Dietary factors enhancing demethylation in vitro. *J Biol Chem* 209: 211-222 (1954).

Brännström, M., Bonn, B., Davis, A., Hilgendorf, C., Palm, J., Rubin, K. and Grime, K. OATP2B1-mediated Uptake of Montelukast in OATP2B1 and Mock Transfected HEK293 Cells. (2014).

Buchdunger, E., Cioffi, C. L., Law, N., Stover, D., Ohno-Jones, S., Druker, B. J. and Lydon, N. B. Abl protein-tyrosine kinase inhibitor STI571 inhibits in vitro signal transduction mediated by c-kit and platelet-derived growth factor receptors. *J Pharmacol Exp Ther* 295: 139-145 (2000).

Bun, S. S., Ciccolini, J., Bun, H., Aubert, C. and Catalin, J. Drug interactions of paclitaxel metabolism in human liver microsomes. *J Chemother* 15: 266-274 (2003).

Burger, H., van Tol, H., Brok, M., Wiemer, E. A., de Bruijn, E. A., Guetens, G., de Boeck, G., Sparreboom, A., Verweij, J. and Nooter, K. Chronic imatinib mesylate exposure leads to reduced intracellular drug accumulation by induction of the ABCG2 (BCRP) and ABCB1 (MDR1) drug transport pumps. *Cancer Biol Ther* 4: 747-752 (2005).

Calapai, G., Casciaro, M., Miroddi, M., Calapai, F., Navarra, M. and Gangemi, S. Montelukast-induced adverse drug reactions: a review of case reports in the literature. *Pharmacology* 94: 60-70 (2014).

Chang, J. T., Staffa, J. A., Parks, M. and Green, L. Rhabdomyolysis with HMG-CoA reductase inhibitors and gemfibrozil combination therapy. *Pharmacoepidemiol Drug Saf* 13: 417-426 (2004).

Chen, Y. and Goldstein, J. A. The transcriptional regulation of the human CYP2C genes. *Curr Drug Metab* 10: 567-578 (2009).

Chen, Y., Liu, L., Monshouwer, M. and Fretland, A. J. Determination of time-dependent inactivation of CYP3A4 in cryopreserved human hepatocytes and assessment of human drug-drug interactions. *Drug Metab Dispos* 39: 2085-2092 (2011).

Cheng, H., Leff, J. A., Amin, R., Gertz, B. J., De Smet, M., Noonan, N., Rogers, J. D., Malbecq, W., Meisner, D. and Somers, G. Pharmacokinetics, bioavailability, and safety of montelukast sodium (MK-0476) in healthy males and females. *Pharm Res* 13: 445-448 (1996).

Chiba, M., Xu, X., Nishime, J. A., Balani, S. K. and Lin, J. H. Hepatic microsomal metabolism of montelukast, a potent leukotriene D4 receptor antagonist, in humans. *Drug Metab Dispos* 25: 1022-1031 (1997).

Chu, X., Philip, G. and Evers, R. Comments on Mougey et al. (2009): Absorption of montelukast is transporter mediated: a common variant of OATP2B1 is associated with reduced plasma concentrations and poor response. Pharmacogenet Genomics 19: 129-138. *Pharmacogenet Genomics* 22: 319-322 (2012).

Cingi, C., Toros, S. Z., Ince, I., Ertugay, C. K., Gurbuz, M. K., Cakli, H., Erdogmus, N., Karasulu, E. and Kaya, E. Does desloratadine alter the serum levels of montelukast when administered in a fixed-dose combination? *Laryngoscope* 123: 2610-2614 (2013).

Clark, S. S., McLaughlin, J., Timmons, M., Pendergast, A. M., Ben-Neriah, Y., Dow, L. W., Crist, W., Rovera, G., Smith, S. D. and Witte, O. N. Expression of a distinctive BCR-ABL oncogene in Ph1-positive acute lymphocytic leukemia (ALL). *Science* 239: 775-777 (1988).

Conney, A. H. Pharmacological implications of microsomal enzyme induction. *Pharmacol Rev* 19: 317-366 (1967).

Conney, A. H., Brown, R. R., Miller, J. A. and Miller, E. C. The metabolism of methylated aminoazo dyes. VI. Intracellular distribution and properties of the demethylase system. *Cancer Res* 17: 628-633 (1957).

Connolly, R. M., Rudek, M. A., Garrett-Mayer, E., Jeter, S. C., Donehower, M. G., Wright, L. A., Zhao, M., Fetting, J. H., Emens, L. A., Stearns, V., Davidson, N. E., Baker, S. D. and Wolff, A. C. Docetaxel metabolism is not altered by imatinib: findings from an early phase study in metastatic breast cancer. *Breast Cancer Res Treat* 127: 153-162 (2011).

Cooper, D. Y., Levin, S., Narasimhulu, S. and Rosenthal, O. Photochemical Action Spectrum of the Terminal Oxidase of Mixed Function Oxidase Systems. *Science* 147: 400-402 (1965).

Copeland, R. A. Evaluation of enzyme inhibitors in drug discovery : a guide for medicinal chemists and pharmacologists. *Methods of biochemical analysis*. Wiley-Interscience, Hoboken, N.J. (2005). 1-397.

Cortes, J. E., Talpaz, M., Beran, M., O'Brien, S. M., Rios, M. B., Stass, S. and Kantarjian, H. M. Philadelphia chromosome-negative chronic myelogenous leukemia with rearrangement of the breakpoint cluster region. Long-term follow-up results. *Cancer* 75: 464-470 (1995).

Crespi, C. L. and Miller, V. P. The use of heterologously expressed drug metabolizing enzymes--state of the art and prospects for the future. *Pharmacol Ther* 84: 121-131 (1999).

Cribb, A. E., Peyrou, M., Muruganandan, S. and Schneider, L. The endoplasmic reticulum in xenobiotic toxicity. *Drug Metab Rev* 37: 405-442 (2005).

Cusatis, G., Gregorc, V., Li, J., Spreafico, A., Ingersoll, R. G., Verweij, J., Ludovini, V., Villa, E., Hidalgo, M., Sparreboom, A. and Baker, S. D. Pharmacogenetics of ABCG2 and adverse reactions to gefitinib. *J Natl Cancer Inst* 98: 1739-1742 (2006).

Dai, D., Zeldin, D. C., Blaisdell, J. A., Chanas, B., Coulter, S. J., Ghanayem, B. I. and Goldstein, J. A. Polymorphisms in human CYP2C8 decrease metabolism of the anticancer drug paclitaxel and arachidonic acid. *Pharmacogenetics* 11: 597-607 (2001).

Daily, E. B. and Aquilante, C. L. Cytochrome P450 2C8 pharmacogenetics: a review of clinical studies. *Pharmacogenomics* 10: 1489-1510 (2009).

Davies, B. and Morris, T. Physiological parameters in laboratory animals and humans. *Pharm Res* 10: 1093-1095 (1993).

de Wit, D., Guchelaar, H. J., den Hartigh, J., Gelderblom, H. and van Erp, N. P. Individualized dosing of tyrosine kinase inhibitors: are we there yet? *Drug Discov Today* (2014).

Delozier, T. C., Kissling, G. E., Coulter, S. J., Dai, D., Foley, J. F., Bradbury, J. A., Murphy, E., Steenbergen, C., Zeldin, D. C. and Goldstein, J. A. Detection of human CYP2C8, CYP2C9, and CYP2J2 in cardiovascular tissues. *Drug Metab Dispos* 35: 682-688 (2007).

Demetri, G. D., Wang, Y., Wehrle, E., Racine, A., Nikolova, Z., Blanke, C. D., Joensuu, H. and von Mehren, M. Imatinib plasma levels are correlated with clinical benefit in patients with unresectable/metastatic gastrointestinal stromal tumors. *J Clin Oncol* 27: 3141-3147 (2009).

Deng, L. J., Wang, F. and Li, H. D. Effect of gemfibrozil on the pharmacokinetics of pioglitazone. *Eur J Clin Pharmacol* 61: 831-836 (2005).

Dewar, A. L., Cambareri, A. C., Zannettino, A. C., Miller, B. L., Doherty, K. V., Hughes, T. P. and Lyons, A. B. Macrophage colony-stimulating factor receptor c-fms is a novel target of imatinib. *Blood* 105: 3127-3132 (2005).

Dickins, M., Elcombe, C. R., Moloney, S. J., Netter, K. J. and Bridges, J. W. Further studies on the dissociation of the isosafrole metabolite-cytochrome P-450 complex. *Biochem Pharmacol* 28: 231-238 (1979).

Dobson, P. D. and Kell, D. B. Carrier-mediated cellular uptake of pharmaceutical drugs: an exception or the rule? *Nat Rev Drug Discov* 7: 205-220 (2008).

Draper, A. J., Madan, A. and Parkinson, A. Inhibition of coumarin 7-hydroxylase activity in human liver microsomes. *Arch Biochem Biophys* 341: 47-61 (1997).

Druker, B. J., Tamura, S., Buchdunger, E., Ohno, S., Segal, G. M., Fanning, S., Zimmermann, J. and Lydon, N. B. Effects of a selective inhibitor of the Abl tyrosine kinase on the growth of Bcr-Abl positive cells. *Nat Med* 2: 561-566 (1996).

Dutreix, C., Peng, B., Mehring, G., Hayes, M., Capdeville, R., Pokorny, R. and Seiberling, M. Pharmacokinetic interaction between ketoconazole and imatinib mesylate (Glivec) in healthy subjects. *Cancer Chemother Pharmacol* 54: 290-294 (2004).

Eadie, L. N., Hughes, T. P. and White, D. L. Interaction of the efflux transporters ABCB1 and ABCG2 with imatinib, nilotinib, and dasatinib. *Clin Pharmacol Ther* 95: 294-306 (2014).

Eagling, V. A., Tjia, J. F. and Back, D. J. Differential selectivity of cytochrome P450 inhibitors against probe substrates in human and rat liver microsomes. *Br J Clin Pharmacol* 45: 107-114 (1998).

Edwards, R. J., Murray, B. P., Singleton, A. M. and Boobis, A. R. Orientation of cytochromes P450 in the endoplasmic reticulum. *Biochemistry* 30: 71-76 (1991).

Eechoute, K., Franke, R. M., Loos, W. J., Scherkenbach, L. A., Boere, I., Verweij, J., Gurney, H., Kim, R. B., Tirona, R. G., Mathijssen, R. H. and Sparreboom, A. Environmental and genetic factors affecting transport of imatinib by OATP1A2. *Clin Pharmacol Ther* 89: 816-820 (2011a).

Eechoute, K., Sparreboom, A., Burger, H., Franke, R. M., Schiavon, G., Verweij, J., Loos, W. J., Wiemer, E. A. and Mathijssen, R. H. Drug transporters and imatinib treatment: implications for clinical practice. *Clin Cancer Res* 17: 406-415 (2011b).

Egorin, M. J., Shah, D. D., Christner, S. M., Yerk, M. A., Komazec, K. A., Appleman, L. R., Redner, R. L., Miller, B. M. and Beumer, J. H. Effect of a proton pump inhibitor on the pharmacokinetics of imatinib. *Br J Clin Pharmacol* 68: 370-374 (2009).

Elcombe, C. R., Bridges, J. W. and Netter, K. J. Proceedings: Properties of the safrole metabolite-cytochrome P-450 complex. *Naunyn Schmiedebergs Arch Pharmacol* 287 Suppl: R72 (1975).

Elens, L., Becker, M. L., Haufroid, V., Hofman, A., Visser, L. E., Uitterlinden, A. G., Stricker, B. and van Schaik, R. H. Novel CYP3A4 intron 6 single nucleotide polymorphism is associated with simvastatin-mediated cholesterol reduction in the Rotterdam Study. *Pharmacogenet Genomics* 21: 861-866 (2011).

EMA. European Medicines Agency. Guideline on the investigation of drug interactions. *URL: http://www.ema.europa.eu/ema/pages/includes/document/open_document.jsp?webContentId=WC500129606 (Accessed October 14, 2014)* (2013).

Enayetallah, A. E., French, R. A., Thibodeau, M. S. and Grant, D. F. Distribution of soluble epoxide hydrolase and of cytochrome P450 2C8, 2C9, and 2J2 in human tissues. *J Histochem Cytochem* 52: 447-454 (2004).

Endres, C. J., Hsiao, P., Chung, F. S. and Unadkat, J. D. The role of transporters in drug interactions. *Eur J Pharm Sci* 27: 501-517 (2006).

Estabrook, R. W., Cooper, D. Y. and Rosenthal, O. The Light Reversible Carbon Monoxide Inhibition of the Steroid C21-Hydroxylase System of the Adrenal Cortex. *Biochem Z* 338: 741-755 (1963).

Fahmi, O. A., Hurst, S., Plowchalk, D., Cook, J., Guo, F., Youdim, K., Dickins, M., Phipps, A., Darekar, A., Hyland, R. and Obach, R. S. Comparison of different algorithms for predicting clinical drug-drug interactions, based on the use of CYP3A4 in vitro data: predictions of compounds as precipitants of interaction. *Drug Metab Dispos* 37: 1658-1666 (2009).

Fahmi, O. A., Maurer, T. S., Kish, M., Cardenas, E., Boldt, S. and Nettleton, D. A combined model for predicting CYP3A4 clinical net drug-drug interaction based on CYP3A4 inhibition, inactivation, and induction determined in vitro. *Drug Metab Dispos* 36: 1698-1708 (2008).

FDA. Drug Development and Drug Interactions: Table of Substrates, Inhibitors and Inducers. *URL: http://www.fda.gov/Drugs/DevelopmentApprovalProcess/DevelopmentResources/DrugInteractionsLabeling/ucm093664.htm (Accessed October 14, 2014)* (2011).

FDA. US Food and Drug Administration. Guidance for industry. Drug interaction studies — Study design, data analysis, implications for dosing, and labeling recommendations. Draft guidance. *URL: http://www.fda.gov/downloads/Drugs/GuidanceComplianceRegulatoryInformation/Guidances/UCM292362.pdf (Accessed October 14, 2014)* (2012).

Feidt, D. M., Klein, K., Hofmann, U., Riedmaier, S., Knobeloch, D., Thasler, W. E., Weiss, T. S., Schwab, M. and Zanger, U. M. Profiling induction of cytochrome p450 enzyme activity by statins using a new liquid chromatography-tandem mass spectrometry cocktail assay in human hepatocytes. *Drug Metab Dispos* 38: 1589-1597 (2010).

Ferguson, S. S., Chen, Y., LeCluyse, E. L., Negishi, M. and Goldstein, J. A. Human CYP2C8 is transcriptionally regulated by the nuclear receptors constitutive androstane receptor, pregnane X receptor, glucocorticoid receptor, and hepatic nuclear factor 4alpha. *Mol Pharmacol* 68: 747-757 (2005).

Filppula, A. M., Neuvonen, P. J. and Backman, J. T. In Vitro Assessment of Time-Dependent Inhibitory Effects on CYP2C8 and CYP3A Activity by Fourteen Protein Kinase Inhibitors. *Drug Metab Dispos* 42: 1202-1209 (2014).

Filppula, A. M., Tornio, A., Niemi, M., Neuvonen, P. J. and Backman, J. T. Gemfibrozil impairs imatinib absorption and inhibits the CYP2C8-mediated formation of its main metabolite. *Clin Pharmacol Ther* 94: 383-393 (2013).

Floyd, J. S., Kaspera, R., Marciante, K. D., Weiss, N. S., Heckbert, S. R., Lumley, T., Wiggins, K. L., Tamraz, B., Kwok, P. Y., Totah, R. A. and Psaty, B. M. A screening study of drug-drug interactions in cerivastatin users: an adverse effect of clopidogrel. *Clin Pharmacol Ther* 91: 896-904 (2012).

Fontana, E., Dansette, P. M. and Poli, S. M. Cytochrome p450 enzymes mechanism based inhibitors: common sub-structures and reactivity. *Curr Drug Metab* 6: 413-454 (2005).

Fowler, S. and Zhang, H. In vitro evaluation of reversible and irreversible cytochrome P450 inhibition: current status on methodologies and their utility for predicting drug-drug interactions. *AAPS J* 10: 410-424 (2008).

Franklin, M. R. Cytochrome P450 metabolic intermediate complexes from macrolide antibiotics and related compounds. *Methods Enzymol* 206: 559-573 (1991).

Frye, R. F., Fitzgerald, S. M., Lagattuta, T. F., Hruska, M. W. and Egorin, M. J. Effect of St John's wort on imatinib mesylate pharmacokinetics. *Clin Pharmacol Ther* 76: 323-329 (2004).

Fujino, H., Yamada, I., Shimada, S., Hirano, M., Tsunenari, Y. and Kojima, J. Interaction between fibrates and statins--metabolic interactions with gemfibrozil. *Drug Metabol Drug Interact* 19: 161-176 (2003).

Fujioka, Y., Kunze, K. L. and Isoherranen, N. Risk assessment of mechanism-based inactivation in drug-drug interactions. *Drug Metab Dispos* 40: 1653-1657 (2012).

Furukawa, T., Wakabayashi, K., Tamura, A., Nakagawa, H., Morishima, Y., Osawa, Y. and Ishikawa, T. Major SNP (Q141K) variant of human ABC transporter ABCG2 undergoes lysosomal and proteasomal degradations. *Pharm Res* 26: 469-479 (2009).

Gambacorti-Passerini, C., Zucchetti, M., Russo, D., Frapolli, R., Verga, M., Bungaro, S., Tornaghi, L., Rossi, F., Pioltelli, P., Pogliani, E., Alberti, D., Corneo, G. and D'Incalci, M. Alpha1 acid glycoprotein binds to imatinib (STI571) and substantially alters its pharmacokinetics in chronic myeloid leukemia patients. *Clin Cancer Res* 9: 625-632 (2003).

Gao, Y., Liu, D., Wang, H., Zhu, J. and Chen, C. Functional characterization of five CYP2C8 variants and prediction of CYP2C8 genotype-dependent effects on in vitro and in vivo drug-drug interactions. *Xenobiotica* 40: 467-475 (2010).

Garfinkel, D. Studies on pig liver microsomes. I. Enzymic and pigment composition of different microsomal fractions. *Arch Biochem Biophys* 77: 493-509 (1958).

Gerbal-Chaloin, S., Pascussi, J. M., Pichard-Garcia, L., Daujat, M., Waechter, F., Fabre, J. M., Carrere, N. and Maurel, P. Induction of CYP2C genes in human hepatocytes in primary culture. *Drug Metab Dispos* 29: 242-251 (2001).

Gertz, M., Davis, J. D., Harrison, A., Houston, J. B. and Galetin, A. Grapefruit juice-drug interaction studies as a method to assess the extent of intestinal availability: utility and limitations. *Curr Drug Metab* 9: 785-795 (2008).

Ghanbari, F., Rowland-Yeo, K., Bloomer, J. C., Clarke, S. E., Lennard, M. S., Tucker, G. T. and Rostami-Hodjegan, A. A critical evaluation of the experimental design of studies of mechanism based enzyme inhibition, with implications for in vitro-in vivo extrapolation. *Curr Drug Metab* 7: 315-334 (2006).

Giacomini, K. M., Balimane, P. V., Cho, S. K., Eadon, M., Edeki, T., Hillgren, K. M., Huang, S. M., Sugiyama, Y., Weitz, D., Wen, Y., Xia, C. Q., Yee, S. W., Zimdahl, H., Niemi, M. and International Transporter, C. International Transporter Consortium commentary on clinically important transporter polymorphisms. *Clin Pharmacol Ther* 94: 23-26 (2013).

Giacomini, K. M. and Sugiyama, Y. (2011). Membrane transporters and drug response. Goodman & Gilman's pharmacological basis of therapeutics. Goodman, L. S., Brunton, L. L., Chabner, B. and Knollmann, B. r. C. New York, McGraw-Hill**:** 89-121.

Gibbs, M. A., Kunze, K. L., Howald, W. N. and Thummel, K. E. Effect of inhibitor depletion on inhibitory potency: tight binding inhibition of CYP3A by clotrimazole. *Drug Metab Dispos* 27: 596-599 (1999).

Gleevec Clinical Pharmacology and Biopharmaceutic Review(s). Food and Drug Administration, Center for drug evaluation and research. *URL: http://www.accessdata.fda.gov/drugsatfda_docs/nda/2001/21335_Gleevec.cfm (Accessed October 14, 2014)* (2001).

Gleevec label. Food and Drug Administration, Center for drug evaluation and research. *URL: http://www.accessdata.fda.gov/drugsatfda_docs/label/2014/021588s040lbl.pdf (Accessed October 14, 2014)* (2014).

Gonzalez, F. J. The 2006 Bernard B. Brodie Award Lecture. Cyp2e1. *Drug Metab Dispos* 35: 1-8 (2007).

Gray, I. C., Nobile, C., Muresu, R., Ford, S. and Spurr, N. K. A 2.4-megabase physical map spanning the CYP2C gene cluster on chromosome 10q24. *Genomics* 28: 328-332 (1995).

Greiner, B., Eichelbaum, M., Fritz, P., Kreichgauer, H. P., von Richter, O., Zundler, J. and Kroemer, H. K. The role of intestinal P-glycoprotein in the interaction of digoxin and rifampin. *J Clin Invest* 104: 147-153 (1999).

Grimm, S. W., Einolf, H. J., Hall, S. D., He, K., Lim, H. K., Ling, K. H., Lu, C., Nomeir, A. A., Seibert, E., Skordos, K. W., Tonn, G. R., Van Horn, R., Wang, R. W., Wong, Y. N., Yang, T. J. and Obach, R. S. The conduct of in vitro studies to address time-dependent inhibition of drug-metabolizing enzymes: a perspective of the pharmaceutical research and manufacturers of America. *Drug Metab Dispos* 37: 1355-1370 (2009).

Gschwind, H. P., Pfaar, U., Waldmeier, F., Zollinger, M., Sayer, C., Zbinden, P., Hayes, M., Pokorny, R., Seiberling, M., Ben-Am, M., Peng, B. and Gross, G. Metabolism and disposition of imatinib mesylate in healthy volunteers. *Drug Metab Dispos* 33: 1503-1512 (2005).

Guengerich, F. P. Common and uncommon cytochrome P450 reactions related to metabolism and chemical toxicity. *Chem Res Toxicol* 14: 611-650 (2001).

Guengerich, F. P. Cytochrome p450 and chemical toxicology. *Chem Res Toxicol* 21: 70-83 (2008).

Guengerich, F. P., Kim, D. H. and Iwasaki, M. Role of human cytochrome P-450 IIE1 in the oxidation of many low molecular weight cancer suspects. *Chem Res Toxicol* 4: 168-179 (1991).

Gurney, H., Wong, M., Balleine, R. L., Rivory, L. P., McLachlan, A. J., Hoskins, J. M., Wilcken, N., Clarke, C. L., Mann, G. J., Collins, M., Delforce, S. E., Lynch, K. and Schran, H. Imatinib disposition and ABCB1 (MDR1, P-glycoprotein) genotype. *Clin Pharmacol Ther* 82: 33-40 (2007).

Halling, J., Petersen, M. S., Damkier, P., Nielsen, F., Grandjean, P., Weihe, P., Lundgren, S., Lundblad, M. S. and Brosen, K. Polymorphism of CYP2D6, CYP2C19, CYP2C9 and CYP2C8 in the Faroese population. *Eur J Clin Pharmacol* 61: 491-497 (2005).

Hamman, M. A., Thompson, G. A. and Hall, S. D. Regioselective and stereoselective metabolism of ibuprofen by human cytochrome P450 2C. *Biochem Pharmacol* 54: 33-41 (1997).

He, L., Vasiliou, K. and Nebert, D. W. Analysis and update of the human solute carrier (SLC) gene superfamily. *Hum Genomics* 3: 195-206 (2009).

Hediger, M. A., Romero, M. F., Peng, J. B., Rolfs, A., Takanaga, H. and Bruford, E. A. The ABCs of solute carriers: physiological, pathological and therapeutic implications of human membrane transport proteinsIntroduction. *Pflugers Arch* 447: 465-468 (2004).

Hegazy, S. K., Mabrouk, M. M., Elsisi, A. E. and Mansour, N. O. Effect of clarithromycin and fluconazole on the pharmacokinetics of montelukast in human volunteers. *Eur J Clin Pharmacol* 68: 1275-1280 (2012).

Heinrich, M. C., Griffith, D. J., Druker, B. J., Wait, C. L., Ott, K. A. and Zigler, A. J. Inhibition of c-kit receptor tyrosine kinase activity by STI 571, a selective tyrosine kinase inhibitor. *Blood* 96: 925-932 (2000).

Hemeryck, A., Lefebvre, R. A., De Vriendt, C. and Belpaire, F. M. Paroxetine affects metoprolol pharmacokinetics and pharmacodynamics in healthy volunteers. *Clin Pharmacol Ther* 67: 283-291 (2000).

Henningsson, A., Marsh, S., Loos, W. J., Karlsson, M. O., Garsa, A., Mross, K., Mielke, S., Vigano, L., Locatelli, A., Verweij, J., Sparreboom, A. and McLeod, H. L. Association of CYP2C8, CYP3A4, CYP3A5, and ABCB1 polymorphisms with the pharmacokinetics of paclitaxel. *Clin Cancer Res* 11: 8097-8104 (2005).

Hirano, M., Maeda, K., Shitara, Y. and Sugiyama, Y. Drug-drug interaction between pitavastatin and various drugs via OATP1B1. *Drug Metab Dispos* 34: 1229-1236 (2006).

Ho, R. H., Tirona, R. G., Leake, B. F., Glaeser, H., Lee, W., Lemke, C. J., Wang, Y. and Kim, R. B. Drug and bile acid transporters in rosuvastatin hepatic uptake: function, expression, and pharmacogenetics. *Gastroenterology* 130: 1793-1806 (2006).

Honkalammi, J., Niemi, M., Neuvonen, P. J. and Backman, J. T. Gemfibrozil is a strong inactivator of CYP2C8 in very small multiple doses. *Clin Pharmacol Ther* 91: 846-855 (2012).

Houston, J. B. and Galetin, A. Methods for predicting in vivo pharmacokinetics using data from in vitro assays. *Curr Drug Metab* 9: 940-951 (2008).

HSDB. Hazardous Substances Data Bank. *URL: http://toxnet.nlm.nih.gov (Search word: montelukast, accessed: May 12, 2014)* (2008).

Hsyu, P. H., Schultz-Smith, M. D., Lillibridge, J. H., Lewis, R. H. and Kerr, B. M. Pharmacokinetic interactions between nelfinavir and 3-hydroxy-3-methylglutaryl coenzyme A reductase inhibitors atorvastatin and simvastatin. *Antimicrob Agents Chemother* 45: 3445-3450 (2001).

Hu, G., Johnson, E. F. and Kemper, B. CYP2C8 exists as a dimer in natural membranes. *Drug Metab Dispos* 38: 1976-1983 (2010).

Hu, S., Franke, R. M., Filipski, K. K., Hu, C., Orwick, S. J., de Bruijn, E. A., Burger, H., Baker, S. D. and Sparreboom, A. Interaction of imatinib with human organic ion carriers. *Clin Cancer Res* 14: 3141-3148 (2008).

Huang, S. M., Strong, J. M., Zhang, L., Reynolds, K. S., Nallani, S., Temple, R., Abraham, S., Habet, S. A., Baweja, R. K., Burckart, G. J., Chung, S., Colangelo, P., Frucht, D., Green, M. D., Hepp, P., Karnaukhova, E., Ko, H. S., Lee, J. I., Marroum, P. J., Norden, J. M., Qiu, W., Rahman, A., Sobel, S., Stifano, T., Thummel, K., Wei, X. X., Yasuda, S., Zheng, J. H., Zhao, H. and Lesko, L. J. New era in drug interaction evaluation: US Food and Drug Administration update on CYP enzymes, transporters, and the guidance process. *J Clin Pharmacol* 48: 662-670 (2008).

Ieiri, I., Kimura, M., Irie, S., Urae, A., Otsubo, K. and Ishizaki, T. Interaction magnitude, pharmacokinetics and pharmacodynamics of ticlopidine in relation to CYP2C19 genotypic status. *Pharmacogenet Genomics* 15: 851-859 (2005).

Ingelman-Sundberg, M. and Sim, S. C. Pharmacogenetic biomarkers as tools for improved drug therapy; emphasis on the cytochrome P450 system. *Biochem Biophys Res Commun* 396: 90-94 (2010).

Isoherranen, N., Hachad, H., Yeung, C. K. and Levy, R. H. Qualitative analysis of the role of metabolites in inhibitory drug-drug interactions: literature evaluation based on the metabolism and transport drug interaction database. *Chem Res Toxicol* 22: 294-298 (2009).

Ito, K., Brown, H. S. and Houston, J. B. Database analyses for the prediction of in vivo drug-drug interactions from in vitro data. *Br J Clin Pharmacol* 57: 473-486 (2004).

Ito, K., Hallifax, D., Obach, R. S. and Houston, J. B. Impact of parallel pathways of drug elimination and multiple cytochrome P450 involvement on drug-drug interactions: CYP2D6 paradigm. *Drug Metabolism and Disposition* 33: 837-844 (2005).

Jaakkola, T., Backman, J. T., Neuvonen, M., Laitila, J. and Neuvonen, P. J. Effect of rifampicin on the pharmacokinetics of pioglitazone. *Br J Clin Pharmacol* 61: 70-78 (2006a).

Jaakkola, T., Backman, J. T., Neuvonen, M. and Neuvonen, P. J. Effects of gemfibrozil, itraconazole, and their combination on the pharmacokinetics of pioglitazone. *Clin Pharmacol Ther* 77: 404-414 (2005).

Jaakkola, T., Backman, J. T., Neuvonen, M., Niemi, M. and Neuvonen, P. J. Montelukast and zafirlukast do not affect the pharmacokinetics of the CYP2C8 substrate pioglitazone. *Eur J Clin Pharmacol* 62: 503-509 (2006b).

Jaakkola, T., Laitila, J., Neuvonen, P. J. and Backman, J. T. Pioglitazone is metabolised by CYP2C8 and CYP3A4 in vitro: potential for interactions with CYP2C8 inhibitors. *Basic Clin Pharmacol Toxicol* 99: 44-51 (2006c).

Jalava, K. M., Partanen, J. and Neuvonen, P. J. Itraconazole decreases renal clearance of digoxin. *Ther Drug Monit* 19: 609-613 (1997).

Jenkins, S. M., Zvyaga, T., Johnson, S. R., Hurley, J., Wagner, A., Burrell, R., Turley, W., Leet, J. E., Philip, T. and Rodrigues, A. D. Studies to further investigate the inhibition of human liver microsomal CYP2C8 by the acyl-beta-glucuronide of gemfibrozil. *Drug Metab Dispos* 39: 2421-2430 (2011).

Jiang, H., Zhong, F., Sun, L., Feng, W., Huang, Z. X. and Tan, X. Structural and functional insights into polymorphic enzymes of cytochrome P450 2C8. *Amino Acids* 40: 1195-1204 (2011).

Kajosaari, L. I., Laitila, J., Neuvonen, P. J. and Backman, J. T. Metabolism of repaglinide by CYP2C8 and CYP3A4 in vitro: effect of fibrates and rifampicin. *Basic Clin Pharmacol Toxicol* 97: 249-256 (2005a).

Kajosaari, L. I., Niemi, M., Backman, J. T. and Neuvonen, P. J. Telithromycin, but not montelukast, increases the plasma concentrations and effects of the cytochrome P450 3A4 and 2C8 substrate repaglinide. *Clin Pharmacol Ther* 79: 231-242 (2006).

Kajosaari, L. I., Niemi, M., Neuvonen, M., Laitila, J., Neuvonen, P. J. and Backman, J. T. Cyclosporine markedly raises the plasma concentrations of repaglinide. *Clin Pharmacol Ther* 78: 388-399 (2005b).

Kalgutkar, A. S., Obach, R. S. and Maurer, T. S. Mechanism-based inactivation of cytochrome P450 enzymes: chemical mechanisms, structure-activity relationships and relationship to clinical drug-drug interactions and idiosyncratic adverse drug reactions. *Curr Drug Metab* 8: 407-447 (2007).

Kanamitsu, S., Ito, K. and Sugiyama, Y. Quantitative prediction of in vivo drug-drug interactions from in vitro data based on physiological pharmacokinetics: use of maximum unbound concentration of inhibitor at the inlet to the liver. *Pharm Res* 17: 336-343 (2000).

Kang, Y. S., Park, S. Y., Yim, C. H., Kwak, H. S., Gajendrarao, P., Krishnamoorthy, N., Yun, S. C., Lee, K. W. and Han, K. O. The CYP3A4*18 genotype in the cytochrome P450 3A4 gene, a rapid metabolizer of sex steroids, is associated with low bone mineral density. *Clin Pharmacol Ther* 85: 312-318 (2009).

Kantola, T., Kivisto, K. T. and Neuvonen, P. J. Erythromycin and verapamil considerably increase serum simvastatin and simvastatin acid concentrations. *Clin Pharmacol Ther* 64: 177-182 (1998).

Karonen, T., Neuvonen, P. J. and Backman, J. T. The CYP2C8 inhibitor gemfibrozil does not affect the pharmacokinetics of zafirlukast. *Eur J Clin Pharmacol* 67: 151-155 (2011).

Karonen, T., Neuvonen, P. J. and Backman, J. T. CYP2C8 but not CYP3A4 is important in the pharmacokinetics of montelukast. *Br J Clin Pharmacol* 73: 257-267 (2012).

Kaspera, R., Naraharisetti, S. B., Tamraz, B., Sahele, T., Cheesman, M. J., Kwok, P. Y., Marciante, K., Heckbert, S. R., Psaty, B. M. and Totah, R. A. Cerivastatin in vitro metabolism by CYP2C8 variants found in patients experiencing rhabdomyolysis. *Pharmacogenet Genomics* 20: 619-629 (2010).

Kawakami, H., Ohtsuki, S., Kamiie, J., Suzuki, T., Abe, T. and Terasaki, T. Simultaneous absolute quantification of 11 cytochrome P450 isoforms in human liver microsomes by liquid chromatography tandem mass spectrometry with in silico target peptide selection. *J Pharm Sci* 100: 341-352 (2011).

Kenny, J. R., Mukadam, S., Zhang, C., Tay, S., Collins, C., Galetin, A. and Khojasteh, S. C. Drug-drug interaction potential of marketed oncology drugs: in vitro assessment of time-dependent cytochrome P450 inhibition, reactive metabolite formation and drug-drug interaction prediction. *Pharm Res* 29: 1960-1976 (2012).

Kerr, B. M., Thummel, K. E., Wurden, C. J., Klein, S. M., Kroetz, D. L., Gonzalez, F. J. and Levy, R. H. Human liver carbamazepine metabolism. Role of CYP3A4 and CYP2C8 in 10,11-epoxide formation. *Biochem Pharmacol* 47: 1969-1979 (1994).

Keskitalo, J. E., Zolk, O., Fromm, M. F., Kurkinen, K. J., Neuvonen, P. J. and Niemi, M. ABCG2 polymorphism markedly affects the pharmacokinetics of atorvastatin and rosuvastatin. *Clin Pharmacol Ther* 86: 197-203 (2009).

Kim, D. W., Tan, E. Y., Jin, Y., Park, S., Hayes, M., Demirhan, E., Schran, H. and Wang, Y. Effects of imatinib mesylate on the pharmacokinetics of paracetamol (acetaminophen) in Korean patients with chronic myelogenous leukaemia. *Br J Clin Pharmacol* 71: 199-206 (2011).

Kim, K. A., Chung, J., Jung, D. H. and Park, J. Y. Identification of cytochrome P450 isoforms involved in the metabolism of loperamide in human liver microsomes. *Eur J Clin Pharmacol* 60: 575-581 (2004).

Kim, K. A., Lee, H. M., Joo, H. J., Park, I. B. and Park, J. Y. Effects of polymorphisms of the SLCO2B1 transporter gene on the pharmacokinetics of montelukast in humans. *J Clin Pharmacol* 53: 1186-1193 (2013a).

Kim, K. A., Park, J. Y., Lee, J. S. and Lim, S. Cytochrome P450 2C8 and CYP3A4/5 are involved in chloroquine metabolism in human liver microsomes. *Arch Pharm Res* 26: 631-637 (2003).

Kim, K. A., Park, P. W., Kim, K. R. and Park, J. Y. Effect of multiple doses of montelukast on the pharmacokinetics of rosiglitazone, a CYP2C8 substrate, in humans. *Br J Clin Pharmacol* 63: 339-345 (2007).

Kim, M. J., Lee, J. W., Oh, K. S., Choi, C. S., Kim, K. H., Han, W. S., Yoon, C. N., Chung, E. S., Kim, D. H. and Shin, J. G. The tyrosine kinase inhibitor nilotinib selectively inhibits CYP2C8 activities in human liver microsomes. *Drug Metab Pharmacokinet* 28: 462-467 (2013b).

Kimura, S., Kako, S., Wada, H., Sakamoto, K., Ashizawa, M., Sato, M., Terasako, K., Kikuchi, M., Nakasone, H., Okuda, S., Yamazaki, R., Oshima, K., Nishida, J., Watanabe, T. and Kanda, Y. Can grapefruit juice decrease the cost of imatinib for the treatment of chronic myelogenous leukemia? *Leuk Res* 35: e11-12 (2011).

Kirchheiner, J., Thomas, S., Bauer, S., Tomalik-Scharte, D., Hering, U., Doroshyenko, O., Jetter, A., Stehle, S., Tsahuridu, M., Meineke, I., Brockmoller, J. and Fuhr, U. Pharmacokinetics and pharmacodynamics of rosiglitazone in relation to CYP2C8 genotype. *Clin Pharmacol Ther* 80: 657-667 (2006).

Kitz, R. and Wilson, I. B. Esters of methanesulfonic acid as irreversible inhibitors of acetylcholinesterase. *J Biol Chem* 237: 3245-3249 (1962).

Klein, K., Thomas, M., Winter, S., Nussler, A. K., Niemi, M., Schwab, M. and Zanger, U. M. PPARA: a novel genetic determinant of CYP3A4 in vitro and in vivo. *Clin Pharmacol Ther* 91: 1044-1052 (2012).

Klingenberg, M. Pigments of rat liver microsomes. *Arch Biochem Biophys* 75: 376-386 (1958).

Klose, T. S., Blaisdell, J. A. and Goldstein, J. A. Gene structure of CYP2C8 and extrahepatic distribution of the human CYP2Cs. *J Biochem Mol Toxicol* 13: 289-295 (1999).

Ko, J. W., Sukhova, N., Thacker, D., Chen, P. and Flockhart, D. A. Evaluation of omeprazole and lansoprazole as inhibitors of cytochrome P450 isoforms. *Drug Metab Dispos* 25: 853-862 (1997).

Koenigs, L. L., Peter, R. M., Thompson, S. J., Rettie, A. E. and Trager, W. F. Mechanism-based inactivation of human liver cytochrome P450 2A6 by 8-methoxypsoralen. *Drug Metab Dispos* 25: 1407-1415 (1997).

Konig, J., Muller, F. and Fromm, M. F. Transporters and drug-drug interactions: important determinants of drug disposition and effects. *Pharmacol Rev* 65: 944-966 (2013).

Korzekwa, K. Case study 4. Predicting the drug interaction potential for inhibition of CYP2C8 by montelukast. *Methods Mol Biol* 1113: 461-469 (2014).

Korzekwa, K. R. In vitro enzyme kinetics applied to drug-metabolizing enzymes. *Drug-drug interactions*. M. Dekker, New York (2002). 33-54.

Kretz, O., Weiss, H. M., Schumacher, M. M. and Gross, G. In vitro blood distribution and plasma protein binding of the tyrosine kinase inhibitor imatinib and its active metabolite, CGP74588, in rat, mouse, dog, monkey, healthy humans and patients with acute lymphatic leukaemia. *Br J Clin Pharmacol* 58: 212-216 (2004).

Kudzi, W., Dodoo, A. N. and Mills, J. J. Characterisation of CYP2C8, CYP2C9 and CYP2C19 polymorphisms in a Ghanaian population. *BMC Med Genet* 10: 124 (2009).

Kyrklund, C., Backman, J. T., Kivisto, K. T., Neuvonen, M., Laitila, J. and Neuvonen, P. J. Rifampin greatly reduces plasma simvastatin and simvastatin acid concentrations. *Clin Pharmacol Ther* 68: 592-597 (2000).

Kyrklund, C., Backman, J. T., Kivisto, K. T., Neuvonen, M., Laitila, J. and Neuvonen, P. J. Plasma concentrations of active lovastatin acid are markedly increased by gemfibrozil but not by bezafibrate. *Clin Pharmacol Ther* 69: 340-345 (2001).

Kyrklund, C., Backman, J. T., Neuvonen, M. and Neuvonen, P. J. Gemfibrozil increases plasma pravastatin concentrations and reduces pravastatin renal clearance. *Clin Pharmacol Ther* 73: 538-544 (2003).

Lai, X. S., Yang, L. P., Li, X. T., Liu, J. P., Zhou, Z. W. and Zhou, S. F. Human CYP2C8: structure, substrate specificity, inhibitor selectivity, inducers and polymorphisms. *Curr Drug Metab* 10: 1009-1047 (2009).

Larson, R. A., Druker, B. J., Guilhot, F., O'Brien, S. G., Riviere, G. J., Krahnke, T., Gathmann, I., Wang, Y. and Group, I. S. Imatinib pharmacokinetics and its correlation with response and safety in chronic-phase chronic myeloid leukemia: a subanalysis of the IRIS study. *Blood* 111: 4022-4028 (2008).

Lawrence, S., Nguyen, D., Bowen, C., Richards-Peterson, L. E. and Skordos, K. The Metabolic Drug-drug Interaction Profile of Dabrafenib: In Vitro Investigations and Quantitative Extrapolation of the P450-mediated DDI Risk. *Drug Metab Dispos* doi: 10.1124/dmd.114.057778 (2014).

le Coutre, P., Kreuzer, K. A., Pursche, S., Bonin, M., Leopold, T., Baskaynak, G., Dorken, B., Ehninger, G., Ottmann, O., Jenke, A., Bornhauser, M. and Schleyer, E. Pharmacokinetics and cellular uptake of imatinib and its main metabolite CGP74588. *Cancer Chemother Pharmacol* 53: 313-323 (2004).

Lecoeur, S., Bonierbale, E., Challine, D., Gautier, J. C., Valadon, P., Dansette, P. M., Catinot, R., Ballet, F., Mansuy, D. and Beaune, P. H. Specificity of in vitro covalent binding of tienilic acid metabolites to human liver microsomes in relationship to the type of hepatotoxicity: comparison with two directly hepatotoxic drugs. *Chem Res Toxicol* 7: 434-442 (1994).

Leo, M. A., Lasker, J. M., Raucy, J. L., Kim, C. I., Black, M. and Lieber, C. S. Metabolism of retinol and retinoic acid by human liver cytochrome P450IIC8. *Arch Biochem Biophys* 269: 305-312 (1989).

Li, A. C., Yu, E., Ring, S. C. and Chovan, J. P. Structural identification of imatinib cyanide adducts by mass spectrometry and elucidation of bioactivation pathway. *Rapid Commun Mass Spectrom* 28: 123-134 (2014).

Li, X. Q., Bjorkman, A., Andersson, T. B., Ridderstrom, M. and Masimirembwa, C. M. Amodiaquine clearance and its metabolism to N-desethylamodiaquine is mediated by CYP2C8: a new high affinity and turnover enzyme-specific probe substrate. *J Pharmacol Exp Ther* 300: 399-407 (2002).

Lilja, J. J., Backman, J. T. and Neuvonen, P. J. Effect of gemfibrozil on the pharmacokinetics and pharmacodynamics of racemic warfarin in healthy subjects. *Br J Clin Pharmacol* 59: 433-439 (2005).

Lin, J. H. Drug-drug interaction mediated by inhibition and induction of P-glycoprotein. *Adv Drug Deliv Rev* 55: 53-81 (2003).

Lin, J. H. and Lu, A. Y. Inhibition and induction of cytochrome P450 and the clinical implications. *Clin Pharmacokinet* 35: 361-390 (1998).

Lin, J. H. and Lu, A. Y. Interindividual variability in inhibition and induction of cytochrome P450 enzymes. *Annu Rev Pharmacol Toxicol* 41: 535-567 (2001).

Lin, Y. S., Dowling, A. L., Quigley, S. D., Farin, F. M., Zhang, J., Lamba, J., Schuetz, E. G. and Thummel, K. E. Co-regulation of CYP3A4 and CYP3A5 and contribution to hepatic and intestinal midazolam metabolism. *Mol Pharmacol* 62: 162-172 (2002).

Link, E., Parish, S., Armitage, J., Bowman, L., Heath, S., Matsuda, F., Gut, I., Lathrop, M. and Collins, R. SLCO1B1 variants and statin-induced myopathy--a genomewide study. *N Engl J Med* 359: 789-799 (2008).

Lopid Label. Pfizer Inc. *URL: http://www.accessdata.fda.gov/drugsatfda_docs/label/2013/018422s053lbl.pdf (Accessed October 14, 2014)* (2013).

Ma, S., Xu, Y. and Shou, M. Characterization of imatinib metabolites in rat and human liver microsomes: differentiation of hydroxylation from N-oxidation by liquid chromatography/atmospheric pressure chemical ionization mass spectrometry. *Rapid Commun Mass Spectrom* 23: 1446-1450 (2009).

MacKichan, J. J. Influence of protein binding and use of unbound (free) drug concentrations. *Applied pharmacokinetics & pharmacodynamics : principles of therapeutic drug monitoring*. Burton, M. E. Lippincott Williams & Wilkins, Baltimore (2006). 82-113.

Madan, A., Graham, R. A., Carroll, K. M., Mudra, D. R., Burton, L. A., Krueger, L. A., Downey, A. D., Czerwinski, M., Forster, J., Ribadeneira, M. D., Gan, L. S., LeCluyse, E. L., Zech, K., Robertson, P., Jr., Koch, P., Antonian, L., Wagner, G., Yu, L. and Parkinson, A. Effects of prototypical microsomal enzyme inducers on cytochrome P450 expression in cultured human hepatocytes. *Drug Metab Dispos* 31: 421-431 (2003).

Madan, A., Usuki, E., Burton, L. A., Ogilvie, B. W. and Parkinson, A. In vitro approaches for studying the inhibition of drug-metabolizing enzymes and identifying the drug-metabolizing enzymes responsible for the metabolism of drugs. *Drug-drug interactions. Drugs and the pharmaceutical sciences*. Rodrigues, A. D. Drug-drug interactions. M. Dekker, New York (2002). 217-294.

Mahon, F. X., Belloc, F., Lagarde, V., Chollet, C., Moreau-Gaudry, F., Reiffers, J., Goldman, J. M. and Melo, J. V. MDR1 gene overexpression confers resistance to imatinib mesylate in leukemia cell line models. *Blood* 101: 2368-2373 (2003).

Malmstrom, K., Schwartz, J., Reiss, T. F., Sullivan, T. J., Reese, J. H., Jauregui, L., Miller, K., Scott, M., Shingo, S., Peszek, I., Larson, P., Ebel, D., Hunt, T. L., Huhn, R. D. and Bachmann, K. Effect of montelukast on single-dose theophylline pharmacokinetics. *Am J Ther* 5: 189-195 (1998).

Mano, Y., Usui, T. and Kamimura, H. The UDP-glucuronosyltransferase 2B7 isozyme is responsible for gemfibrozil glucuronidation in the human liver. *Drug Metab Dispos* 35: 2040-2044 (2007).

Marull, M. and Rochat, B. Fragmentation study of imatinib and characterization of new imatinib metabolites by liquid chromatography-triple-quadrupole and linear ion trap mass spectrometers. *J Mass Spectrom* 41: 390-404 (2006).

Mathew, P., Cuddy, T., G., T. W. and D., S. An open-label study on the pharmacokinetics (PK) of pitavastatin (NK-104) when administered concomitantly with fenofibrate or gemfibrozil in healthy volunteers. *Clin Pharmacol Ther* 75: [abstract] (2004).

Mayhew, B. S., Jones, D. R. and Hall, S. D. An in vitro model for predicting in vivo inhibition of cytochrome P450 3A4 by metabolic intermediate complex formation. *Drug Metab Dispos* 28: 1031-1037 (2000).

McFayden, M. C., Melvin, W. T. and Murray, G. I. Regional distribution of individual forms of cytochrome P450 mRNA in normal adult human brain. *Biochem Pharmacol* 55: 825-830 (1998).

Melet, A., Marques-Soares, C., Schoch, G. A., Macherey, A. C., Jaouen, M., Dansette, P. M., Sari, M. A., Johnson, E. F. and Mansuy, D. Analysis of human cytochrome P450 2C8 substrate specificity using a substrate pharmacophore and site-directed mutants. *Biochemistry* 43: 15379-15392 (2004).

Melo, J. V. The diversity of BCR-ABL fusion proteins and their relationship to leukemia phenotype. *Blood* 88: 2375-2384 (1996).

Meyer, U. A. Overview of enzymes of drug metabolism. *J Pharmacokinet Biopharm* 24: 449-459 (1996).

Miller, D. B. and Spence, J. D. Clinical pharmacokinetics of fibric acid derivatives (fibrates). *Clin Pharmacokinet* 34: 155-162 (1998).

Mizuno, T., Terada, T., Kamba, T., Fukudo, M., Katsura, T., Nakamura, E., Ogawa, O. and Inui, K. ABCG2 421C>A polymorphism and high exposure of sunitinib in a patient with renal cell carcinoma. *Ann Oncol* 21: 1382-1383 (2010).

Mougey, E. B., Feng, H., Castro, M., Irvin, C. G. and Lima, J. J. Absorption of montelukast is transporter mediated: a common variant of OATP2B1 is associated with reduced plasma concentrations and poor response. *Pharmacogenet Genomics* 19: 129-138 (2009).

Mougey, E. B., Lang, J. E., Wen, X. and Lima, J. J. Effect of citrus juice and SLCO2B1 genotype on the pharmacokinetics of montelukast. *J Clin Pharmacol* 51: 751-760 (2011).

Muller, P. Y. and Milton, M. N. The determination and interpretation of the therapeutic index in drug development. *Nat Rev Drug Discov* 11: 751-761 (2012).

Murray, M. Drug-mediated inactivation of cytochrome P450. *Clin Exp Pharmacol Physiol* 24: 465-470 (1997).

Muschler, E., Lal, J., Jetter, A., Rattay, A., Zanger, U., Zadoyan, G., Fuhr, U. and Kirchheiner, J. The role of human CYP2C8 and CYP2C9 variants in pioglitazone metabolism in vitro. *Basic Clin Pharmacol Toxicol* 105: 374-379 (2009).

Nadin, L. and Murray, M. Participation of CYP2C8 in retinoic acid 4-hydroxylation in human hepatic microsomes. *Biochem Pharmacol* 58: 1201-1208 (1999).

Nakagomi-Hagihara, R., Nakai, D. and Tokui, T. Inhibition of human organic anion transporter 3 mediated pravastatin transport by gemfibrozil and the metabolites in humans. *Xenobiotica* 37: 416-426 (2007a).

Nakagomi-Hagihara, R., Nakai, D., Tokui, T., Abe, T. and Ikeda, T. Gemfibrozil and its glucuronide inhibit the hepatic uptake of pravastatin mediated by OATP1B1. *Xenobiotica* 37: 474-486 (2007b).

Nakajima, M., Fujiki, Y., Noda, K., Ohtsuka, H., Ohkuni, H., Kyo, S., Inoue, M., Kuroiwa, Y. and Yokoi, T. Genetic polymorphisms of CYP2C8 in Japanese population. *Drug Metab Dispos* 31: 687-690 (2003).

Nakajima, M., Nakamura, S., Tokudome, S., Shimada, N., Yamazaki, H. and Yokoi, T. Azelastine N-demethylation by cytochrome P-450 (CYP)3A4, CYP2D6, and CYP1A2 in human liver microsomes: evaluation of approach to predict the contribution of multiple CYPs. *Drug Metab Dispos* 27: 1381-1391 (1999).

Naraharisetti, S. B., Lin, Y. S., Rieder, M. J., Marciante, K. D., Psaty, B. M., Thummel, K. E. and Totah, R. A. Human liver expression of CYP2C8: gender, age, and genotype effects. *Drug Metab Dispos* 38: 889-893 (2010).

Narjoz, C., Favre, A., McMullen, J., Kiehl, P., Montemurro, M., Figg, W. D., Beaune, P., de Waziers, I. and Rochat, B. Important role of CYP2J2 in protein kinase inhibitor degradation: a possible role in intratumor drug disposition and resistance. *PLoS One* 9: e95532 (2014).

Nebert, D. W. and Russell, D. W. Clinical importance of the cytochromes P450. *Lancet* 360: 1155-1162 (2002).

Nebot, N., Crettol, S., d'Esposito, F., Tattam, B., Hibbs, D. E. and Murray, M. Participation of CYP2C8 and CYP3A4 in the N-demethylation of imatinib in human hepatic microsomes. *Br J Pharmacol* 161: 1059-1069 (2010).

Nelson, D. R. The cytochrome p450 homepage. *Hum Genomics* 4: 59-65 (2009).

Nelson, D. R., Zeldin, D. C., Hoffman, S. M., Maltais, L. J., Wain, H. M. and Nebert, D. W. Comparison of cytochrome P450 (CYP) genes from the mouse and human genomes, including nomenclature recommendations for genes, pseudogenes and alternative-splice variants. *Pharmacogenetics* 14: 1-18 (2004).

Newton, D. J., Wang, R. W. and Lu, A. Y. Cytochrome P450 inhibitors. Evaluation of specificities in the in vitrometabolism of therapeutic agents by human liver microsomes. *Drug Metab Dispos* 23: 154-158 (1995).

Nicolas, J. M., Chanteux, H., Rosa, M., Watanabe, S. and Stockis, A. Effect of gemfibrozil on the metabolism of brivaracetam in vitro and in human subjects. *Drug Metab Dispos* 40: 1466-1472 (2012).

Niemi, M., Backman, J. T., Granfors, M., Laitila, J., Neuvonen, M. and Neuvonen, P. J. Gemfibrozil considerably increases the plasma concentrations of rosiglitazone. *Diabetologia* 46: 1319-1323 (2003a).

Niemi, M., Backman, J. T., Juntti-Patinen, L., Neuvonen, M. and Neuvonen, P. J. Coadministration of gemfibrozil and itraconazole has only a minor effect on the pharmacokinetics of the CYP2C9 and CYP3A4 substrate nateglinide. *Br J Clin Pharmacol* 60: 208-217 (2005a).

Niemi, M., Backman, J. T., Kajosaari, L. I., Leathart, J. B., Neuvonen, M., Daly, A. K., Eichelbaum, M., Kivisto, K. T. and Neuvonen, P. J. Polymorphic organic anion transporting polypeptide 1B1 is a major determinant of repaglinide pharmacokinetics. *Clin Pharmacol Ther* 77: 468-478 (2005b).

Niemi, M., Backman, J. T., Neuvonen, M. and Neuvonen, P. J. Effects of gemfibrozil, itraconazole, and their combination on the pharmacokinetics and pharmacodynamics of repaglinide: potentially hazardous interaction between gemfibrozil and repaglinide. *Diabetologia* 46: 347-351 (2003b).

Niemi, M., Backman, J. T., Neuvonen, M., Neuvonen, P. J. and Kivisto, K. T. Rifampin decreases the plasma concentrations and effects of repaglinide. *Clin Pharmacol Ther* 68: 495-500 (2000).

Niemi, M., Backman, J. T. and Neuvonen, P. J. Effects of trimethoprim and rifampin on the pharmacokinetics of the cytochrome P450 2C8 substrate rosiglitazone. *Clin Pharmacol Ther* 76: 239-249 (2004).

Niemi, M., Leathart, J. B., Neuvonen, M., Backman, J. T., Daly, A. K. and Neuvonen, P. J. Polymorphism in CYP2C8 is associated with reduced plasma concentrations of repaglinide. *Clin Pharmacol Ther* 74: 380-387 (2003c).

Niemi, M., Neuvonen, P. J. and Kivisto, K. T. Effect of gemfibrozil on the pharmacokinetics and pharmacodynamics of glimepiride. *Clin Pharmacol Ther* 70: 439-445 (2001).

Niemi, M., Pasanen, M. K. and Neuvonen, P. J. Organic anion transporting polypeptide 1B1: a genetically polymorphic transporter of major importance for hepatic drug uptake. *Pharmacol Rev* 63: 157-181 (2011).

Niemi, M., Tornio, A., Pasanen, M. K., Fredrikson, H., Neuvonen, P. J. and Backman, J. T. Itraconazole, gemfibrozil and their combination markedly raise the plasma concentrations of loperamide. *Eur J Clin Pharmacol* 62: 463-472 (2006).

Nikolova, Z., Peng, B., Hubert, M., Sieberling, M., Keller, U., Ho, Y. Y., Schran, H. and Capdeville, R. Bioequivalence, safety, and tolerability of imatinib tablets compared with capsules. *Cancer Chemother Pharmacol* 53: 433-438 (2004).

Nishimura, M., Yaguti, H., Yoshitsugu, H., Naito, S. and Satoh, T. Tissue distribution of mRNA expression of human cytochrome P450 isoforms assessed by high-sensitivity real-time reverse transcription PCR. *Yakugaku Zasshi* 123: 369-375 (2003).

Niwa, T. and Yamazaki, H. Comparison of cytochrome P450 2C subfamily members in terms of drug oxidation rates and substrate inhibition. *Curr Drug Metab* 13: 1145-1159 (2012).

O'Brien, S. G., Meinhardt, P., Bond, E., Beck, J., Peng, B., Dutreix, C., Mehring, G., Milosavljev, S., Huber, C., Capdeville, R. and Fischer, T. Effects of imatinib mesylate (STI571, Glivec) on the pharmacokinetics of simvastatin, a cytochrome P450 3A4 substrate, in patients with chronic myeloid leukaemia. *Br J Cancer* 89: 1855-1859 (2003).

Obach, R. S. The importance of nonspecific binding in in vitro matrices, its impact on enzyme kinetic studies of drug metabolism reactions, and implications for in vitro-in vivo correlations. *Drug Metab Dispos* 24: 1047-1049 (1996).

Obach, R. S. Prediction of human clearance of twenty-nine drugs from hepatic microsomal intrinsic clearance data: An examination of in vitro half-life approach and nonspecific binding to microsomes. *Drug Metab Dispos* 27: 1350-1359 (1999).

Obach, R. S. Inhibition of drug-metabolizing enzymes and drug-drug interactions in drug discovery and development. *Drug-drug interactions in pharmaceutical development* Li, A. P. Wiley-interscience, Hoboken, N.J. (2008). 75-95.

Obach, R. S., Baxter, J. G., Liston, T. E., Silber, B. M., Jones, B. C., MacIntyre, F., Rance, D. J. and Wastall, P. The prediction of human pharmacokinetic parameters from preclinical and in vitro metabolism data. *J Pharmacol Exp Ther* 283: 46-58 (1997).

Obach, R. S., Walsky, R. L. and Venkatakrishnan, K. Mechanism-based inactivation of human cytochrome p450 enzymes and the prediction of drug-drug interactions. *Drug Metab Dispos* 35: 246-255 (2007).

Obach, R. S., Walsky, R. L., Venkatakrishnan, K., Gaman, E. A., Houston, J. B. and Tremaine, L. M. The utility of in vitro cytochrome P450 inhibition data in the prediction of drug-drug interactions. *J Pharmacol Exp Ther* 316: 336-348 (2006).

Ogilvie, B. W., Usuki, E., Yerino, P. and Parkinson, A. In vitro approaches for studying the inhibition of drug-metabolizing enzymes and identifying the drug-metabolizing enzymes responsible for the metabolism of a drug (reaction phenotyping) with emphasis on cytochrome P450. *Drug-drug interactions*. Rodrigues, A. D. Informa Healthcare, New York (2008). 231-358.

Ogilvie, B. W., Zhang, D., Li, W., Rodrigues, A. D., Gipson, A. E., Holsapple, J., Toren, P. and Parkinson, A. Glucuronidation converts gemfibrozil to a potent, metabolism-dependent inhibitor of CYP2C8: implications for drug-drug interactions. *Drug Metab Dispos* 34: 191-197 (2006).

Ohtsuki, S., Schaefer, O., Kawakami, H., Inoue, T., Liehner, S., Saito, A., Ishiguro, N., Kishimoto, W., Ludwig-Schwellinger, E., Ebner, T. and Terasaki, T. Simultaneous absolute protein quantification of transporters, cytochromes P450, and UDP-glucuronosyltransferases as a novel approach for the characterization of individual human liver: comparison with mRNA levels and activities. *Drug Metab Dispos* 40: 83-92 (2012).

Ohyama, K., Nakajima, M., Nakamura, S., Shimada, N., Yamazaki, H. and Yokoi, T. A significant role of human cytochrome P450 2C8 in amiodarone N-deethylation: an approach to predict the contribution with relative activity factor. *Drug Metab Dispos* 28: 1303-1310 (2000).

Okerholm, R. A., Keeley, F. J., Peterson, F. E. and Glazko, A. J. The metabolism of gemfibrozil. *Proc R Soc Med* 69 Suppl 2: 11-14 (1976).

Omura, T. and Sato, R. A new cytochrome in liver microsomes. *J Biol Chem* 237: 1375-1376 (1962).

Paggiaro, P. and Bacci, E. Montelukast in asthma: a review of its efficacy and place in therapy. *Ther Adv Chronic Dis* 2: 47-58 (2011).

Pane, F., Frigeri, F., Sindona, M., Luciano, L., Ferrara, F., Cimino, R., Meloni, G., Saglio, G., Salvatore, F. and Rotoli, B. Neutrophilic-chronic myeloid leukemia: a distinct disease with a specific molecular marker (BCR/ABL with C3/A2 junction). *Blood* 88: 2410-2414 (1996).

Parikh, S., Ouedraogo, J. B., Goldstein, J. A., Rosenthal, P. J. and Kroetz, D. L. Amodiaquine metabolism is impaired by common polymorphisms in CYP2C8: implications for malaria treatment in Africa. *Clin Pharmacol Ther* 82: 197-203 (2007).

Park, J. Y., Kim, K. A., Kang, M. H., Kim, S. L. and Shin, J. G. Effect of rifampin on the pharmacokinetics of rosiglitazone in healthy subjects. *Clin Pharmacol Ther* 75: 157-162 (2004).

Pasanen, M. K., Neuvonen, M., Neuvonen, P. J. and Niemi, M. SLCO1B1 polymorphism markedly affects the pharmacokinetics of simvastatin acid. *Pharmacogenet Genomics* 16: 873-879 (2006).

Pearson, J. T., Hill, J. J., Swank, J., Isoherranen, N., Kunze, K. L. and Atkins, W. M. Surface plasmon resonance analysis of antifungal azoles binding to CYP3A4 with kinetic resolution of multiple binding orientations. *Biochemistry* 45: 6341-6353 (2006).

Pechandova, K., Buzkova, H., Matouskova, O., Perlik, F. and Slanar, O. Genetic polymorphisms of CYP2C8 in the Czech Republic. *Genet Test Mol Biomarkers* 16: 812-816 (2012).

Pedersen, R. S., Brasch-Andersen, C., Sim, S. C., Bergmann, T. K., Halling, J., Petersen, M. S., Weihe, P., Edvardsen, H., Kristensen, V. N., Brosen, K. and Ingelman-Sundberg, M. Linkage disequilibrium between the CYP2C19*17 allele and wildtype CYP2C8 and CYP2C9 alleles: identification of CYP2C haplotypes in healthy Nordic populations. *Eur J Clin Pharmacol* 66: 1199-1205 (2010).

Pelkonen, O. and Turpeinen, M. In vitro-in vivo extrapolation of hepatic clearance: biological tools, scaling factors, model assumptions and correct concentrations. *Xenobiotica* 37: 1066-1089 (2007).

Pelkonen, O., Turpeinen, M., Hakkola, J., Honkakoski, P., Hukkanen, J. and Raunio, H. Inhibition and induction of human cytochrome P450 enzymes: current status. *Arch Toxicol* 82: 667-715 (2008).

Peng, B., Dutreix, C., Mehring, G., Hayes, M. J., Ben-Am, M., Seiberling, M., Pokorny, R., Capdeville, R. and Lloyd, P. Absolute bioavailability of imatinib (Glivec) orally versus intravenous infusion. *J Clin Pharmacol* 44: 158-162 (2004a).

Peng, B., Hayes, M., Resta, D., Racine-Poon, A., Druker, B. J., Talpaz, M., Sawyers, C. L., Rosamilia, M., Ford, J., Lloyd, P. and Capdeville, R. Pharmacokinetics and pharmacodynamics of imatinib in a phase I trial with chronic myeloid leukemia patients. *J Clin Oncol* 22: 935-942 (2004b).

Peng, B., Lloyd, P. and Schran, H. Clinical pharmacokinetics of imatinib. *Clin Pharmacokinet* 44: 879-894 (2005).

Peng, C. C., Shi, W., Lutz, J. D., Kunze, K. L., Liu, J. O., Nelson, W. L. and Isoherranen, N. Stereospecific metabolism of itraconazole by CYP3A4: dioxolane ring scission of azole antifungals. *Drug Metab Dispos* 40: 426-435 (2012).

Perloff, E. S., Mason, A. K., Dehal, S. S., Blanchard, A. P., Morgan, L., Ho, T., Dandeneau, A., Crocker, R. M., Chandler, C. M., Boily, N., Crespi, C. L. and Stresser, D. M. Validation of cytochrome P450 time-dependent inhibition assays: a two-time point IC50 shift approach facilitates kinact assay design. *Xenobiotica* 39: 99-112 (2009).

Picard, N., Cresteil, T., Djebli, N. and Marquet, P. In vitro metabolism study of buprenorphine: evidence for new metabolic pathways. *Drug Metab Dispos* 33: 689-695 (2005).

Picard, S., Titier, K., Etienne, G., Teilhet, E., Ducint, D., Bernard, M. A., Lassalle, R., Marit, G., Reiffers, J., Begaud, B., Moore, N., Molimard, M. and Mahon, F. X. Trough imatinib plasma levels are associated with both cytogenetic and molecular responses to standard-dose imatinib in chronic myeloid leukemia. *Blood* 109: 3496-3499 (2007).

Polasek, T. M., Elliot, D. J., Lewis, B. C. and Miners, J. O. Mechanism-based inactivation of human cytochrome P4502C8 by drugs in vitro. *J Pharmacol Exp Ther* 311: 996-1007 (2004).

Proctor, N. J., Tucker, G. T. and Rostami-Hodjegan, A. Predicting drug clearance from recombinantly expressed CYPs: intersystem extrapolation factors. *Xenobiotica* 34: 151-178 (2004).

Prueksaritanont, T., Ma, B. and Yu, N. The human hepatic metabolism of simvastatin hydroxy acid is mediated primarily by CYP3A, and not CYP2D6. *Br J Clin Pharmacol* 56: 120-124 (2003).

Prueksaritanont, T., Richards, K. M., Qiu, Y., Strong-Basalyga, K., Miller, A., Li, C., Eisenhandler, R. and Carlini, E. J. Comparative effects of fibrates on drug metabolizing enzymes in human hepatocytes. *Pharm Res* 22: 71-78 (2005).

Pursche, S., Schleyer, E., von Bonin, M., Ehninger, G., Said, S. M., Prondzinsky, R., Illmer, T., Wang, Y., Hosius, C., Nikolova, Z., Bornhauser, M. and Dresemann, G. Influence of enzyme-inducing antiepileptic drugs on trough level of imatinib in glioblastoma patients. *Curr Clin Pharmacol* 3: 198-203 (2008).

Rae, J. M., Johnson, M. D., Lippman, M. E. and Flockhart, D. A. Rifampin is a selective, pleiotropic inducer of drug metabolism genes in human hepatocytes: studies with cDNA and oligonucleotide expression arrays. *J Pharmacol Exp Ther* 299: 849-857 (2001).

Rahman, A., Korzekwa, K. R., Grogan, J., Gonzalez, F. J. and Harris, J. W. Selective biotransformation of taxol to 6 alpha-hydroxytaxol by human cytochrome P450 2C8. *Cancer Res* 54: 5543-5546 (1994).

Raucy, J. L., Mueller, L., Duan, K., Allen, S. W., Strom, S. and Lasker, J. M. Expression and induction of CYP2C P450 enzymes in primary cultures of human hepatocytes. *J Pharmacol Exp Ther* 302: 475-482 (2002).

Reese, M. J., Wurm, R. M., Muir, K. T., Generaux, G. T., St John-Williams, L. and McConn, D. J. An in vitro mechanistic study to elucidate the desipramine/bupropion clinical drug-drug interaction. *Drug Metab Dispos* 36: 1198-1201 (2008).

Richter, T., Murdter, T. E., Heinkele, G., Pleiss, J., Tatzel, S., Schwab, M., Eichelbaum, M. and Zanger, U. M. Potent mechanism-based inhibition of human CYP2B6 by clopidogrel and ticlopidine. *J Pharmacol Exp Ther* 308: 189-197 (2004).

Rifkind, A. B., Lee, C., Chang, T. K. and Waxman, D. J. Arachidonic acid metabolism by human cytochrome P450s 2C8, 2C9, 2E1, and 1A2: regioselective oxygenation and evidence for a role for CYP2C enzymes in arachidonic acid epoxygenation in human liver microsomes. *Arch Biochem Biophys* 320: 380-389 (1995).

Rochat, B., Zoete, V., Grosdidier, A., von Grunigen, S., Marull, M. and Michielin, O. In vitro biotransformation of imatinib by the tumor expressed CYP1A1 and CYP1B1. *Biopharm Drug Dispos* 29: 103-118 (2008).

Rodriguez-Antona, C., Niemi, M., Backman, J. T., Kajosaari, L. I., Neuvonen, P. J., Robledo, M. and Ingelman-Sundberg, M. Characterization of novel CYP2C8 haplotypes and their contribution to paclitaxel and repaglinide metabolism. *Pharmacogenomics J* 8: 268-277 (2008).

Rostami-Hodjegan, A. and Tucker, G. T. 'In silico' simulations to assess the 'in vivo' consequences of 'in vitro' metabolic drug-drug interactions. *Drug Discov Today Tech* 1: 441-448 (2004).

Rostami-Hodjegan, A. and Tucker, G. T. Simulation and prediction of in vivo drug metabolism in human populations from in vitro data. *Nat Rev Drug Discov* 6: 140-148 (2007).

Rowland, M., Peck, C. and Tucker, G. Physiologically-based pharmacokinetics in drug development and regulatory science. *Annu Rev Pharmacol Toxicol* 51: 45-73 (2011).

Rowland Yeo, K., Rostami Hodjegan, A. and Tucker, G. T. Abundance of cytochromes P450 in human liver: a meta-analysis. *In: BPS Winter Meeting; 2003, Dec 16-18; GKT School of Biomedical Sciences, Guys Campus, Kings College London. Br J Clinical Pharmacol* 57: 687-688 (2004).

Rowland Yeo, K., Walsky, R. L., Jamei, M., Rostami-Hodjegan, A. and Tucker, G. T. Prediction of time-dependent CYP3A4 drug-drug interactions by physiologically based pharmacokinetic modelling: impact of inactivation parameters and enzyme turnover. *Eur J Pharm Sci* 43: 160-173 (2011).

Roy, A. and Pahan, K. Gemfibrozil, stretching arms beyond lipid lowering. *Immunopharmacol Immunotoxicol* 31: 339-351 (2009).

Ryan, K. J. and Engel, L. L. Hydroxylation of steroids at carbon 21. *J Biol Chem* 225: 103-114 (1957).

Sager, J. E., Lutz, J. D., Foti, R. S., Davis, C., Kunze, K. L. and Isoherranen, N. Fluoxetine- and Norfluoxetine-Mediated Complex Drug-Drug Interactions: In Vitro to In Vivo Correlation of Effects on CYP2D6, CYP2C19, and CYP3A4. *Clin Pharmacol Ther* 95: 653-662 (2014).

Sahi, J., Black, C. B., Hamilton, G. A., Zheng, X., Jolley, S., Rose, K. A., Gilbert, D., LeCluyse, E. L. and Sinz, M. W. Comparative effects of thiazolidinediones on in vitro P450 enzyme induction and inhibition. *Drug Metab Dispos* 31: 439-446 (2003).

Sasongko, L., Link, J. M., Muzi, M., Mankoff, D. A., Yang, X., Collier, A. C., Shoner, S. C. and Unadkat, J. D. Imaging P-glycoprotein transport activity at the human blood-brain barrier with positron emission tomography. *Clin Pharmacol Ther* 77: 503-514 (2005).

Schmidli, H., Peng, B., Riviere, G. J., Capdeville, R., Hensley, M., Gathmann, I., Bolton, A. E., Racine-Poon, A. and Group, I. S. Population pharmacokinetics of imatinib mesylate in patients with chronic-phase chronic myeloid leukaemia: results of a phase III study. *Br J Clin Pharmacol* 60: 35-44 (2005).

Schneck, D. W., Birmingham, B. K., Zalikowski, J. A., Mitchell, P. D., Wang, Y., Martin, P. D., Lasseter, K. C., Brown, C. D., Windass, A. S. and Raza, A. The effect of gemfibrozil on the pharmacokinetics of rosuvastatin. *Clin Pharmacol Ther* 75: 455-463 (2004).

Schoch, G. A., Yano, J. K., Sansen, S., Dansette, P. M., Stout, C. D. and Johnson, E. F. Determinants of cytochrome P450 2C8 substrate binding: structures of complexes with montelukast, troglitazone, felodipine, and 9-cis-retinoic acid. *J Biol Chem* 283: 17227-17237 (2008).

Schoch, G. A., Yano, J. K., Wester, M. R., Griffin, K. J., Stout, C. D. and Johnson, E. F. Structure of human microsomal cytochrome P450 2C8. Evidence for a peripheral fatty acid binding site. *J Biol Chem* 279: 9497-9503 (2004).

Shimada, T., Yamazaki, H., Mimura, M., Inui, Y. and Guengerich, F. P. Interindividual variations in human liver cytochrome P-450 enzymes involved in the oxidation of drugs, carcinogens and toxic chemicals: studies with liver microsomes of 30 Japanese and 30 Caucasians. *J Pharmacol Exp Ther* 270: 414-423 (1994).

Shitara, Y., Hirano, M., Sato, H. and Sugiyama, Y. Gemfibrozil and its glucuronide inhibit the organic anion transporting polypeptide 2 (OATP2/OATP1B1:SLC21A6)-mediated hepatic uptake and CYP2C8-mediated metabolism of cerivastatin: analysis of the mechanism of the clinically relevant drug-drug interaction between cerivastatin and gemfibrozil. *J Pharmacol Exp Ther* 311: 228-236 (2004).

Silverman, R. B. Mechanism-based enzyme inactivators. *Methods Enzymol* 249: 240-283 (1995).

Silverman, R. B. and Invergo, B. J. Mechanism of inactivation of gamma-aminobutyrate aminotransferase by 4-amino-5-fluoropentanoic acid. First example of an enamine mechanism for a gamma-amino acid with a partition ratio of 0. *Biochemistry* 25: 6817-6820 (1986).

Simonson, S. G., Raza, A., Martin, P. D., Mitchell, P. D., Jarcho, J. A., Brown, C. D., Windass, A. S. and Schneck, D. W. Rosuvastatin pharmacokinetics in heart transplant recipients administered an antirejection regimen including cyclosporine. *Clin Pharmacol Ther* 76: 167-177 (2004).

Simonsson, U. S., Jansson, B., Hai, T. N., Huong, D. X., Tybring, G. and Ashton, M. Artemisinin autoinduction is caused by involvement of cytochrome P450 2B6 but not 2C9. *Clin Pharmacol Ther* 74: 32-43 (2003).

Singh, R., Ting, J. G., Pan, Y., Teh, L. K., Ismail, R. and Ong, C. E. Functional role of Ile264 in CYP2C8: mutations affect haem incorporation and catalytic activity. *Drug Metab Pharmacokinet* 23: 165-174 (2008).

Singulair Clinical Pharmacology and Biopharmaceutic Review(s). Food and Drug Administration, Center for drug evaluation and research. *URL: http://www.accessdata.fda.gov/drugsatfda_docs/nda/98/020829s000_Singular_Clin_Pharm_Biopharm.pdf (Accessed October 14, 2014)* (1998).

Singulair Label. Merck & Co., Inc. *URL: http://www.accessdata.fda.gov/drugsatfda_docs/label/2013/021409s043lbl.pdf (Accessed October 14, 2014)* (2013).

Singulair Pharmacology Review(s). Food and Drug Administration, Center for drug evaluation and research. *URL: http://www.accessdata.fda.gov/drugsatfda_docs/nda/2002/21-409_Singulair_Pharmr.pdf (Accessed October 14, 2014)* (2002).

Sinz, M., Wallace, G. and Sahi, J. Current industrial practices in assessing CYP450 enzyme induction: preclinical and clinical. *AAPS J* 10: 391-400 (2008).

Smith, H. E., Jones, J. P., 3rd, Kalhorn, T. F., Farin, F. M., Stapleton, P. L., Davis, C. L., Perkins, J. D., Blough, D. K., Hebert, M. F., Thummel, K. E. and Totah, R. A. Role of cytochrome P450 2C8 and 2J2 genotypes in calcineurin inhibitor-induced chronic kidney disease. *Pharmacogenet Genomics* 18: 943-953 (2008).

Smith, P., Bullock, J. M., Booker, B. M., Haas, C. E., Berenson, C. S. and Jusko, W. J. The influence of St. John's wort on the pharmacokinetics and protein binding of imatinib mesylate. *Pharmacotherapy* 24: 1508-1514 (2004a).

Smith, P. F., Bullock, J. M., Booker, B. M., Haas, C. E., Berenson, C. S. and Jusko, W. J. Induction of imatinib metabolism by hypericum perforatum. *Blood* 104: 1229-1230 (2004b).

Soyama, A., Hanioka, N., Saito, Y., Murayama, N., Ando, M., Ozawa, S. and Sawada, J. Amiodarone N-deethylation by CYP2C8 and its variants, CYP2C8*3 and CYP2C8 P404A. *Pharmacol Toxicol* 91: 174-178 (2002).

Soyama, A., Saito, Y., Hanioka, N., Murayama, N., Nakajima, O., Katori, N., Ishida, S., Sai, K., Ozawa, S. and Sawada, J. I. Non-synonymous single nucleotide alterations found in the CYP2C8 gene result in reduced in vitro paclitaxel metabolism. *Biol Pharm Bull* 24: 1427-1430 (2001).

Sparano, B. A., Egorin, M. J., Parise, R. A., Walters, J., Komazec, K. A., Redner, R. L. and Beumer, J. H. Effect of antacid on imatinib absorption. *Cancer Chemother Pharmacol* 63: 525-528 (2009).

Spence, J. D., Munoz, C. E., Hendricks, L., Latchinian, L. and Khouri, H. E. Pharmacokinetics of the combination of fluvastatin and gemfibrozil. *Am J Cardiol* 76: 80A-83A (1995).

Stage, T. B., Christensen, M. M., Feddersen, S., Beck-Nielsen, H. and Brosen, K. The role of genetic variants in CYP2C8, LPIN1, PPARGC1A and PPARgamma on the trough steady-state plasma concentrations of rosiglitazone and on glycosylated haemoglobin A1c in type 2 diabetes. *Pharmacogenet Genomics* 23: 219-227 (2013).

Stevens, J. C. and Wrighton, S. A. Interaction of the enantiomers of fluoxetine and norfluoxetine with human liver cytochromes P450. *J Pharmacol Exp Ther* 266: 964-971 (1993).

Stringer, R. A., Strain-Damerell, C., Nicklin, P. and Houston, J. B. Evaluation of recombinant cytochrome P450 enzymes as an in vitro system for metabolic clearance predictions. *Drug Metab Dispos* 37: 1025-1034 (2009).

Tafinlar label. Food and Drug Administration, Center for Drug Evaluation and research. *URL: http://www.accessdata.fda.gov/drugsatfda_docs/label/2014/202806s002lbl.pdf (Accessed October 14, 2014)* (2014).

Tapaninen, T., Karonen, T., Backman, J. T., Neuvonen, P. J. and Niemi, M. SLCO2B1 c.935G>A single nucleotide polymorphism has no effect on the pharmacokinetics of montelukast and aliskiren. *Pharmacogenet Genomics* 23: 19-24 (2013).

Tapaninen, T., Neuvonen, P. J. and Niemi, M. Grapefruit juice greatly reduces the plasma concentrations of the OATP2B1 and CYP3A4 substrate aliskiren. *Clin Pharmacol Ther* 88: 339-342 (2010).

Templeton, I., Peng, C. C., Thummel, K. E., Davis, C., Kunze, K. L. and Isoherranen, N. Accurate prediction of dose-dependent CYP3A4 inhibition by itraconazole and its metabolites from in vitro inhibition data. *Clin Pharmacol Ther* 88: 499-505 (2010).

Templeton, I. E., Thummel, K. E., Kharasch, E. D., Kunze, K. L., Hoffer, C., Nelson, W. L. and Isoherranen, N. Contribution of itraconazole metabolites to inhibition of CYP3A4 in vivo. *Clin Pharmacol Ther* 83: 77-85 (2008).

Teng, J. F., Mabasa, V. H. and Ensom, M. H. The role of therapeutic drug monitoring of imatinib in patients with chronic myeloid leukemia and metastatic or unresectable gastrointestinal stromal tumors. *Ther Drug Monit* 34: 85-97 (2012).

Testa, B. and Kramer, S. D. The biochemistry of drug metabolism--an introduction: part 1. Principles and overview. *Chem Biodivers* 3: 1053-1101 (2006).

Thomas, J., Wang, L., Clark, R. E. and Pirmohamed, M. Active transport of imatinib into and out of cells: implications for drug resistance. *Blood* 104: 3739-3745 (2004).

Thum, T. and Borlak, J. Gene expression in distinct regions of the heart. *Lancet* 355: 979-983 (2000).

Tirona, R. G. Molecular mechanisms of drug transporter regulation. *Handb Exp Pharmacol*: 373-402 (2011).

Tirona, R. G., Leake, B. F., Merino, G. and Kim, R. B. Polymorphisms in OATP-C: identification of multiple allelic variants associated with altered transport activity among European- and African-Americans. *J Biol Chem* 276: 35669-35675 (2001).

Todd, P. A. and Ward, A. Gemfibrozil. A review of its pharmacodynamic and pharmacokinetic properties, and therapeutic use in dyslipidaemia. *Drugs* 36: 314-339 (1988).

Tomlinson, B., Hu, M., Lee, V. W., Lui, S. S., Chu, T. T., Poon, E. W., Ko, G. T., Baum, L., Tam, L. S. and Li, E. K. ABCG2 polymorphism is associated with the low-density lipoprotein cholesterol response to rosuvastatin. *Clin Pharmacol Ther* 87: 558-562 (2010).

Tornio, A., Filppula, A. M., Kailari, O., Neuvonen, M., Nyronen, T. H., Tapaninen, T., Neuvonen, P. J., Niemi, M. and Backman, J. T. Glucuronidation Converts Clopidogrel to a Strong Time-Dependent Inhibitor of CYP2C8: A Phase II Metabolite as a Perpetrator of Drug-Drug Interactions. *Clin Pharmacol Ther* 96: 498-507 (2014).

Tornio, A., Neuvonen, P. J. and Backman, J. T. The CYP2C8 inhibitor gemfibrozil does not increase the plasma concentrations of zopiclone. *Eur J Clin Pharmacol* 62: 645-651 (2006).

Tornio, A., Niemi, M., Neuvonen, M., Laitila, J., Kalliokoski, A., Neuvonen, P. J. and Backman, J. T. The effect of gemfibrozil on repaglinide pharmacokinetics persists for at least 12 h after the dose: evidence for mechanism-based inhibition of CYP2C8 in vivo. *Clin Pharmacol Ther* 84: 403-411 (2008).

Tornio, A., Niemi, M., Neuvonen, P. J. and Backman, J. T. Stereoselective interaction between the CYP2C8 inhibitor gemfibrozil and racemic ibuprofen. *Eur J Clin Pharmacol* 63: 463-469 (2007).

Tornio, A., Pasanen, M. K., Laitila, J., Neuvonen, P. J. and Backman, J. T. Comparison of 3-hydroxy-3-methylglutaryl coenzyme A (HMG-CoA) reductase inhibitors (statins) as inhibitors of cytochrome P450 2C8. *Basic Clin Pharmacol Toxicol* 97: 104-108 (2005).

Totah, R. A. and Rettie, A. E. Cytochrome P450 2C8: substrates, inhibitors, pharmacogenetics, and clinical relevance. *Clin Pharmacol Ther* 77: 341-352 (2005).

Tozer, T. N. and Rowland, M. Drug interactions. *Introduction to pharmacokinetics and pharmacodynamics : the quantitative basis of drug therapy*. Lippincott Williams & Wilkins, Philadelphia (2006). 483-526.

Tracy, T. S. Atypical cytochrome p450 kinetics: implications for drug discovery. *Drugs R D* 7: 349-363 (2006).

Treiber, G., Wex, T., Schleyer, E., Troeger, U., Hosius, C. and Malfertheiner, P. Imatinib for hepatocellular cancer--focus on pharmacokinetic/pharmacodynamic modelling and liver function. *Cancer Lett* 260: 146-154 (2008).

Ullrich, V. and Schnabel, K. H. Formation and binding of carbanions by cytochrome P-450 of liver microsomes. *Drug Metab Dispos* 1: 176-183 (1973).

Walsky, R. L., Astuccio, A. V. and Obach, R. S. Evaluation of 227 drugs for in vitro inhibition of cytochrome P450 2B6. *J Clin Pharmacol* 46: 1426-1438 (2006).

Walsky, R. L., Gaman, E. A. and Obach, R. S. Examination of 209 drugs for inhibition of cytochrome P450 2C8. *J Clin Pharmacol* 45: 68-78 (2005a).

Walsky, R. L. and Obach, R. S. Validated assays for human cytochrome P450 activities. *Drug Metab Dispos* 32: 647-660 (2004).

Walsky, R. L., Obach, R. S., Gaman, E. A., Gleeson, J. P. and Proctor, W. R. Selective inhibition of human cytochrome P4502C8 by montelukast. *Drug Metab Dispos* 33: 413-418 (2005b).

van Erp, N., Gelderblom, H., van Glabbeke, M., Van Oosterom, A., Verweij, J., Guchelaar, H. J., Debiec-Rychter, M., Peng, B., Blay, J. Y. and Judson, I. Effect of cigarette smoking on imatinib in patients in the soft tissue and bone sarcoma group of the EORTC. *Clin Cancer Res* 14: 8308-8313 (2008).

van Erp, N. P., Gelderblom, H., Karlsson, M. O., Li, J., Zhao, M., Ouwerkerk, J., Nortier, J. W., Guchelaar, H. J., Baker, S. D. and Sparreboom, A. Influence of CYP3A4 inhibition on the steady-state pharmacokinetics of imatinib. *Clin Cancer Res* 13: 7394-7400 (2007).

Van Hecken, A., Depre, M., Verbesselt, R., Wynants, K., De Lepeleire, I., Arnout, J., Wong, P. H., Freeman, A., Holland, S., Gertz, B. and De Schepper, P. J. Effect of montelukast on the pharmacokinetics and pharmacodynamics of warfarin in healthy volunteers. *J Clin Pharmacol* 39: 495-500 (1999).

VandenBrink, B. M., Foti, R. S., Rock, D. A., Wienkers, L. C. and Wahlstrom, J. L. Evaluation of CYP2C8 inhibition in vitro: utility of montelukast as a selective CYP2C8 probe substrate. *Drug Metab Dispos* 39: 1546-1554 (2011).

Wang, D., Guo, Y., Wrighton, S. A., Cooke, G. E. and Sadee, W. Intronic polymorphism in CYP3A4 affects hepatic expression and response to statin drugs. *Pharmacogenomics J* 11: 274-286 (2011).

Wang, H. and LeCluyse, E. L. Role of orphan nuclear receptors in the regulation of drug-metabolising enzymes. *Clin Pharmacokinet* 42: 1331-1357 (2003).

Wang, J., Hughes, T. P., Kok, C. H., Saunders, V. A., Frede, A., Groot-Obbink, K., Osborn, M., Somogyi, A. A., D'Andrea, R. J. and White, D. L. Contrasting effects of diclofenac and ibuprofen on active imatinib uptake into leukaemic cells. *Br J Cancer* 106: 1772-1778 (2012).

Wang, J. S., Neuvonen, M., Wen, X., Backman, J. T. and Neuvonen, P. J. Gemfibrozil inhibits CYP2C8-mediated cerivastatin metabolism in human liver microsomes. *Drug Metab Dispos* 30: 1352-1356 (2002).

Wang, Y., Wang, M., Qi, H., Pan, P., Hou, T., Li, J., He, G. and Zhang, H. Pathway-Dependent Inhibition of Paclitaxel Hydroxylation by Kinase Inhibitors and Assessment of Drug-Drug Interaction Potentials. *Drug Metab Dispos* doi: 10.1124/dmd.113.053793 (2014).

Wang, Y., Zhou, L., Dutreix, C., Leroy, E., Yin, Q., Sethuraman, V., Riviere, G. J., Yin, O. Q., Schran, H. and Shen, Z. X. Effects of imatinib (Glivec) on the pharmacokinetics of metoprolol, a CYP2D6 substrate, in Chinese patients with chronic myelogenous leukaemia. *Br J Clin Pharmacol* 65: 885-892 (2008).

Wang, Y. H., Jones, D. R. and Hall, S. D. Prediction of cytochrome P450 3A inhibition by verapamil enantiomers and their metabolites. *Drug Metabolism and Disposition* 32: 259-266 (2004).

Wen, X., Wang, J. S., Backman, J. T., Kivisto, K. T. and Neuvonen, P. J. Gemfibrozil is a potent inhibitor of human cytochrome P450 2C9. *Drug Metab Dispos* 29: 1359-1361 (2001).

Wen, X., Wang, J. S., Backman, J. T., Laitila, J. and Neuvonen, P. J. Trimethoprim and sulfamethoxazole are selective inhibitors of CYP2C8 and CYP2C9, respectively. *Drug Metab Dispos* 30: 631-635 (2002).

Venkatakrishnan, K., Obach, R. S. and Rostami-Hodjegan, A. Mechanism-based inactivation of human cytochrome P450 enzymes: strategies for diagnosis and drug-drug interaction risk assessment. *Xenobiotica* 37: 1225-1256 (2007).

Venkatakrishnan, K., von Moltke, L. L., Obach, R. S. and Greenblatt, D. J. Drug metabolism and drug interactions: application and clinical value of in vitro models. *Curr Drug Metab* 4: 423-459 (2003).

Westlind-Johnsson, A., Malmebo, S., Johansson, A., Otter, C., Andersson, T. B., Johansson, I., Edwards, R. J., Boobis, A. R. and Ingelman-Sundberg, M. Comparative analysis of CYP3A expression in human liver suggests only a minor role for CYP3A5 in drug metabolism. *Drug Metab Dispos* 31: 755-761 (2003).

Widmer, N., Decosterd, L. A., Csajka, C., Leyvraz, S., Duchosal, M. A., Rosselet, A., Rochat, B., Eap, C. B., Henry, H., Biollaz, J. and Buclin, T. Population pharmacokinetics of imatinib and the role of alpha-acid glycoprotein. *Br J Clin Pharmacol* 62: 97-112 (2006).

Viibryd Clinical Pharmacology and Biopharmaceutics Review(s). Food and Drug Administration, Center for Drug Evaluation and Research. . *URL: http://www.accessdata.fda.gov/drugsatfda_docs/nda/2011/022567Orig1s000ClinPharmR.pdf (Accessed October 14, 2014)* (2010).

Wilkinson, G. R. Clearance approaches in pharmacology. *Pharmacol Rev* 39: 1-47 (1987).

Wilkinson, G. R. and Shand, D. G. Commentary: a physiological approach to hepatic drug clearance. *Clin Pharmacol Ther* 18: 377-390 (1975).

Williams, P. A., Cosme, J., Vinkovic, D. M., Ward, A., Angove, H. C., Day, P. J., Vonrhein, C., Tickle, I. J. and Jhoti, H. Crystal structures of human cytochrome P450 3A4 bound to metyrapone and progesterone. *Science* 305: 683-686 (2004).

Wolbold, R., Klein, K., Burk, O., Nussler, A. K., Neuhaus, P., Eichelbaum, M., Schwab, M. and Zanger, U. M. Sex is a major determinant of CYP3A4 expression in human liver. *Hepatology* 38: 978-988 (2003).

von Moltke, L. L., Greenblatt, D. J., Schmider, J., Wright, C. E., Harmatz, J. S. and Shader, R. I. In vitro approaches to predicting drug interactions in vivo. *Biochem Pharmacol* 55: 113-122 (1998).

Wu, X., Zuo, J., Guo, T. and Yuan, L. CYP2C8 polymorphism frequencies among Han, Uighur, Hui, and Mongolian Chinese populations. *Genet Test Mol Biomarkers* 17: 104-108 (2013).

Xenotech. CYP inhibition flyer. *URL: http://www.xenotechllc.com/Flyers/Inhibition/CYP-Inhibition-flyer.aspx (Accessed May 5, 2014)* (2011).

Xtandi Clinical Pharmacology and Biopharmaceutic Review(s). Food and Drug Administration, Center for Drug Evaluation and Research. *URL: http://www.accessdata.fda.gov/drugsatfda_docs/nda/2012/203415Orig1s000ClinPharmR.pdf (Accessed October 14, 2014)* (2012).

Yamano, K., Yamamoto, K., Kotaki, H., Takedomi, S., Matsuo, H., Sawada, Y. and Iga, T. Correlation between in vivo and in vitro hepatic uptake of metabolic inhibitors of cytochrome P-450 in rats. *Drug Metab Dispos* 27: 1225-1231 (1999).

Yamazaki, H., Shibata, A., Suzuki, M., Nakajima, M., Shimada, N., Guengerich, F. P. and Yokoi, T. Oxidation of troglitazone to a quinone-type metabolite catalyzed by cytochrome P-450 2C8 and P-450 3A4 in human liver microsomes. *Drug Metab Dispos* 27: 1260-1266 (1999).

Yamazaki, H., Suzuki, M., Tane, K., Shimada, N., Nakajima, M. and Yokoi, T. In vitro inhibitory effects of troglitazone and its metabolites on drug oxidation activities of human cytochrome P450 enzymes: comparison with pioglitazone and rosiglitazone. *Xenobiotica* 30: 61-70 (2000).

Yamazaki, M., Li, B., Louie, S. W., Pudvah, N. T., Stocco, R., Wong, W., Abramovitz, M., Demartis, A., Laufer, R., Hochman, J. H., Prueksaritanont, T. and Lin, J. H. Effects of fibrates on human organic anion-transporting polypeptide 1B1-, multidrug resistance protein 2- and P-glycoprotein-mediated transport. *Xenobiotica* 35: 737-753 (2005).

Yang, J., Liao, M., Shou, M., Jamei, M., Yeo, K. R., Tucker, G. T. and Rostami-Hodjegan, A. Cytochrome p450 turnover: regulation of synthesis and degradation, methods for determining rates, and implications for the prediction of drug interactions. *Curr Drug Metab* 9: 384-394 (2008).

Yano, J. K., Wester, M. R., Schoch, G. A., Griffin, K. J., Stout, C. D. and Johnson, E. F. The structure of human microsomal cytochrome P450 3A4 determined by X-ray crystallography to 2.05-A resolution. *J Biol Chem* 279: 38091-38094 (2004).

Yasar, U., Lundgren, S., Eliasson, E., Bennet, A., Wiman, B., de Faire, U. and Rane, A. Linkage between the CYP2C8 and CYP2C9 genetic polymorphisms. *Biochem Biophys Res Commun* 299: 25-28 (2002).

Yeung, C. K., Fujioka, Y., Hachad, H., Levy, R. H. and Isoherranen, N. Are circulating metabolites important in drug-drug interactions?: Quantitative analysis of risk prediction and inhibitory potency. *Clin Pharmacol Ther* 89: 105-113 (2011).

Yoshida, K., Maeda, K. and Sugiyama, Y. Transporter-mediated drug--drug interactions involving OATP substrates: predictions based on in vitro inhibition studies. *Clin Pharmacol Ther* 91: 1053-1064 (2012).

Young, R. N. Discovery and development of montelukast (Singulair). *Case studies in modern drug discovery and development*. Huang, X. and Aslanian, R. G. John Wiley & Sons, Hoboken, NJ (2012). 154-195.

Yu, L., Shi, D., Ma, L., Zhou, Q. and Zeng, S. Influence of CYP2C8 polymorphisms on the hydroxylation metabolism of paclitaxel, repaglinide and ibuprofen enantiomers in vitro. *Biopharm Drug Dispos* 34: 278-287 (2013).

Zanger, U. M. and Schwab, M. Cytochrome P450 enzymes in drug metabolism: regulation of gene expression, enzyme activities, and impact of genetic variation. *Pharmacol Ther* 138: 103-141 (2013).

Zanger, U. M., Turpeinen, M., Klein, K. and Schwab, M. Functional pharmacogenetics/genomics of human cytochromes P450 involved in drug biotransformation. *Anal Bioanal Chem* 392: 1093-1108 (2008).

Zeldin, D. C., DuBois, R. N., Falck, J. R. and Capdevila, J. H. Molecular cloning, expression and characterization of an endogenous human cytochrome P450 arachidonic acid epoxygenase isoform. *Arch Biochem Biophys* 322: 76-86 (1995).

Zetia Clinical Pharmacology and Biopharmaceutic Review(s). Food and Drug Administration, Center for Drug Evaluation and Research. *URL: http://www.accessdata.fda.gov/drugsatfda_docs/nda/2002/21445_Zetia_biopharmr_P1.pdf (Accessed October 14, 2014)* (2001).

Zhang, H., Davis, C. D., Sinz, M. W. and Rodrigues, A. D. Cytochrome P450 reaction-phenotyping: an industrial perspective. *Expert Opin Drug Metab Toxicol* 3: 667-687 (2007).

Zhang, L., Strong, J. M., Qiu, W., Lesko, L. J. and Huang, S. M. Scientific perspectives on drug transporters and their role in drug interactions. *Mol Pharm* 3: 62-69 (2006a).

Zhang, L., Zhang, Y. D., Strong, J. M., Reynolds, K. S. and Huang, S. M. A regulatory viewpoint on transporter-based drug interactions. *Xenobiotica* 38: 709-724 (2008).

Zhang, W., Yu, B. N., He, Y. J., Fan, L., Li, Q., Liu, Z. Q., Wang, A., Liu, Y. L., Tan, Z. R., Fen, J., Huang, Y. F. and Zhou, H. H. Role of BCRP 421C>A polymorphism on rosuvastatin pharmacokinetics in healthy Chinese males. *Clin Chim Acta* 373: 99-103 (2006b).

Zhang, Y. and Benet, L. Z. The gut as a barrier to drug absorption: combined role of cytochrome P450 3A and P-glycoprotein. *Clin Pharmacokinet* 40: 159-168 (2001).

Zhao, J. J., Rogers, J. D., Holland, S. D., Larson, P., Amin, R. D., Haesen, R., Freeman, A., Seiberling, M., Merz, M. and Cheng, H. Pharmacokinetics and bioavailability of montelukast sodium (MK-0476) in healthy young and elderly volunteers. *Biopharm Drug Dispos* 18: 769-777 (1997).

Zhao, P., Zhang, L., Grillo, J. A., Liu, Q., Bullock, J. M., Moon, Y. J., Song, P., Brar, S. S., Madabushi, R., Wu, T. C., Booth, B. P., Rahman, N. A., Reynolds, K. S., Gil Berglund, E., Lesko, L. J. and Huang, S. M. Applications of physiologically based pharmacokinetic (PBPK) modeling and simulation during regulatory review. *Clin Pharmacol Ther* 89: 259-267 (2011).

ORIGINAL PUBLICATIONS